Water Authority
of Western Australia

WATER RESOURCES DIRECTORATE

The Development And Calibration Of The Penman Equation For Application To Pan And Forest Evaporation Studies

Report No.WH 38

May 1987

Water Authority
of Western Australia

WATER RESOURCES DIRECTORATE

Hydrology Branch

The Development And Calibration Of The Penman Equation For Application To Pan And Forest Evaporation Studies

R W Edgeloe
I C Loh
R W Bell

Report No.WH 38

May 1987

SYNOPSIS

This report describes the physical basis for the Penman Monteith equation for estimation of evapotranspiration, and presents a detailed derivation of the equation. The data requirements for the equation were investigated and a method of estimating net radiation from measurements of direct short-wave radiation was developed.

The Penman equation was applied to a Class A evaporation pan and showed the significant effects of heat storage of water in the pan, and the direct loss of energy for evaporation by the reflection of incident shortwave radiation off the sides and bottom of the pan.

Rates of evaporation of intercepted rainfall was found to be of order 40% of wet canopy evaporation rates calculated from dry canopy climatogoical data. Forest transpiration rates are much lower than this due to the operation of leaf stomata in restricting transpiration.

The results of this work indicates that the rate of evaporation of intercepted water can be up to 4 times greater than the rate of pan evaporation in the winter months.

The Development and Calibration of the Penman Equation for Application to Pan and Forest Evaporation Studies

Appendices

LIST OF TABLES

Appendices

LIST OF TABLES

1. INTRODUCTION

The Hydrology Branch of the Water Authority of Western Australia is currently involved in investigating and developing reforestation strategies for catchment areas in the south-west of Western Australia.

Reforestation programmes have been established at Stene's Farm in the Collie Catchment (figs. 1, 2) (Anderson. et. al., 1982) and are presently being applied to other cleared areas in the same region.

Although there are indications that reforestation will lower the levels of the underlying groundwater, there is as yet no direct experimental confirmation that reforestation will control salinity (Sadler & Williams, 1981).

To confirm that water tables can be lowered by reforestation and to determine the amount of water used by different tree species the approach of computer simulation modelling was undertaken by the Water Resources Branch. The models used include combinations of hillslope, groundwater, water balance and interception models.

Of major importance to all these models are accurate estimates of the evapotranspiration losses of different tree species.

The evapotranspiration from each species is determined by the available energy input, the aerodynamic properties, the meteorological conditions and most importantly the availability of water that is free to evaporate.

During periods of rain when the tree canopies are wet, water is free to evaporate at the potential rate given by the Penman equation (Penman, 1948). However when the canopies are dry, evapotranspiration is limited to water that is released through the stomata of the leaves. The dry canopy rate can then be of order 3 times less than that for a wet canopy. (Holmes & Wronski, 1981).

This work was concerned only with the determination of the wet canopy rate. Later work will investigate the effects of the stomata on the transpiration rates.

The results of this work can then be applied to a larger scale to determine the effects of the reforestation strategies and assist in the selection of appropriate tree species.

The approach has been to apply the Penman equation to short term meteorological data that had been collected at the Ernies Climat Station (Edgeloe & Loh 1983) to predict class A pan evaporation by calibrating the penman equation with observed data via a pan albedo which allows for the short-wave radiation that is reflected off the pan wall and base.

Additional information regarding the aerodynamics of tree canopies were estimated from measurements of wind run profiles taken at one reforestation site in the Collie Region (Arboretum Site).

The problems of the traditional approach of using pan evaporation to estimate forest evapotranspriation is also briefly discussed in this work.

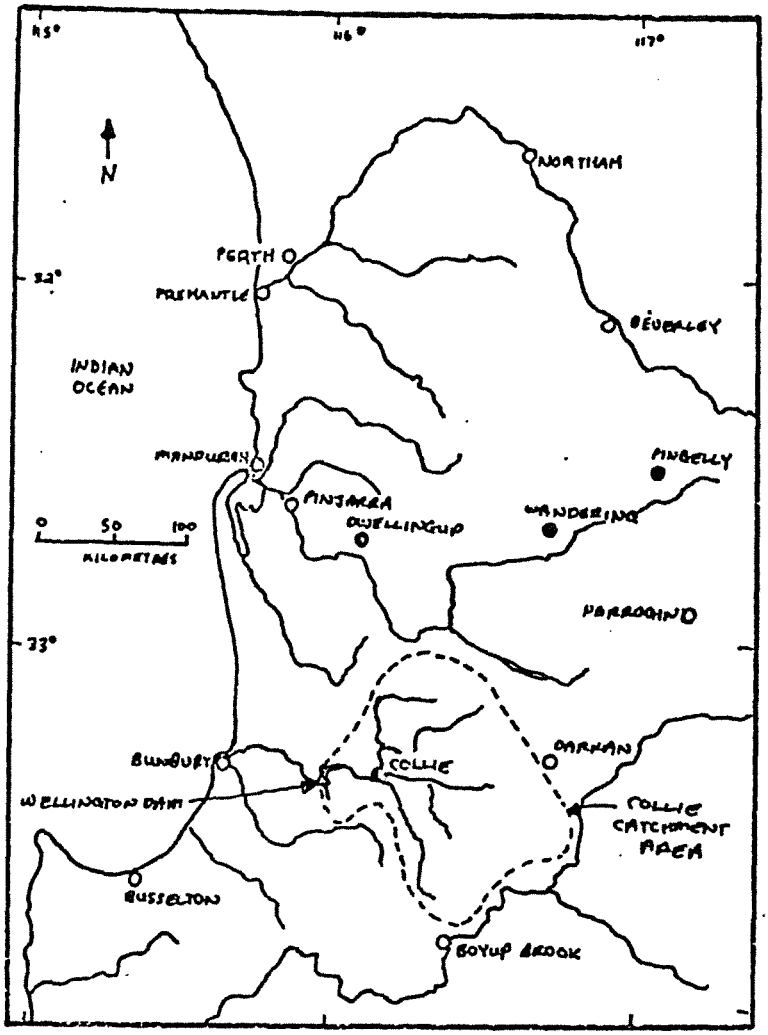

Figure 1 Locality Plan

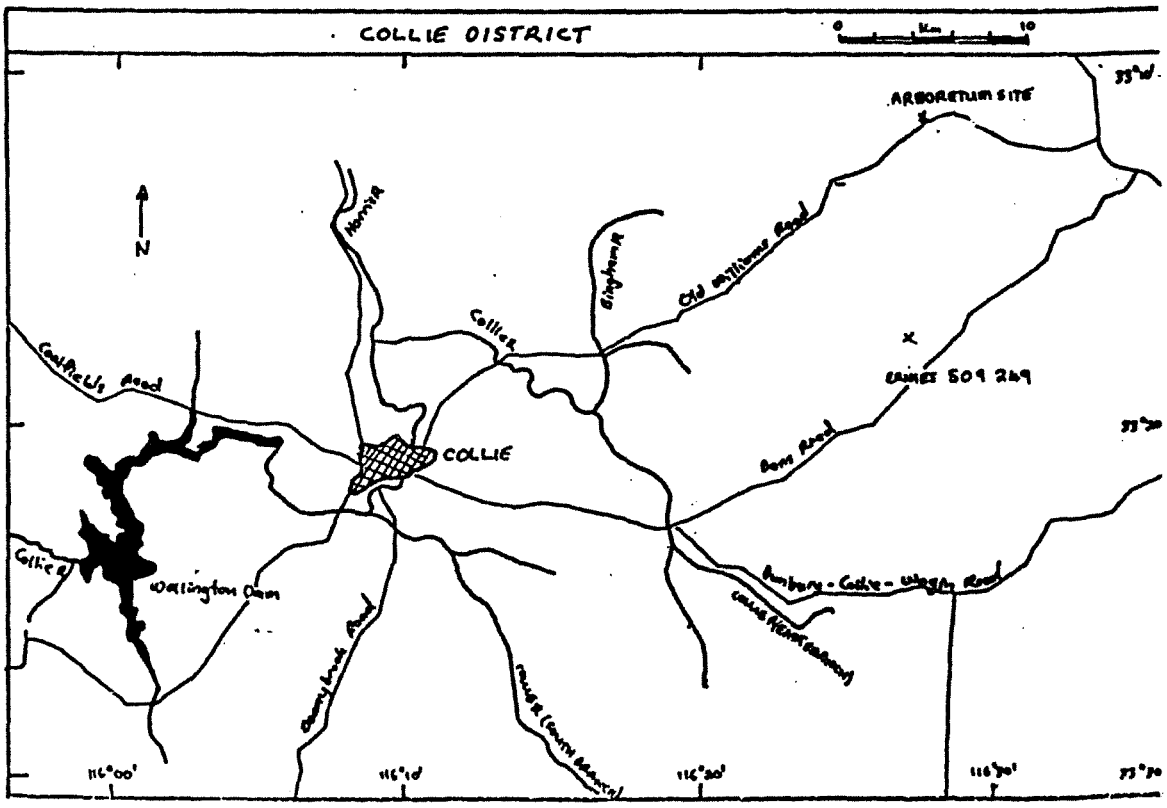

Figure 2 Collie District

2. Derivation of Penman Monteith Equation

2.1 General

The Penman Monteith equation combines aerodynamic and energy balance principles into a single equation which requires information of conditions at only one level above the vegetation.

Penman (1948) considered two theoretical approaches to evaporation from saturated surfaces. The first using an aerodynamic basis in which evaporation is regarded as being due to the turbulent transport of water vapour by the process of eddy diffusion. The second using an energy basis in which evaporation is considered as one of the ways in which incoming radiation is degraded. Neither approach was new but a combination was suggested that eliminated the difficult need of measuring the temperature and humidity at the evaporating surface. This provided for the first time an opportunity to make theoretical estimates of evaporation rates from standard meteorological data.

Monteith (1965) considered vegetation to be represented by a "big leaf" model and modified the Penman equation to include an additional resistance to vapour flow due to the surface resistance of the vegetation. This is commonly termed the Penman Monteith equation.

The derivation of the Penman Monteith equation will be considered here, together with the underlying assumptions involved. The derivation will closely follow that given by Shuttleworth (1979).

A simplified derivation following Chapman (1979) is given in Appendix A.

Evaporation occurs when water is converted from the liquid phase to the vapour phase and is then transferred into the atmoshphere. For this process to occur an input of energy is required. The rate of evaporation is then controlled by the rate at which this energy, stored in water vapour can diffuse away from a surface.

An analogy with electrical resistance can be used to conveniently express the molecular and turbulent diffusion that occurs at different stages of the transfer path.

Evaporation from a natural surface can hence be expressed on a physical basis by models which describe the effects of molecular and turbulent diffusion resistances on the partition of the available energy.

Here the basic physical concepts of available energy diffusion and turbulence will be outlined, and then they will be combined to form the Penman Monteith equation.

2.2 Energy

2.2.1 Latent Heat

In the liquid phase strong intermolecular forces act between water molecules keeping them at a separation of just over one molecular diameter.

As this separation increases, the attractive force decreases as illustrated in Figure 3. In the vapour phase the molecules are about ten or more molecular diameters apart and hence attractive forces are much smaller.

Thus to change water from a liquid to a vapour, work must be done against the attractive forces. The amount of energy required is directly relatcd to the number of molecules, which is in turn directly related to the mass of water involved.

This amount of energy required per unit mass of liquid water is called the latent heat of vaporisation of water, λ, and at $10^{o}C$ is 2.47×10^{6} JKg^{-1}. This changes by about 0.1% per ^{o}C because the initial separation of the molecules making up the liquid varies with temperature. As this variation is only small it is taken to be a constant.

The amount of energy transferred away from a surface in evaporation is numerically equal to the product of the mass flow (i.e. the evaporation E, in kg $m^{-2}s^{-1}$) and the latent heat of vapourization, λ. This energy flow is denoted λE.

2.2.2 Liquid-Vapour Transfer at a Water Surface

For water vapour to form there must be an exchange of water molecules with a free water surface somewhere within the system being considered.

In wet conditions this surface could be on the surface of the vegetation or soil, while under dry conditions it could be within the vegetation or soil.

Figure 4 schematically shows the exchange of individual water molecules at the liquid vapour interface.

At the water surface the energy of any water molecule has been found to be dependent on the surface temperature of the liquid Ts.

The number of molecules with energy greater than a particular value ε is given by

$$N_\varepsilon = \exp(-\varepsilon/k'Ts) \qquad (1)$$

where Ts = surface temperature (^oK)
k' = Boltzman's constant.

For a molecule to leave the surface it must have an energy greater than (λ/n), where n is the number of molecules per unit volume of liquid water. The rate at which molecules leave the surface is thus given by

$$\beta = k_1 \exp\left(\frac{-\lambda/n}{k' Ts}\right) \qquad (2)$$

where k_1 = constant

Molecules in the vapour above the liquid approach the surface at a rate, n, which is dependent on the vapour pressure, e, of the water vapour in contact with the surface.

A fraction, r, of these water vapour molecules are immediately reflected on collision with the surface while the remaining fraction, (1-r), are absorbed.

The number of molecules absorbed per unit time is given by

$$n\,(1-r) = k_2\,(1-r)\,e \qquad (3)$$

where k_2 = constant

The net evaporation rate, E, is given by the difference between these two rates, ie.

$$E = k_1 \exp\left(\frac{-\lambda/n}{k' Ts}\right) \quad k_2\,(1\ r)\,e \qquad (4)$$

2.2.3 Saturation

If evaporation occurs within a closed system at a rate E, then as molecules leave the surface the concentration of the water vapour and its equivalent vapour pressure (e) increase until such times as the two rates in equation (4) are equal and there is no longer any evaporation (E=0).

The air is then said to be saturated and cannot absorb any more water molecules. At a given temperature this situation occurs at a particular vapour pressure, the saturation vapour pressure, e_s.

Thus substituting E=0 into equation (4) and rearranging gives

$$e_s = (k_1/(k_2\,(1-r)))\ \exp\left(\frac{-\lambda/n}{k' Ts}\right) \qquad (5)$$

So e_s is a unique function of Ts and can be measured experimentally.

Figure 5 shows the variation of e_s with Ts

The gradient of this relationship is given by

$$\Delta = (e_s (T_2) - e_s (T_1))/(T_2-T_1) \quad (6)$$

where T_1, T_2 are temperatures.

Mills (1975) made a comparison of some formulae for the calculation of saturation vapour pressure and found that a 5th order polynomial provided the best accuracy and was the most efficient for a computer formulation.

The equation given was

$$e_s = \sum_{i=0}^{5} a_i T^i \text{ (mb)} \quad (7)$$

where $a_0 = 6.10671$
$a_1 = 0.44425$
$a_2 = 0.014221$
$a_3 = 2.7091 \times 10^{-4}$
$a_4 = 2.7411 \times 10^{-6}$
$a_5 = 2.7256 \times 10^{-9}$

T = temperature ^{o}C

and thus

$$\Delta = \sum_{i=0}^{5} i a_i T^{i-1} \quad (8)$$

This was based on a least squares fit over the range $5^{o}C$ to $40^{o}C$.

2.2.4 Sensible Heat

Large quantities of the energy input to a surface are exchanged between the surface and the atmosphere by thermal conduction and thermal convection and hence is not available for evaporation.

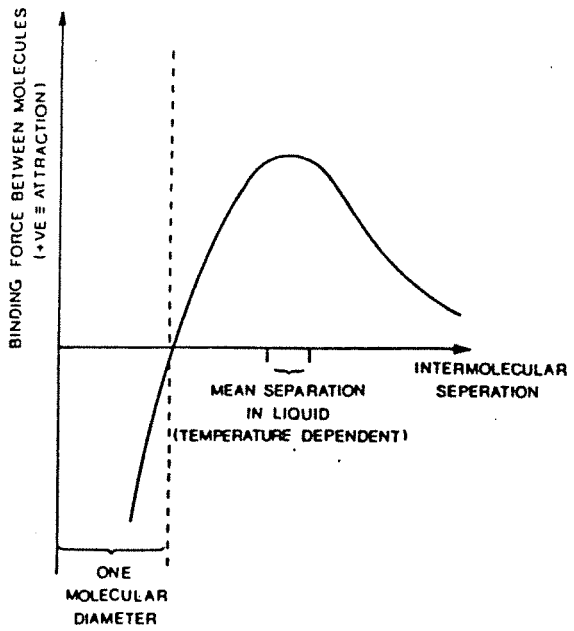

FIGURE 3

SCHEMATIC DIAGRAM OF THE ATTRACTIVE FORCE BETWEEN WATER MOLECULES AS A FUNCTION OF THE SEPARATION BETWEEN THEM

Shuttleworth,(1979)

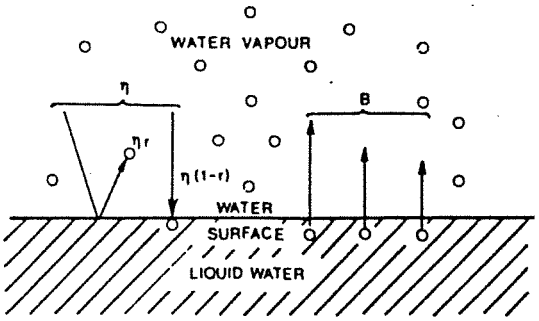

FIGURE 4

SCHEMATIC DIAGRAM OF THE EXCHANGE OF WATER MOLECULES BETWEEN LIQUID WATER AND WATER VAPOUR. B IS THE RATE AT WHICH MOLECULES 'BOIL OFF' FROM THE SURFACE: η IS THE RATE AT WHICH THEY COLLIDE WITH THE SURFACE; A FRACTION r ARE REFLECTED ON COLLISION

Shuttleworth,(1979)

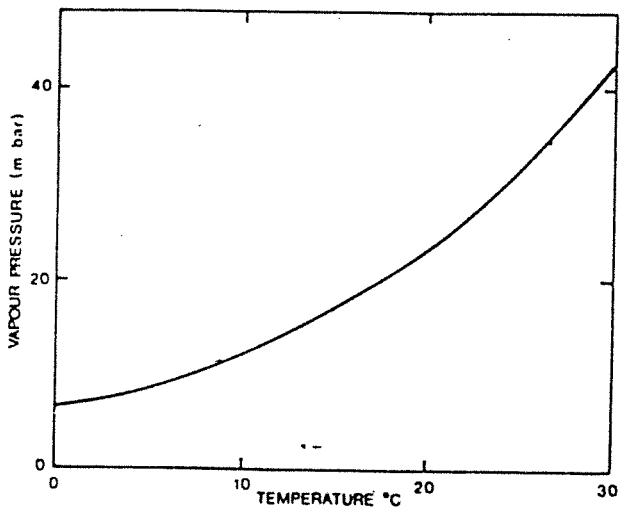

FIGURE 5

VARIATION OF SATURATED VAPOUR PRESSURE WITH TEMPERATURE

Shuttleworth,(1979)

Close to the surface thermal conduction is dominant, while further from the surface and of more importance, thermal convection is the primary exchange mechanism.

Thermal convection occurs when mass motions of the air result in the transport and mixing of the heat content of the air between different levels in the atmosphere.

The flow of energy between the surface and the atmosphere by the combined processes of thermal conduction and thermal convection is known as "sensible" heat flux because it is the transfer which determines air temperature, a property of the air that we can "sense".

In the daytime, when the ground is generally hotter than the atmosphere, the flux of sensible heat is commonly away from the surface. At night however the flux is generally towards the surface as it supports the outward flux of radiation as shown in Figure 9.

If the surface of the vegetation is wet, the evaporation rate is often very high, particularly for tall vegetation, and even during the day can exceed the energy reaching the surface as radiation. In such situations there will be an inward flux of sensible heat to provide the additional energy requirement.

2.2.5 Radiation

The sun provides a radiant energy input to the earth equivalent to that of a black body at 6000 K.

After being modified by its transit through the atmosphere the radiation becomes confined to short wavelengths in the band 0.3 to 3 μm, and forms the total short wave energy input, S_T.

A significant part of this short-wave energy S_D, reaches the ground in a diffuse or non-directional form after scattering. This fraction is typically 15 to 25% in clear sky conditions, and approaching 100% in overcast conditions.

Appendix B gives the method of Fleming (1971) for the calculation of the short-wave radiation reaching a surface on a clear day.

Part of this short-wave radiation reaching the ground is reflected by the surface. The fraction reflected, termed the "albedo" is dependent on the angle of incidence of the solar beam and the type of surface.

There is an additional exchange of energy between the surface and the atmosphere in the form of long-wave radiation (3 to 100 μm).

This radiation arises from "black body" radiation from the surface and the atmosphere. There is generally a net loss of energy from the earth's surface in the form of long-wave radiation.

The balance of outgoing L_u, and incoming L_b, long-wave radiation, often termed the back radiation R_B, is governed by atmospheric temperature, humidity and cloudiness and is given by Wiesner (1970) as

$$R_B = \theta\, T_a^4\, (0.56 - 0.09\, e_a^{1/2})(0.1 + 0.9\, n/N) \qquad (9)$$

where θ = Stephans constant
T_a = air temperature (^oK)
e_a = water vapour pressure at T_a (mm Hg)
n/N = ratio of actual to possible hours of bright sunshine for locality and date.

Linacre (1975) denotes the outgoing radiation, L_u, as terrestrial radiation and estimates it from:

$$L_u = AT^4 \ (cal/cm^2\ min) \qquad (10)$$

where $A = 8.13 \times 10^{-11}$
T = air temperature (^oK)

and denotes the incoming radiation, L_d, as sky radiation. An estimate of R_B is given by

$$R_B = 32 \times 10^{-5} (1+4\ n/N)(100-T)\ (cal/cm^2 min) \quad (11)$$

where T = air temperature (^oC)

Baumgartner (1967) gives

$$L_u = \varepsilon\ \theta\ T^4 \quad (12)$$

where T = surface temperature (^oK)
θ = 8.26×10^{-10} (cal cm^{-2} min^{-1} deg^{-4})
ε = emissivity
= 0.97 for forests
= 0.96 for meadows
= 0.95 for arable lands
= 0.93 for bare soil

Estimates of the sky radiation were investigated by Anderson (1952) in a study of evaporation from Lake Hefner. He found that although sky radiation (or atmospheric radiation) is a function of many variables such as the distributions of moisture, temperature, ozone and carbon dioxide, most estimates of L_D were made only from the air temperature and humidity near the place of observation. The formulas developed are thus considered only to be empirical and agree only statistically with actual observations. For a clear sky these formulas are of the form,

$$L_D = \theta T^4 (a-b(\exp(-\gamma e_a))) \quad (13)$$

$$L_D = \theta T^4 (a+b \sqrt{e_a}) \quad (14)$$

$$L_D = \theta T^4 (aP-be_a)/T_a \quad (15)$$

$$L_D = \theta T^4 (a+b \log e_a) \quad (16)$$

where a, b, γ = constants
θ = Stephan's constant
T_a = air temperature near ground (^oK)
e_a = vapour pressure of air near ground
p = air pressure near ground

If clouds are present then the sky radiation is increased by the additional radiation emitted by water and ice particles at the bottom of the clouds. Low clouds emit more radiation than high clouds, the former being generally warmer and denser than the latter.

The extent of cloud cover also has an influence on the radiation. As the amount of radiation from the central part of the sky is more dominant clouds near the horizon do not influence radiation as much as clouds in the central part of the sky.

T.V.A. (1972) accounts for the influence of cloudiness by an expression of the form

$$q_{ac} = q_a (1 + KC^2) \qquad (17)$$

where q_{ac} = sky radiation from cloudy sky
q_a = sky radiation from clear sky
K = factor depending on type of cloud and cloud height (Table 2.1)
C = part of sky covered by clouds in tenths of the total sky.
CFAC = $(1+KC^2)$ = cloud factor

For time periods less than a day, K is also a function of solar altitude, α.

TABLE 2.1. Factor K in formula for Sky Radiation from a Cloudy Sky.

Cloud Type	K
Cirrus	0.04
Cirrostratus	0.08
Attocummulus	0.17
Altostratus	0.20
Cummulus	0.20
Stratus	0.24

The relationships between the cloud factor, CFAC, and the cloud amount are shown in Figure 6.

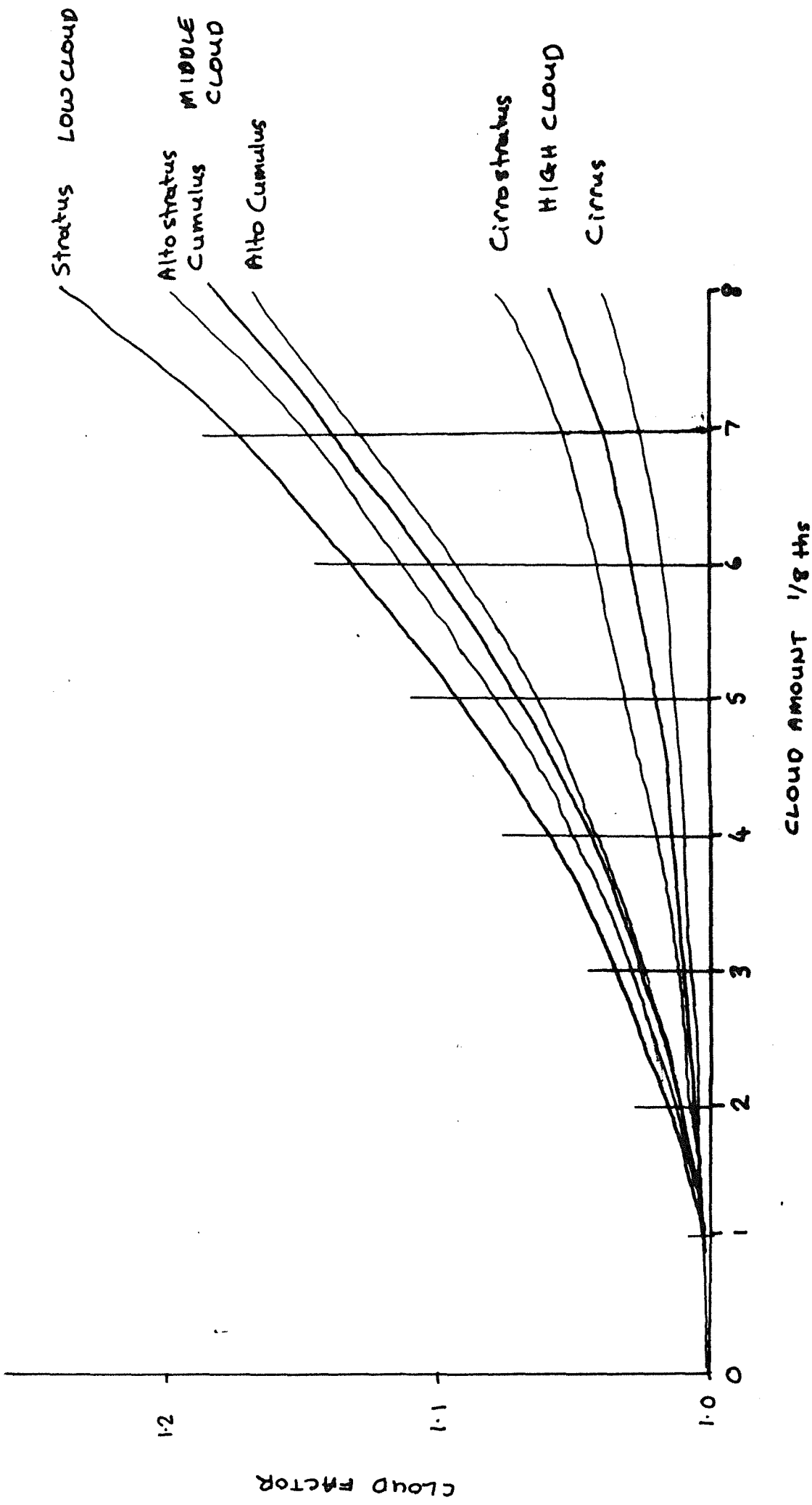

FIGURE 6 Cloud Factor

For simplicity, the cloud types have been grouped into low, middle and high cloud as given in Table 2.2 and in Figure 6.

The associated cloud factors are given in Table 2.3. These factors can be determined from cloud type and cloud amount data and be applied to clear sky estimates of L_D to give estimates for a cloudy sky.

Cloud type and amount information is generally available at 9am and 3pm each day, so factors are applied uniformly of the 12 hour period corresponding to each reading.

In periods where rainfall occurs the cloud factor is set to a value of 1.2.

Problems with the cloud amount data are described in section 3.

The need to estimate the long-wave radiation arises because the Pyranometers used by the Public Works Department only measure direct and diffuse short-wave radiation S_T (Hawkins (1983)). Net radiometers are required to remove the need to estimate the long-wave radiation component. This is further discussed in section 3.

Figure 7 illustrates schematically the radiation balance at the earth's surface. In this diagram, S_T, is the total incoming short-wave solar radiation in direct and diffuse forms as recorded by the W.A.W.A. S_R is that short-wave radiation immediately reflected at the surface, while L_D and L_u are respectively the downward (sky) long-wave radiation and the upward (terrestrial) long-wave radiation from the surface.

For lack of a better model for short term simulations, Schofield (1982) related net radiation R_N to solar radiation, S_T, by an equation of the form

$$R_N = \delta_n S_T \qquad (18)$$

where δ_n = constant = 0.83

TABLE 2.2 Cloud Type Groupings

Low Cloud	(surface to 2500m)
Cumulonimbus	(Cb)
Cummulus	(Cu)
Stratocumulus	(Sc)
Stratus	(St)
Fractostratus	(Fs)
Middle Cloud	(2500m to 6000m)
Altostratus	(As)
Nimbostratus	(Ns)
Altocumulus	(Ac)
High Cloud	(> 6000m)
Cirrocumulus	(Cc)
Cirrostratus	(Cs)
Cirrus	(Ci)

TABLE 2.3 Cloud Factors

Cloud Factors CFAC

Cloud Amount C (1/8ths)	Low Cloud	Middle Cloud	High Cloud
0	1.000	1.000	1.000
1	1.000	1.000	1.000
2	1.016	1.012	1.008
3	1.036	1.028	1.008
4	1.060	1.044	1.016
5	1.096	1.072	1.020
6	1.134	1.106	1.030
7	1.176	1.140	1.042
8	1.240	1.186	1.060

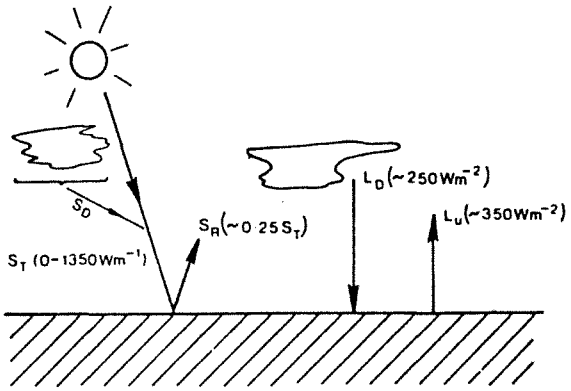

FIGURE 7

SCHEMATIC DIAGRAM OF THE RADIATION BALANCE AT THE EARTH's SURFACE. S_T IS THE TOTAL SHORTWAVE RADIATION, OF WHICH S_D IS THE DIFFUSE COMPONENT; S_R IS THE REFLECTED SHORTWAVE RADIATION, WHILE L_D AND L_u ARE THE INCOMING AND OUTGOING COMPONENTS OF LONGWAVE RADIATION

Shuttleworth, (1979)

δ_n is meant to account for both albedo effects and back radiation effects. The limitations of this simple approach is that at night when S_T becomes zero, it is implied the net radiation R_N is zero.

This is not so as there will always be long-wave radiation emitted by the surface and the atmosphere and hence in some cases an important source or sink of energy is being omitted.

This effect is not important for time scales greater than a day, but for shorter time scales as used here, it is very important to get the correct diurnal variation in the available energy from radiation R_N.

For the modelling work here the terrestrial radiation, L_u, is estimated from the approach of Baumgartner (1967) using equation (12) with an average value of emissivity, ε, equal to 0.96. ie.

$$L_u = 0.96\ \theta T_a^4 \qquad (19)$$

where $\theta = 5.6697 \times 10^{-8}$ $(W/m^{2o}K^4)$
T_a = air temperature (^oK)

The constant arises because the body emitting the radiation is not a true black body but is a "grey body" and hence emits less radiation.

The sky radiation is evaluated for clear sky conditions using the Idso-Jackson formula T.V.A. (1972).

$$L_D = \theta Ta^4\ (1-c\ \exp(-d(273-T_a)^2)) \qquad (20)$$
$\theta = 5.6697 \times 10^{-8}$ $(W/m^{2o}K^4)$
T_a = air temperature (^oK)
$c = 0.261$
$d = 7.77 \times 10^{-4}$ $(^oK^{-2})$

This empirical equation was developed on clear sky data from Phoenix, Arizona, Australia, the Indian Ocean and Point Barrow, Alaska.

Idso and Jackson (1969) thus concluded that the relationship holds for any latitude and any natural air temperature.

The effect of the additional long-wave radiation from clouds is included by multiplying equation (20) by the cloud factor, CFAC, defined in equation (17) and in Table 2.3.

Thus the net long-wave radiation is formulated as

$$R_B = L_u - L_D \tag{21}$$

where L_u is given by equation (19) and L_D by CFAC times equation (20) ie

$$R_B = 0.96\theta T_a^4 - CFAC\ \theta T_a^4 (1 - c \exp(-d(273 - T_a)^2)) \tag{22}$$

where $\theta = 5.6697 \times 10^{-8}$ $(W/m^2{}^oK^4)$

T_a = air temperature (^oK)

CFAC= cloud factor from Table 2.3

$c = 0.261$

$d = 7.77 \times 10^{-4}$ $(^oK^{-2})$

The total net radiation then becomes

$$R_N = S_T (1 - r) - R_B \tag{23}$$

where S_T = measured direct and diffuse short-wave solar radiation (W/m^2)

r = albedo

R_B = net back radiation (W/m^2)

The albedo, r, is a variable factor depending on surface conditions and must be selected from the estimates considered most appropriate.

Values of albedo are given by T.V.A. (1972) and are listed in Table 2.4. The value of albedo for a water surface is a function of solar altitude α, and cloud cover and type. Appendix C gives the procedure for calculating the albedo of a water surface.

TABLE 2.4 Values of Albedo
(after T.V.A. (1972))

Condition	albedo
Meadows and Fields	0.14*
Leaf and Needle Forest	0.07-0.09*
Dark, Extended Mixed Forest	0.045*
Heath	0.10*
Flat Ground, grass covered	0.25-0.33
Flat Ground, rock	0.12-0.15
Sand	0.18
Vegetation in Early summer, Leaves with high water content	0.19
Vegetation in Late Summer, Leaves with low water content	0.29
Fresh Snow	0.83
Old Snow	0.42-0.70

* may be too low

2.2.6 Heat Storage

The most dominant form of heat storage when considering a ground surface is from the heat flux, G, into the soil. This depends to a large extent on the shading of the soil surface by plant canopies.

The amount of energy transferred into a soil surface is dependent on the type of plant canopy as shown in Figure 8. In this diagram the total histogram area for each cover type represents the net radiation available at the soil surface. The smaller histograms are proportional to soil heat flux in each cover type.

In the consideration of short term variations, G is important, but on an annual or daily basis the soil heat flux is usually not of interest as its net value tends toward zero.

Soil heat flux can be measured using transducers placed below the soil surface at a depth of about 5cm.

Rouse and Wilson (1972) used three transducers at a depth of 5cm and connected them in series to measure soil heat flux. Soil heat flux was then calculated at the surface by

$$G = G_Z + C.\Delta Ts/\Delta\dagger.\Delta Z \qquad (24)$$

where G_Z = measured soil heat flux at 5cm depth
C = heat capacity of the soil
$\Delta Ts/\Delta t$ = change of soil temperature with time (1 hr) in the layer Δz between the soil surface and the transducer.

The heat capacity, C, of the soil was found from

$$C = C_m X_m + C_o X_o + C_w \theta \qquad (25)$$

where C_m = heat capacity of soil mineral matter
C_o = heat capacity of soil organic matter
C_w = heat capacity of water
X_m = volume fraction of mineral matter
X_o = volume fraction of soil matter
θ = volume fraction of water

Data from Southern Ontario for a sweet corn plot on sandy loam gave

$X_m = 0.459$
$X_o = 0.024$

hence reducing equation (25) to

$$C = 0.225 + C_w\theta$$

Moisture content of the surface layer was determined gravimetrically from samples in the morning at the site and it was assumed to stay constant through the day.

Where soil heat flux measurements are not made, then some estimates can be made if required.

Linacre (1975) noted G is practically zero over a day or longer but suggested it could be estimated if the temperature gradient variation at the soil surface were known, by;

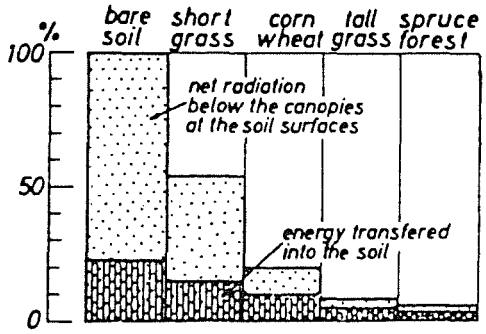

FIG. 8 Heat flux into the soil as a function of net radiation at the soil surface beneath plant canopies, in percent of the net radiation above the canopies ($S = 100$ percent).

Baumgartner (1967)

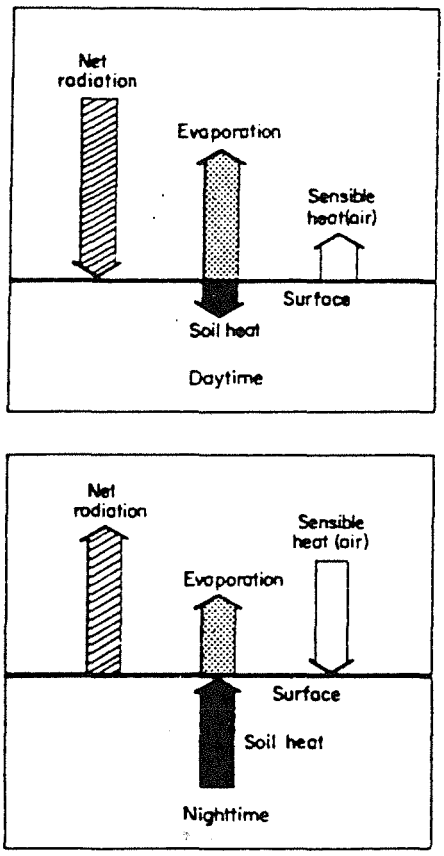

FIG. 9 Schematic representation of the daytime and nighttime energy balance.

$$G = -k^1 \partial T/\partial Z$$
$$= \sqrt{2}\ (CK/D)\ To \sin (wt + \Pi/4) \qquad (26)$$

where k^1 = thermal conductivity of the surface soil
$\partial T/\partial z$ = temperature gradient of the soil surface
C = thermal capacity = ρS
ρ = soils density
S = soils specific heat
K = thermal diffusivity
D = damping depth
To = amplitude of surface temperature variations
w = frequency of surface temperature changes
t = time

If temperature gradients are not known then estimates of G from R_N can be made. The limitations are however that if R_N only includes short-wave radiation, then at night R_N will be zero and hence G will be zero. This is not the case as seen in Figure 9.

Hicks (1973) found G to lie in the range $R_N/4$ to $R_N/8$ and used these to give an error band for estimates of Potential Evaporation. Using measured data, the ratio of G/R_N for soils was found to peak at 0.22 at noon and dropped to 0.11 near dawn and dusk.

In the study here for soils and vegetation, G will be neglected although it is recognised that it is significant during the night.

If a water body is being considered, then G represents the flux of heat into the water body.

Black and Rosher (1980) in a study of the Peel Inlet found that for a shallow water body, unacceptably high values of evaporation are calculated if the subsurface flux, G, is neglected. G can be measured in this case with a modified soil flux plate, but in the absence of such an instrument it can be estimated from water temperature changes.

An average value can be found using the heat equation

$$H = mC\Delta T \quad (27)$$

where H = heat (J)
m = mass of water (g)
C = specific heat of water ($J/g^{o}C$)
ΔT = change in temperature (^{o}C)

Furthermore

$$m = v\rho = dA\rho \quad (28)$$

where V = volume of water (cm^3)
ρ = density (g/cm^3)
d = depth of water (cm)
A = unit area ($1cm^2$)

Thus

$$H = dA\rho\ C\Delta T \quad (29)$$

and

$$G = \frac{H}{At}$$

$$= \frac{d\rho C\Delta T}{t} \quad (30)$$

where G = (W/cm^2)
d = (cm)
ρ = (g/cm^3)
ΔT = (^{o}C)
t = (sec)

Thus by monitoring the water temperature changes the value of G can be estimated.

Additional storages neglected in the modelling here are Physical Storage and Biochemical Storage. (Schofield (1982)).

2.3 Diffusion

2.3.1 Basic Concept

Diffusion is the random exchange of molecules or groups of molecules between adjacent positions.

Such movement takes place when there are variations in particular entities from one position to the next. For a particular volume of fluid these entities may be its heat content, momentum content or the concentration of its consistuent parts. If the concentration of an entity at two positions is different, then there will be a net transfer, or flow, in response to the different concentration.

2.3.2 Molecular Diffusion

The process of molecular motion in air is extremely rapid. Molecules have a root mean square velocity of about 500 ms^{-1} and a mean free path between collisons of about 5×10^{-8}m.

This molecular agitation is responsible for molecular diffusion, the rapid movement being responsible for the transfer, while the high collision rate ensures rapid equilibrium of molecules with new conditions at each location.

The rate of transfer of momentum, heat and vapour, those entities of most relevance to evaporation, are proportional to their gradients of concentration.

Consider for example the transfer of water vapour expressed as a mass flux per unit area, E,

$$E = -D_v \frac{\partial X}{\partial Z} \qquad (31)$$

where D_v = molecular diffusion coefficient of vapour (m^2/s)

$\frac{\partial X}{\partial Z}$ = water vapour concentration gradient

Similarly the rate of heat transfer H per unit area is related to the gradient of its heat capacity by

$$H = -D_h \frac{\partial(\rho C_p T)}{\partial Z} \qquad (32)$$

where D_h = molecular diffusion coefficient of heat (m^2/s)

ρC_p = volumetric heat capacity

ρ = density of air

C_p = specific heat

T = air temperature

Also if u is the velocity of air perpendicular to the z axis, then the air possesses momentum in this plane with a concentration, ρu, and there can be a momentum transfer, giving rise to a viscous force or shearing stress per unit area, τ, where

$$\tau = D_m \frac{\partial(\rho u)}{\partial Z} \qquad (33)$$

where D_m = molecular diffusion coefficient of momentum (m^2/s)

As the same process is responsible for all three of these transfers, the diffusion coefficients, D_v, D_h and D_m are similar in size, around 0.18 m^2/s, and all increase by about 0.7% per degree celcius at normal temperatures.

The flow of latent heat is generally used to represent the evaporation rate, thus equation (31) is usually rewritten in terms of the latent heat flux, λE, which is related to the atmospheric vapour pressure gradient $\partial e/dz$ by

$$\lambda E = -\frac{\rho C_p}{\gamma} D_v \frac{\partial e}{\partial Z} \qquad (34)$$

where γ = psychrometric constant

$$= \frac{C_p . P}{\varepsilon \lambda} \qquad (35)$$

= 0.66 $mb\,^oC\text{-}1$ at 20°C and 1000mb

C_p = specific heat of air ($J\ kg^{-1}\ ^oC^{-1}$)

p = atmospheric pressure (mb)

λ = latent heat of vaporisation (Jkg^{-1})

ε = water air molecular ratio = 0.622

e = vapour pressure of air (mb)

Assuming no spatial variation in the density of the air, ρ, equations (32) and (33) can be approximated by

$$H = -\rho Cp\ D_H\ \partial T/\partial Z \qquad (36)$$

$$\tau = \rho\ D_m\ \partial u/\partial Z \qquad (37)$$

As Δ, λ and hence γ are functions of temperature, Saxton (1972) combined these as a single function of temperature to simplify calculations, by

$$\Delta/\gamma = 0.672 + 4.28 \times 10^{-2} T + 1.13 \times 10^{-3} T^2 + 1.66 \times 10^{-5}\ T^3 + 1.70 \times 10^{-7}\ T^4 \qquad (38)$$

where Δ = gradient of saturated vapour pressure curve (mb $^oC^{-1}$)

γ = psychrometric constant (mb $^oC^{-1}$)

T = air temperature (^oC)

This simplification will be used in the derivation of the Penman Monteith equation to follow.

2.4 Turbulence

2.4.1 Introduction

When wind blows over a natural surface it is retarded by an interaction with the surface, which gives rise to an apparently random and haphazard movement of air above the surface.

This phenomenon, known as turbulence, is initiated by the non uniformity at the surface, and propogates upwards into the atmosphere. The turbulent mixing that is generated provides an efficient mechanism for the transfer of entities through the atmosphere, away from the surface, far more efficiently than simple molecular diffusion.

Turbulence is the primary process responsible for the exchange of mass, momentum and heat between air close to the surface and air at higher levels in the atmosphere.

Although much of the turbulence is generated by frictional retardation of the wind, its transfer properties can either be enhanced or diminished, if there is a gradient in mean air temperature away from the surface.

In the absence of any wind, then turbulent transfer would occur by free convection if a temperature gradient existed. This is known as "free convection".

The combined processes of frictional turbulence and free convection are generally known as "mixed convection".

Usually this situation is treated theoretically with frictional turbulence being considered the primary transfer mechanism and semi-empirical corrections being made for the effects of free convection.

In the situation of a "neutral" atmosphere, it is assumed no temperature gradient exists and hence only frictional turbulence occurs.

2.4.2 Forced Convection

In general, the windspeed u(z) measured at a height z above an extensive horizontal surface, uniformly populated with roughness elements, usually vegetation, is found to increase logarithmically with (z-d) in neutral conditions, as illustrated in Figure 10.

The zero plane displacement, d, is generally regarded as a constant which is a characteristic of the surface cover, although Sceicz and Long (1969) suggest that it may vary with windspeed.

The zero plane displacement has been found to vary with both the height of the roughness elements, h, and their spacing. Various authors have given values of d as a function of h. Some of these are given in Table 2.5.

The empirical observation of a logarithmic wind profile can be expressed formally as

$$u(z) = k_3 \, (\ln(z-d) - \ln (z_o)) \qquad (39)$$

where z_o, the roughness length is also taken as a characteristic of the surface.

Both d and z_o can be found by fitting the assumed windspeed profile to experimental measurements of windspeed profiles measured in the field (Riou, 1984).

This was done on limited windspeed data available above the forest canopy at Ernies and gave d = 0.62h and z_o = 0.1h. This is presented in Appendix D.

Such estimates must be made when there is no temperature gradient and is thus very difficult. Estimates of z_o vary as given in Table 2.5.

The transfer of momentum by turbulent diffusion can be described similarly to molecular diffusion, ie.

$$\tau = K_M \, \partial u/\partial Z \qquad (40)$$

where K_M = eddy diffusivity for momentum.

TABLE 2.5 Roughness length and zero plane displacements

Author	d	z_o
Cowan (1968)	0.64h	0.13h
Jarvis et al (1976)	0.7h	0.1h
Leuning and Attiwill (1978)	0.7h	0.1h
Schofield (1983)	0.75h	0.1h
Tajchman (1971)	0.7h	0.09h
Hicks et al (1975)	0.8h	0.06h
Monteith (1973)	0.63h	0.13h

h = vegetation height

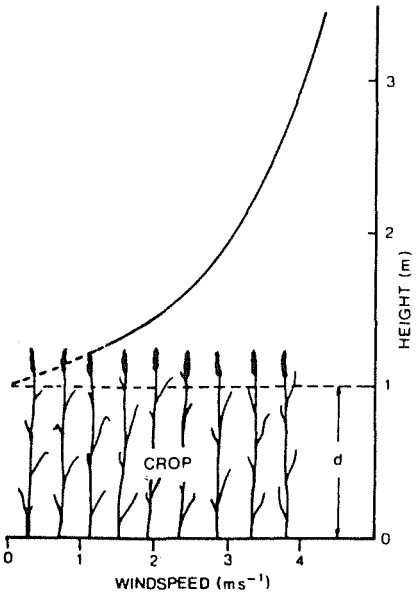

FIGURE 10

SCHEMATIC DIAGRAM OF THE VARIATION IN MEAN WINDSPEED OBSERVED OVER AN EXTENSIVE, UNIFORM STAND OF VEGETATION IN NEUTRAL CONDITIONS.

Shuttleworth,(1979)

The eddy diffusivity is analogous to the molecular diffusion coefficient.

The turbulent boundary layer through which the turbulent exchange takes place is defined as the height range through which the shear stress, τ, is constant.

Equations (39) and (40) applied in this boundary layer require that K_m must be proportional to (z-d) viz.

$$K_m = k_4 (z-d) \tag{41}$$

Thus it follows from equations (39), (40) and (41) that

$$\tau = k_3 k_4 \tag{42}$$

where the product $(k_3 k_4)$ has dimensions of $(\text{velocity})^2$. It is usual to rewrite this product as u_*^2, with u_* called the frictional velocity.

In order that this equivalence should always be valid, it is necessary for k_3 and k_4 to be proportional to u_* and that they should be reciprocals, i.e.

$$k_4 = k u_* \tag{43}$$

$$k_3 = u_*/k \tag{44}$$

and hence it follows

$$\tau = \rho u_*^2 \tag{45}$$

while equation (39) becomes

$$u(z) = u_*/k \ln ((z-d)/z_o) \tag{46}$$

k is a constant assumed independent of the surface and is termed Von Karman's constant, and is usually assigned a value 0.41.

It follows from equations (41) and (43) that the turbulent transfer coefficient, K_m, is given by

$$K_m = K u_* (z-d) \qquad (47)$$

or from equation (46)

$$K_m = k^2 (z-d) \partial u/\partial(\ln (z-d)) \qquad (48)$$

which can be determined from the logarithmic gradient of the measured wind profile, once d is known.

Similar to the definition of eddy diffusivity for momentum transfer (K_m), as given by equation (40), it is possible to define similar entities for the turbulent transfer of sensible heat and latent heat from the equations

$$H = -\rho C_P K_H \partial T/\partial Z \qquad (49)$$

and

$$\lambda E = -\rho \frac{C_P K_V}{\gamma} \partial e/dz \qquad (50)$$

which have an obvious analogy with the molecular diffusion equations, (34), (36) and (37).

The turbulent transfer mechanism responsible for the exchange of all these entities is considered the same and hence it is usual to assume $K_m = K_h = K_v$ are the same over the height range of the near-surface turbulent boundary layer. This is only provided there is no temperature gradient away from the aerodynamically rough surface.

2.4.3 Mixed Convection

If a temperature gradient exists away from the surface then the transfer by forced convection will be modified by free convection.

When air temperature decreases with height, then any parcel of air created at the surface and moved upward by forced convection, will tend to continue to rise because it will be warmer and lighter than the air into which it has moved. This situation is described as an unstable atmosphere.

On the other hand, when temperature increases with height, upward motion is retarded and the atmosphere is said to be stable.

The behaviour of the turbulent transfer mechanism in stable and unstable conditions differs from forced convection in neutral conditions. It is usual to empirically describe these differences in terms of parameters which reflect the relative efficiency of the free and forced convection mechanisms.

Free, or bouyancy generated, turbulent transfer is related to the square of the windspeed gradient and is generally accounted for by a dimensionless parameter, the Richardson number R_i,

$$R_i = \frac{g}{T} \frac{\partial T}{\partial Z} \Big/ \left(\frac{\partial u}{\partial Z}\right)^2 \qquad (51)$$

where g = acceleration due to gravity (m/s^2)
T = temperature (^oK)

In stable conditions R_i is positive, and in unstable conditions R_i is negative.

Webb (1975) also gives the Obukhov length, L, as useful in classifying stability.

$$L = -u_*^3 \, CpT/(kgH) \qquad (52)$$

It is noted that strictly the bouyancy effect of water vapour should be included by replacing the heat flux H by H + 0.07 E and the temperature gradient dT/dz by T/dz + 0.07 (λ/Cp) dq/dz, where q is the specific humidity. This correction is rarely used.

The transfer coefficients for momentum (equation (47)), sensible heat and latent heat can be redefined for a general mixed convection situation by

$$K_m = ku_* (z-d)\Phi_m \tag{53}$$

$$K_h = ku_* (z-d)\Phi_h \tag{54}$$

$$K_v = ku_*(z-d)\Phi_v \tag{55}$$

where the functions Φ_m, Φ_b and Φ_v modify the forced convection to describe the mixed convection situation.

In stable conditions the best available data indicates an inter relationship of the form

$$\Phi_v = \Phi_h = \Phi_m = (1-5\ R_i)^{-1} \tag{56}$$

where R_i is positive, while in unstable conditions where R_i is negative

$$\Phi_v = \Phi_h = \Phi_m^2 = (1-16\ R_i)^{-1/2} \tag{57}$$

These factors are included via equations (53), (54) and (55) as empirical corrections to the one dimensional diffusion equations (40), (49) and (50).

Riou (1984), gives a modified wind profile that accounts for deviations from the logarithmic shape, due to mixed convection and atmospheric instability by

$$u(z) = \frac{u_*}{k} \left(\ln \left(\frac{z-d}{z_o}\right) + 4L^{-1} (z-d)\right) \tag{58}$$

where L is the Obukhov length, which is negative in this case.

In the application and derivation of the Penman Monteith equation to be used here, only neutral conditions and hence only forced convection will be considered and accounted for.

To account for mixed convection then temperature gradient measurements are required, and this means a mimimum of two temperature profile readings. At present no such data is available.

2.5 Resistance

2.5.1 Introduction

A useful simplification can be gained by applying the differential diffusion equations in an integraded form.

In cases where the (one dimensional) flux can be considered as a constant, this integration becomes very straight forward.

Equation (34) which describes the molecular diffusion of latent heat between two points at which the vapour pressures are el and e2 respectively is

$$E = \frac{C_p D_V}{\gamma} \frac{\partial e}{\partial Z} \qquad (34)$$

which in integrated form is

$$E = -\frac{\rho C_P}{\gamma} (e_2 - e_1) \Big/ \int_{Z_1}^{Z_2} dz/Dv \qquad (59)$$

where γ = psychrometric constant

C_P = specific heat of air

ρ = density of air

D_V = molecular diffusion coefficient of vapour (latent heat)

This integration is independent of the detailed mechanism responsible for the diffusion.

Similarly the turbulent transfer equation for latent heat

$$\lambda E = -\frac{\rho C_p}{\gamma} K_V \frac{\partial e}{\partial z} \qquad (50)$$

can be integrated to give

$$\lambda E = -\frac{\rho C_p}{\gamma} (e_2 - e_1) / \int_{Z_1}^{Z_2} dz/Kv \qquad (60)$$

where K_v = eddy diffusivity for latent heat.

Equations (59) and (60) have a similarity to Ohm's law for electrical current,

$$i = \frac{V}{R} \qquad (61)$$

where i = current
V = potential difference
R = resistance

Based on this analogy the entities

$$[\int_{Z_1}^{Z_2} d_z/D_v] \quad \text{and} \quad [\int_{Z_1}^{Z_2} d_z/K_v]$$

are termed the 'resistances' in these equations.

Similar resistances can be defined for the transfer of both momentum and sensible heat.

The use of the concept of resistances in models of the exchange between a surface and the atmosphere allows a description which is mathematically similar at each stage in the transfer path. However the mechanism changes from molecular diffusion close to the surface to turbulent diffusion in the atmospheric boundary layer.

Each physical process can be considered here in terms of an equivalent resistance.

2.5.2 Atmospheric Resistance

The eddy diffusivities K_m, K_h, K_v are used to describe the turbulent transfer away from an aerodynamically rough surface.

The equivalent resistances for these transfers between any two levels z_1 and z_2 can be given

$$r_m^{1,2} = dz/K_m(z) \tag{62}$$

$$r_h^{1,2} = dz/K_h(z) \tag{63}$$

$$r_v^{1,2} = dz/K_v(z) \tag{64}$$

When the turbulent diffusion processes between different levels in or above a bare canopy are considered, the resistances in the form of equations (62), (63) and (64) are used.

More commonly, the bulk resistance to turbulent transfer between some effective source level and the level in the atmosphere z_h where the meteorological measurements are made, is required.

This is taken to be the total turbulent transfer resistance between the reference level, z_h and (z_o+d), the level at which the logarithmic profile, extrapolated into the canopy from above, would predict zero windspeed in neutral conditions (Figure 10).

The value of the bulk transfer resistance for momentum in a neutral atmosphere is obtained by combining

$$u(z) = \frac{u_*}{k} \ln((z-d)/Z_o) \tag{46}$$

and

$$K_m = ku_*(z-d) \tag{47}$$

to give

$$K_m = \frac{k^2\, u(z)\, (z-d)}{\ln((z-d)/Z_o)} \tag{65}$$

and integrating this between (z_o+d) and z_h according to equation (62) to give

$$r_m = \frac{(\ln (z-d)/Z_o)^2}{k^2 u(z)} \qquad (66)$$

In neutral conditions it is usual to assume that the bulk transfer resistances for sensible and latent heat, r_h and r_v are equal to r_m so

$$r_h = r_v = r_m \qquad (67)$$

when $R_i = 0$

If the atmosphere is not neutral then it is necessary to take into account the stability corrections described by equations (51) to (57).

2.5.3 Boundary Layer Resistance

For sensible and latent heat, molecular diffusion through a boundary layer close to the surface of the element gives rise to a "boundary layer resistance".

In the case of momentum, the situation is different since the transfer can occur at enhanced rates as a result of additional interaction of pressure forces on the element.

Hence the boundary layer resistance for momentum, r_{bm}, is usually significantly less than for the heat fluxes, r_{bv} and r_{bh}

The effective boundary layer resistance for momentum is defined by

$$r_{bm} = \rho\bar{u}/\tau = \bar{u}/u_*^2 \qquad (68)$$

where $\bar{u}$ = mean canopy windspeed

An "excess resistance", r_b, due to the transfer of sensible and latent heat fluxes is conveniently expressed in the form of the non-dimensional parameter B^{-1} such that

$$r_b = \frac{B^{-1}}{u_*} \tag{69}$$

The size and variation of the excess resistance has been studied and it is found that it was not strongly related to the surface roughness but depends on u_*.

An empirical relationship of the form

$$B^{-1} = Cu_*^{1/3} \tag{70}$$

can be used for first approximations

$$\text{i.e.} \quad r_b = C/u_*^{2/3} \tag{71}$$

where C is of order 5.6 with u_* in units m/s.

Then if the excess aerodynamic resistance is mainly in the boundary layer, the boundary layer resistance for sensible and latent heat may be estimated from that computed for momentum using

$$\begin{aligned} r_{bh,v} &= r_{bm} + r_B \\ &= r_{bm} + Cu_*^{-2/3} \end{aligned} \tag{72}$$

2.5.4 Stomatal Resistance

The sensible heat and momentum fluxes can be considered to originate on the surface of the vegetation elements making up the canopy.

However, if the canopy is dry, the latent heat flux arises as a result of evaporation from cell walls inside the stomatal cavities within the vegetation. This escapes to the leaf surface by molecular diffusion through the stomatal pores.

Once at the surface, the water vapour can diffuse through the leaf boundary layer and then into the atmosphere along the same path as momentum and sensible heat.

This additional resistance that applies to latent heat is termed the "stomatal resistance".

In wet conditions, when the vapour source is on the surface of the vegetation, the stomatal resistance is effectively zero.

A typical leaf is usually considered small enough for temperature gradients across its surface to be ignored.

The atmosphere in the stomatal cavities within the leaf can be considered to be at saturation vapour pressure corresponding to leaf temperature.

Water potentials in leaves are rarely below -40 bars, and at this potential the equilibrium humidity is still 97% of saturation.

With this simplification it immediately follows that the flow of water vapour to the leaf surface, i.e. transpiration, can be described by

$$\lambda E = \frac{\rho Cp}{\gamma} \frac{(es(T) - e_o)}{r_{st}} \qquad (73)$$

where r_{st} = stomatal resistance
T = leaf temperature
e_s = saturation vapour pressure
e_o = vapour pressure adjacent to leaf surface

2.6 Natural Evaporation

2.6.1 The Energy Budget

If an energy balance is considered over a plant community, then an amount A, termed the "available energy" will result from the balance of the energy input to the vegetation as radiation minus any energy removed in other directions other than vertically upwards, or stored somewhere within the community.

The size of the total heat flux, $(H+ \lambda E)$ from a plant community is subsequently limited to the available energy.

In general, the available energy, A, may be expressed as

$$A = R_N - D - G - J - P \qquad (74)$$

where R_N = net radiation as previously described
D = horizontal flux divergence
G = soil heat flux
J = physical storage
P = biochemical storage

The horizontal flux divergence, D, is often neglected, usually because it is difficult to estimate rather than because it is unimportant.

Ideally proper account should be taken of it in estimates, but no such account can be taken here.

The physical storage, J, is the total rate at which energy is stored within a column of unit cross-sectional area extending from the surface to the level at which R_N is being aeasured, ie

$$J = J_H + J_V + J_{veg} \qquad (75)$$

where J_H = rate of change of sensible heat in the column
J_v = rate of change of latent heat in the column
J_{veg} = rate of change of the heat content of the vegetation itself

J_H and J_v are usually negligible unless the measurement height, z, of R_N is greater than 10m. (Schofield (1982)).

In such cases as tall forests, J_H and J_v may occassionally exceed 10-20 W/m^2.

J_{veg} is entirely negligible in grass but may be tens of W/m^2 in forests where it may exceed J_H and J_v

The biochemcial storage, P, is the energy released or absorbed by the biochemical processes involved in photosynthesis and respiration within the plant community.

P is usually quite small and has been estimated as about 2 percent of net radiation in daytime conditions.

Table 2.6 shows typical values of an energy budget of vegetation.

In the modelling to be considered here, horizontal flux divergence, D, physical storage, J, and biochemical storage P, are all neglected.

In mathematical models of the vegetation/atmosphere interaction involving energy partition at several different levels in the canopy, it is necessary to consider the energy available at each height. The radiation intercepted at each level normally forms the basis of this calculation, with the additional energy terms included where relevant.

TABLE 2.6 Typical energy budget over vegetation (Wm^{-2}) Schofield (1982)

	R_N	D	G	J	P	H
Near sunrise	0	± 5	- 5	+10	+ 3	- 8
Midday	+500	±25	+25	+ 2	+12	+461
Near sunset	0	±15	+ 5	-10	+ 2	+ 3
Midnight	- 50	±10	-25	- 2	- 3	- 20

2.6.2 Resistance Networks

2.6.2 (i) Multilayer Models

For real stands of vegetation, the network of resistances involved in the partition of available energy into sensible heat and evaporation is very complex.

However if considered in one dimension only, computer models can be used to describe the processes.

These models involve a simultaneous iterative solution of the energy balance and resistances operating at each level.

This requires estimates of the resistances operating at each level, ie the stomatal and boundary layer resistances as well the effective eddy diffusion resistances operating between the levels, as illustrated in Figure 11.

The model starts by calculating the available energy relevant to each height and then uses the assumed resistance chain to calculate canopy profiles of temperature and humidity.

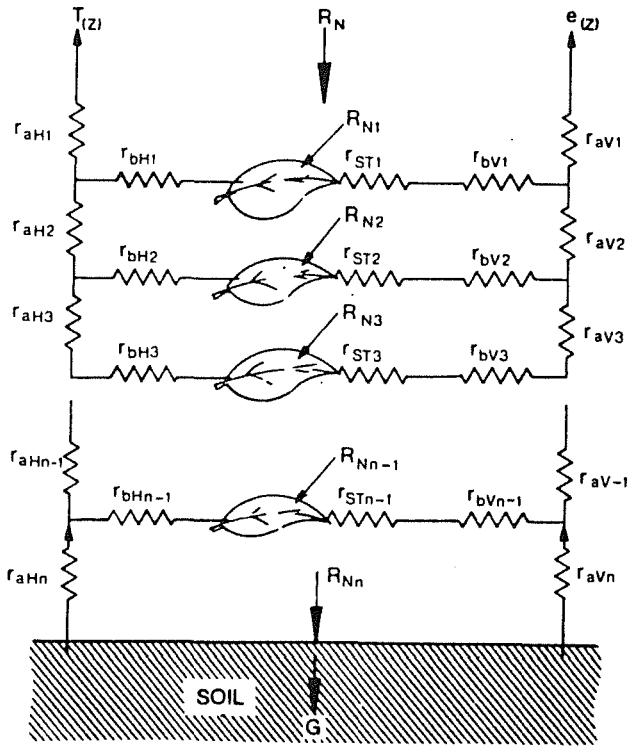

FIGURE 11

DIAGRAM OF THE RESISTANCE NETWORK USED TO PARTITION ENERGY INTO LATENT AND SENSIBLE HEAT IN 'MULTI-LAYER' MODELS OF THE VEGETATION/ATMOSPHERE INTERACTION. THE RESISTANCE r_{STn} IS THE STOMATAL RESISTANCE APPLICABLE AT EACH HEIGHT, WHILE r_{bHn} AND r_{bVn} ARE THE BOUNDARY LAYER RESISTANCES. r_{aHn} AND r_{aVn} ARE THE EDDY DIFFUSION RESISTANCES BETWEEN LEVELS

V = LATENT HEAT
H = SENSIBLE HEAT

Shuttleworth, (1979)

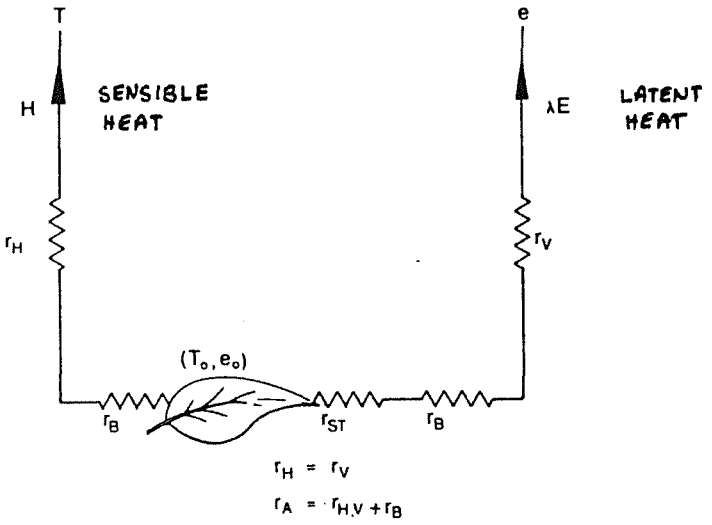

FIGURE 1a SCHEMATIC DIAGRAM OF THE RESISTANCE NETWORK USED IN 'SINGLE-SOURCE' MODELS OF THE VEGETATION/ATMOSPHERIC INTERACTION. r_{ST} AND r_B ARE THE BULK STOMATAL AND BOUNDARY LAYER RESISTANCES; r_H AND r_V ARE USUALLY TAKEN AS EQUAL AND COMBINED IN SERIES WITH THE BOUNDARY LAYER RESISTANCE TO GIVE THE 'AERODYNAMIC' RESISTANCE r_A ($r_A = r'_H + r_B = r'_V + r_B$). r_A IS THEN THE 'BULK TRANSFER RESISTANCE', GIVEN BY EQUATIONS (66) AND (67)

Shuttleworth, (1979)

Such models require extensive input data and are subsequently restricted in predictive use. However they do provide useful yardsticks against which to test simpler models more suitable to predictive application.

2.6.2 (ii) Single Source Models

By combining the in canopy resistances (the stomatal and boundary layer resistances) in parallel and assuming they act at a single level in the canopy, a bulk stomatal and boundary layer resistance, r_{st} and r_b, result.

The single level chosen is assumed to be an "effective source height" somewhere close to the apparent sink of momentum.

In single source models of this type it is no longer relevant to separate the "boundary layer" and "eddy diffusivity" resistances since they are now assumed to act in series on all the fluxes involved. It is more usual to combine them as a single "aerodynamic resistance", r_a which is the bulk transfer resistance given by equation (66) ie

$$r_a = (\ln((z-d)/z_o))^2 / \; k^2 \, u(z) \qquad (76)$$

Figure 12 illustrates a single source model for the partition of energy into latent and sensible heat fluxes. The latent heat flux still differs from the sensible heat flux in that it is subject to the additional stomatal resistance, rst, in dry canopy conditions.

2.6.2 (iii) Penman-Monteith Equation

This equation is the fundamental expression used in simple one-dimensional descriptions of the evaporation processes, and, is the basis of all the more empirical techniques used in estimating evaporation. It is derived from the previous underlying principles applied to a single source model as shown in Figure 12.

Temperature and vapour pressure measured at "screen height" above the vegetation have values of T and e respectively. The effective temperature and vapour pressure adjacent to the dry leaf surface are T_o and e_o respectively. Inside the stomata the air is saturated with a vapour pressure $e_s\ (T_o)$

According to single source model formulations, the latent heat flux is given by

$$\lambda E = \frac{\rho Cp}{\gamma} \frac{(e_s(T_o) - e(T))}{r_a + r_{st}} \qquad (77)$$

while the sensible heat is given by

$$H = \frac{\rho Cp(To-T)}{r_a} \qquad (78)$$

Combining equation (78) with the mean gradient of the saturated vapour pressure curve, Δ, given by equation (6) gives

$$H = \frac{\rho Cp}{\Delta} \frac{(e_s(T_o) - e_s(T))}{r_a} \qquad (79)$$

while conservation of energy requires

$$H = A - \lambda E \qquad (80)$$

Substituting equation (80) into (79) gives

$$A - \lambda E = \frac{\rho Cp}{\Delta} (e_s(To - e_s(T))/ra \qquad (81)$$

Eliminating $e_s\ (T_o)$ by combining equations (77) and (81) gives the Penman Monteith equation

$$\lambda E = \frac{\Delta/\gamma\ A + \frac{\rho Cp}{\gamma} \frac{(e_s(T) - e(T))}{r_a}}{(\Delta/\gamma + 1 + r_s/r_a)} \qquad (82)$$

where $r_a = \frac{(\ln((z-d)/z_o))^2}{k^2 u(z)}$ (76)

2.6.3 Water Balance Models

The single source evaporation model as represented by equation (82), the Penman Monteith equation, is directly applicable to a single layer water balance model.

Interception models such as those of Shuttleworth (1979) (Figure 13) and Schofield (1982, 1983) (Figure 14) related evaporation from canopy storages to potential evaporation rates calculated from wet canopy rates in equation (82) by setting r_s =0.

To truly model the water balance, transpiration losses should also be included in the model.

The transpiration losses would come from a soil moisture store, and hence to get a true water balance of the simplest level possible, an interception store and soil store would be needed in the model.

Transpiration rates may also vary as a function of soil moisture availability (as reflected in r_s) and of leaf wetness (as represented by the canopy storage).

Although this type of model won't be developed here, it is envisaged that such a model will be required in the future.

The data set presently available is sufficient to operate such a model, but more information on the parameters related to interception and soil moisture change is required.

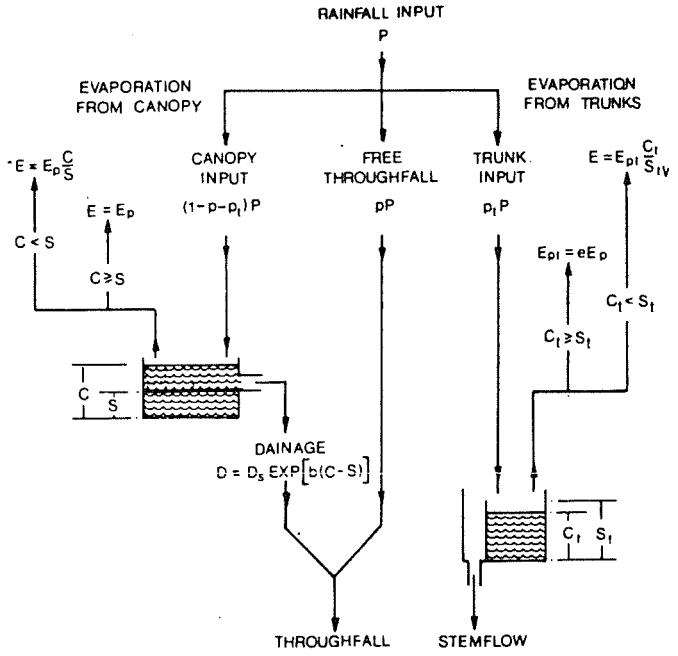

FIGURE 13 CONCEPTUAL FRAMEWORK OF THE RUTTER MODEL OF RAINFALL INTERCEPTION FROM FOREST VEGETATION

Shuttleworth,(1979)

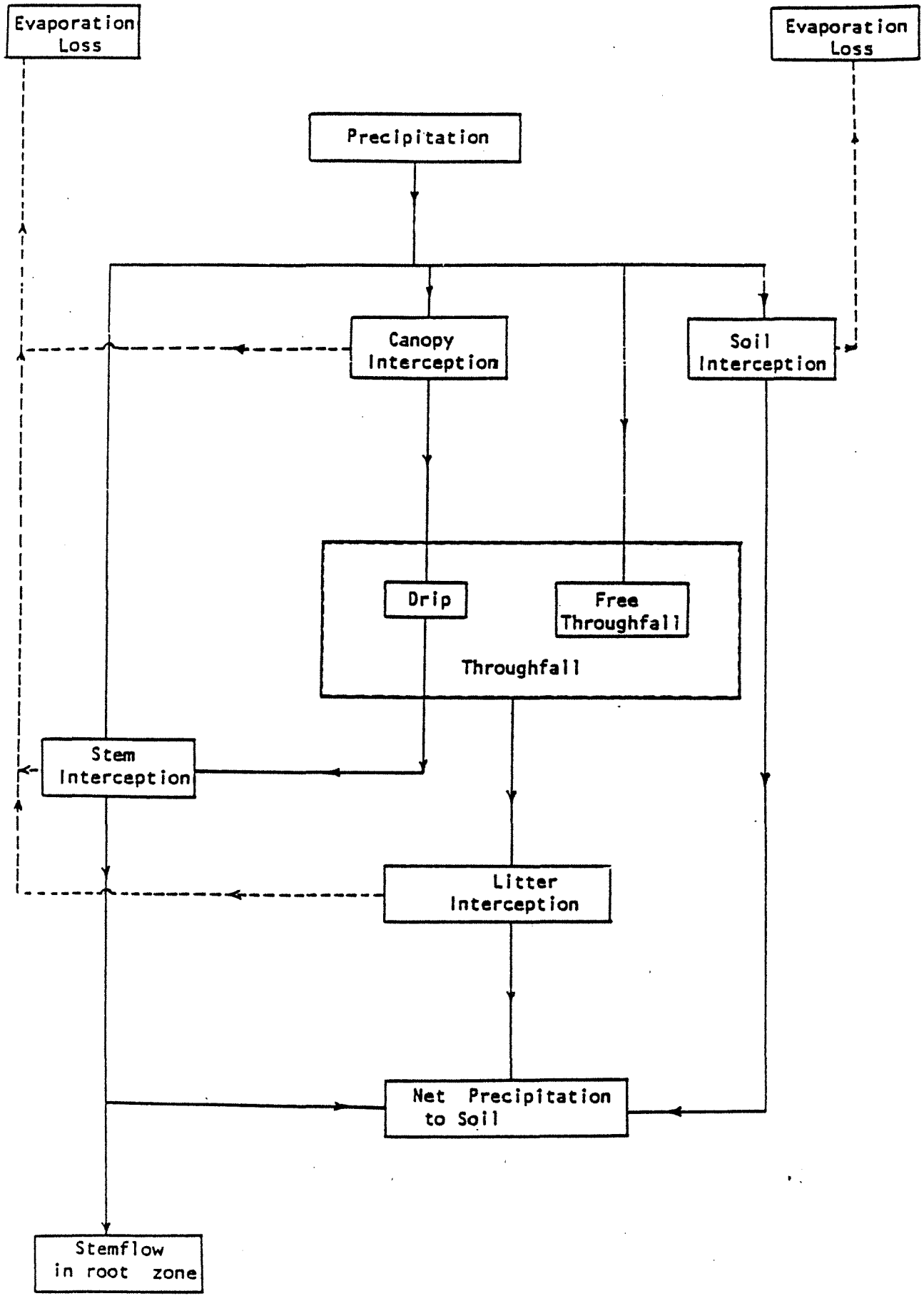

Figure 14 : Interception Model Processes

Schofield (1983)

3. Data Limitations

3.1 Required Data

The Climat Stations initially operated by the Public Works Department (Figure 15) were set up under the auspices of the Representative Basins Program to enable sufficient data to be collected for estimates of potential evapotranspiration to be made.

It was recommended by Stone (1979) that the Penman Combination equation be used for calculating potential evapotranspiration. The data required from the Climat Station are thus

- air temperature
- humidity
- windrun
- net radiation

The model used here requires this data at 15 minute intervals.

The main requirement on the data set is that all 4 parameters are available. If any one is missing then either the data set must be filled in (Edgeloe and Loh (1983)) or discarded.

Ernies Climat Station, (509 249) was used as the source data for the potential evaporation estimates to be made here.

For additional application to interception and water balance models, rainfall is also required at the 15 minute time intervals.

As will be discussed later, additional information on cloud cover and type, and sunshire hours is required for estimation of the net radiation.

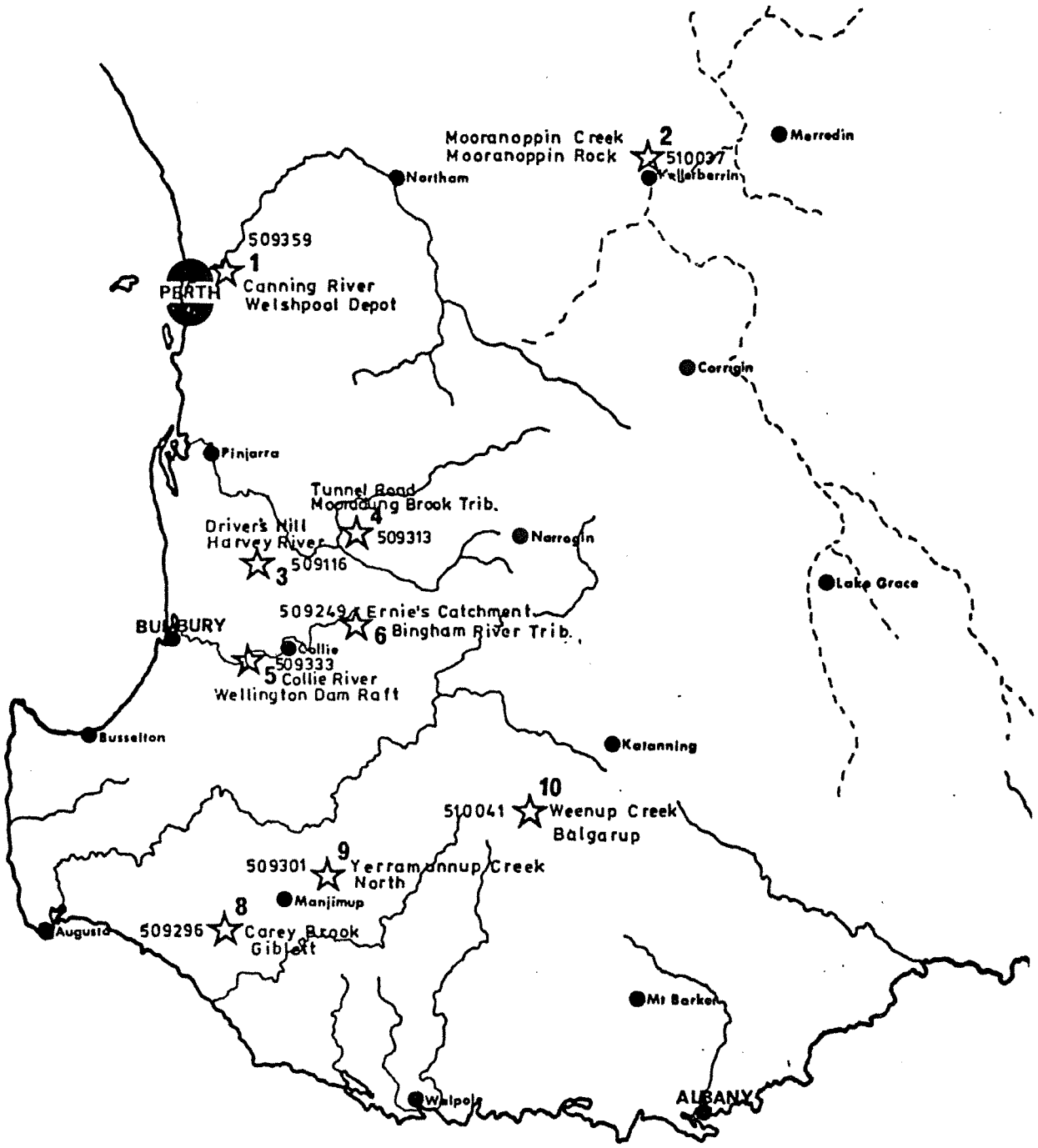

Figure 15 ☆ Location of Climat Stations

Stone (1979)

3.2 Data Collection

3.2.1 General

In general, the information from the various transducers is recorded on Rauchfuss DT/14 digital event recorders (Stone (1979)).

Information is stored on punched tapes which record events from each of the transducers. An event is recorded when a predetermined change of the parameter being measured occurs.

Problems with this type of recorder include

- jammed tape
- torn tape
- faulty circuit boards
- incorrect hole spacing
- faulty clock
- cable plugs

The major cause of lost record is due to clock faults which produce runaways on the time channel.

With the advent of solid state recorders these problems should be eliminated in the future.

3.2.2 Wind run

The anemometers used by the W.R.S. are described in detail by Hawkins (1982a).

Rimco R-CCA 5" cup anemometers are used. These give one contact per 0.2km of wind run and have a starting threshold of 0.5 m/s.

Generally two anemometers are used, a primary and secondary, and are located at a height of 2.34 m (ie 2m above the water level in the evaporation pan).

During the period 1/10/82 to 22/9/83 the secondary anemometer No. 27059 at Ernies had been faulty and some doubt exists as to the quality of its record.

Thus in creating the required data sets, the primary recorder has been used where possible. The secondary has only been used to fill in missing data.

The secondary at Ernies was repaired and shifted nearer to the primary on 20/12/83 and hence the records from both should correspond well from this date onwards.

After applying correction curves to wind run data, an accuracy of $\pm$ 0.5 m/s is expected for the primary.

Although this is greater than desirable it must be accepted.

A great problem also exists in that the anemometers are calibrated in wind tunnels at much higher speeds than generally occur on site. Thus the low end calibration is poor. The lowest possible speed in the Murdoch University wind tunnel is 5 m/s (Hawkins, 1982b).

3.2.3 Air Temperature

Rimco TR/TM temperature transducers are used to record 0.5^{o}C temperature changes. They consist of a mercury-in-stainless steel temperature bulb connected via a micro bore capillary tube to a bourdon tube which activates the contact mechanism via a lever system.

An accuracy of $\pm$ 2.0^{o}C has been found in calibration tests (Stone (1979)). This large range is due mainly to the comparison which was between the Rimco transducer and a Stevenson screen thermometer. In general an accuracy of $\pm$ 0.5^{o}C is maintained, and is desirable.

3.2.4 Relative Humidity

Although large inaccuracies had occurred with humidity transducers in the past, a hair transducer has been installed at Ernies, and with significant post processing of the data, should provide reasonable results. No accurate figures can be placed on the accuracy of these results, although they should be in the range $\pm$5%.

Missing humidity records have been filled in for the period August 1976 to December 1977 by Edgeloe and Loh (1983) for Ernies Climat Station.

Refinements in the measurement of humidity are desirable. The biggest problem seems to be in obtaining a reliable continuous humidity recorder.

3.2.5 Net Radiation

The WRS at present does not measure true net radiation even though it is required for evaporation estimates.

Instead only direct and diffuse short-wave radiation are measured using Rimco integrating pyranometers (Hawkins, 1983).

These use silicon cells as radiation detectors, and generate a direct current proportional to the intensity of the solar radiation.

Radiation in the range of 0.3 µm to 4 µm (short-wave) is detected. Thus to get true net radiation, estimates of surface albedo and back radiation (net long-wave) must be made as discussed in section 2.2.5.

This necessitates the collection of cloud type and amount and sunshine duration data to produce the cloud factor as discussed in section 2.2.5 and in section 3.3.

An accuracy of $\pm$10% is currently obtained with the pyranometers modified to give an event every 0.036 mega joules per m^2. This represents an accuracy of 40 W/m^2 over a 15 minute period.

To measure true net radiation then a CSIRO Funk net radiometer would be required (Funk (1958)).

This instrument involves considerable effort with respect to maintenance, but gives invaluable information.

Long wave radiation (>3 μm) can be measured separately using an Eppley pyrgeometer (Rouse (1984)) but this instrument has a number of problems. The main problem is attributable to the absorption of solar (short-wave) radiation on the dome, which then radiates a long-wave flux to the sensor. (Enz, et al (1975)). Rouse (1984) thus used it only in an inverted position, where under low albedo the short-wave is reduced.

With the instrument set up presently available, only total incoming short-wave radiation can be measured. Approximations of albedo and the back radiation are then required to give the net radiation estimate.

Two pyranometers are required to measure albedo directly. One mounted upwards, and the other inverted to measure the reflected short-wave radiation.

The albedo of the surface (α) over which the measurements are made is then the ratio of the downward short-wave radiation over the reflected upward short-wave radiation.

The albedo can have considerable diurnal variations depending on the surface type. It may be important to recognise and account for these variations in short term modelling.

A useful, although costly addition to the existing Rimco pyranometer at Ernie's would be a CSIRO Funk net radiometer. This could give good estimates of net radiation over different surface types, particularly over forest canopies.

If it is assumed that the forest canopy emits the same long wave radiation as the measurement site surface (ie temperature and emissivity the same) and knowing or estimating the albedos of each surface, then the net radiation over the forest canopy, R_F, would be given by

$$R_F = R_S + S_d \ (\alpha_s - \alpha_F) \qquad (83)$$

where R_F = net radiation over forest canopy (W/m^2)
R_S = net radiation measured at climate station
S_d = direct and diffuse short-wave radiation at climat station measured by the pyranometer
α_s = albedo at climat station
α_F = albedo of forest canopy

If an additional inverted pyranometer were used then α_s could also be measured directly and then only α_F would need be estimated.

This would then give net radiation estimates to an accuracy much better than the present estimates of net radiation. It would also give valuable information on the energy balance of a forest canopy.

The most desirable arrangement would be the direct above canopy measurement of net radiation (together with the other climatic variables).

As a check on the magnitude of the radiation being recorded at Ernies, a simple clear sky model was used as in Appendix B. This showed the radiation being recorded was reasonable and that no gross errors were recorded.

3.3 Cloud Factor

As discussed in section 2.2.5 it is necessary to evaluate a cloud factor, CFAC, for determination of downward long-wave radiation.

The calculation of CFAC requires 9am and 3pm cloud types and cloud amounts. In addition, sunshine durations are used to modify the cloud factors.

The Bureau of Meteorology stations which record this information for the south west of Western Australia are listed in Table 3.1.

TABLE 3.1 Bureau of Meteorology stations which record sunshine hours and cloud cover and type.

C.B.M. Stn. No.	Location
010244	Bakers Hill (CSIRO)
009637	Denmark Research Stn
009538	Dwellingup Forestry
009592	Pemberton Forestry
009034	Perth Regional Office
009642	Wokalup

For the calculations of longwave radiation at Ernies, the information from Dwellingup Forestry was used. This information is presented in Appendix E for July 1982 and December 1982.

After CFAC is calculated according to cloud type and amount it is then further modified according to the sunshine hours.

If during each 12 hour period there is no, or very little sunshine, then the cloud factor is set at 1.24 to represent very cloudy conditions.

If there is a significant reduction in sunshine hours then the cloud factor is set to a minimum of 1.176. This represents highly overcast conditions that may not have been reflected in the twice daily cloud observations.

Further if the humidity is high (>90%), then the moist air will increase the long-wave radiation, and hence the cloud factor is arbitrarily set to a minimum of 1.176.

On the short-term, during calculations if a period of rain is encountered, then the cloud factor is set to 1.2 for that 15 minute period.

Although the use of a cloud factor seems unjustified, it does slightly improve results and does have a very sound basis.

If true net radiation results were available then cloud factors would not be necessary.

The cloud factors used for July 1982 and December 1982 are given in Appendix E.

4. Pan Evaporation

4.1 General

The biggest problem in application of the available data set to the Penman Monteith equation has been in the uncertainty of the net radiation.

The final method that has been discussed here for estimating the net radiation was a result of applying the Penman equation to an evaporation pan, and in a sense calibrating the Penman equation for a pan albedo which allows for the short-wave radiation reflected of the pan wall and base.

Only by modelling the Class A evaporation pan were the energy terms in the Penman equation determined with any accuracy or reliability. As a result of this application to a pan, a great deal has been learnt of the aerodynamics and energy balance of the pan.

4.2 Description of Class A Pan

Hawkins (1981) describes the Class A pan set up used by the W.R.S. as shown in Figure 16.

Prior to 1968 the sunken tank type evaporimeter was standard in Australia while after this date the Class A pan was adopted as the standard for all readings.

The Class A pan is said to have the following advantages over sunken pans;

(i) pans installed above the ground are inexpensive
(ii) ease of installation and maintenance
(iii) they stay cleaner than sunken pans as ingress of dirt by wind and splashing is largely eliminated,
(iv) any leakage that develops after installation is relatively easy to detect and rectify. Hounam (1964)

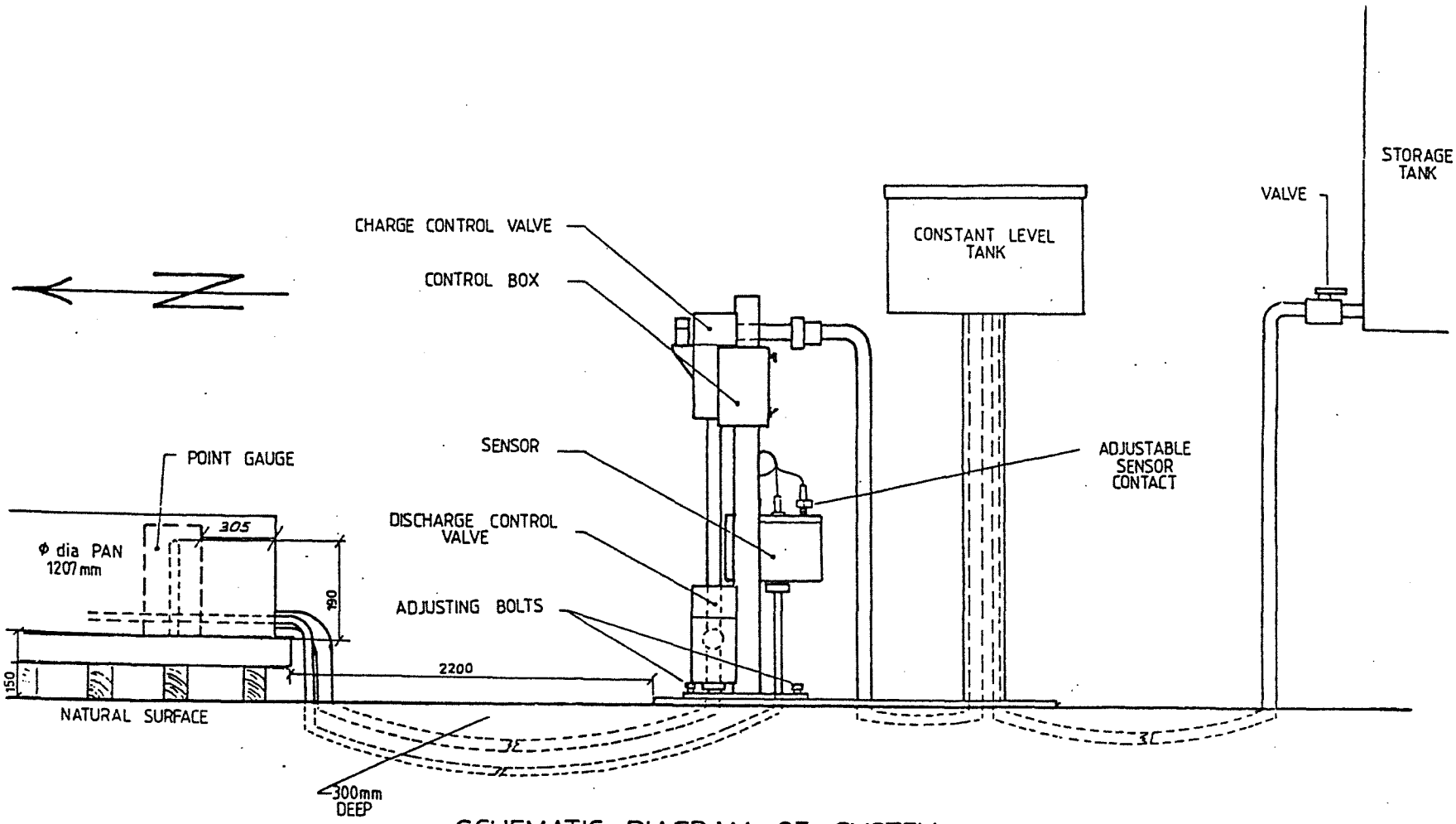

SCHEMATIC DIAGRAM OF SYSTEM

FIGURE 16

The major disadvantage of the above ground pan as an indicator of lake evaporation is that the sides of the pan intercept incident radiation, and the aerodynamics of the pan are different to those of a lake.

The pan is constructed of galvanised iron and has an internal diameter of 1207 mm and a depth of 254 mm. The bottom of the pan is supported 150 mm above the ground by a wooden platform of joists and bearers.

Water level is maintained at 190 mm depth.

A birdguard is fitted to all pans to prevent birds or animals having access to the water in the pan. The standard installation used by the Hydrology Branch has a birdguard 310 mm high and 1234 mm in diameter, covered with 12.5 x 0.9 mm galvanised chicken wire.

In order to attempt to compensate for the error introduced by the effect of the birdguard on the aerodynamics and thermal characteristics of the pan, an Australian Standard factor of +7% is applied to all records obtained to obtain the evaporation from a pan without a birdguard. This implies the birdguard reduces the pan evaporation by 7%.

Under field conditions, the Class A pan has proved grossly inaccurate (Stone (1979)). The pan has an accuracy of at most $\pm$0.2mm. Under windy conditions the accuracy is more like $\pm$0.6 mm.

This is still only a small amount of water, but it can represent a significant portion of a winter day's evaporation.

Thus during the winter period when evaporation is low, the pan accuracy will be far more critical than during the summer when evaporation is much higher.

The inaccuracies in pan data are not constant and hence a "field" scaling factor cannot be used.

4.3 Modification to the Penman Formula

The effects of the birdguard, the pan material and the heat storage in the pan constitute the largest uncertainties in pan evaporation estimates.

Cunningham (1974) investigated the factors affecting Class A pan evaporation so that an evaporimeter could be built which would more closely simulate evaporation from a shallow salt pond.

The final pan developed had only a small negligible side lip, insulated sides and was painted grey inside.

The lip and birdguard on a pan affects its aerodynamic resistance. By reducing the lip height, the roughness length, z_o, is reduced and the aerodynamic resistance r_a is increased.

This subsequently reduces evaporation. Cunningham (1974) observed this effect but his data was very scattered.

No values for z_o or d for a pan have been found in the literature so some estiamtes need to be made.

The zeroplane displacement, d, is that level at which the wind speed is zero, so as an estimate set this to the level of the water surface ie 0.34 metres above ground level.

The roughness length can then be estimated to take account of the birdguard and lip effects.

A roughness length up to 0.01 metres is possible for the pan. Greater than this gives evaporations which are too large in July 1982 due to the aerodynamics of the pan alone.

Schofield (1982) quotes z_o for a water surface as varying from 0.1 to 10^{-4}m and gives the aerodynamic resistance of an open water surface as 200 s/m.

A range of z_o values was considered here.

Basically a smaller roughness length, z_o, gives a higher aerodynamic resistance, r_a, and hence a lower evaporation.

Thus if the birdguard increases the roughness length, it would be expected that evaporation would be increased. On the other hand, the birdguard will tend to shade the pan and hence reduce the evaporation.

Hoy and Stephens (1979) in a study of lake evaporation investigated the effects of a birdguard on Class A pan evaporation at Yallourn in Victoria. It was concluded, that on the basis of 30 months data, the effect of the birdguard was to reduce the evaporation by 7%. This was an evaporation weighted figure and it was not clear how much of this constant resulted from systematic differences in the Class A pans themselves. On a monthly basis the birdguard factor was greatest in summer and least in winter (Figure 17) although the seasonal variation about the mean of 1.07 was of similar magnitude to the maximum error expected.

Van Dijk (1975) also studied the effect of a birdguard for 5 Australian stations in different climatic regions and produced the factor of +7% that is now widely used throughout Australia. A great variation in the factors was evident in this data. It was also found that the presence of the birdguard reduce the daily mean and maximum pan water temperatures by 0.3^{o}C and 1.4^{o}C respectively compared to the observations from the unguarded pans, with corresponding daily standard errors of 2.1^{o}C and 2.7^{o}C. There was also some evidence that the birdguard reduced the rainfall in the pan and hence this would also effect the evaporation recorded.

It is clear then from this that the effects of the birdguard on the evaporation from a Class A pan, cannot simply be represented by a constant factor.

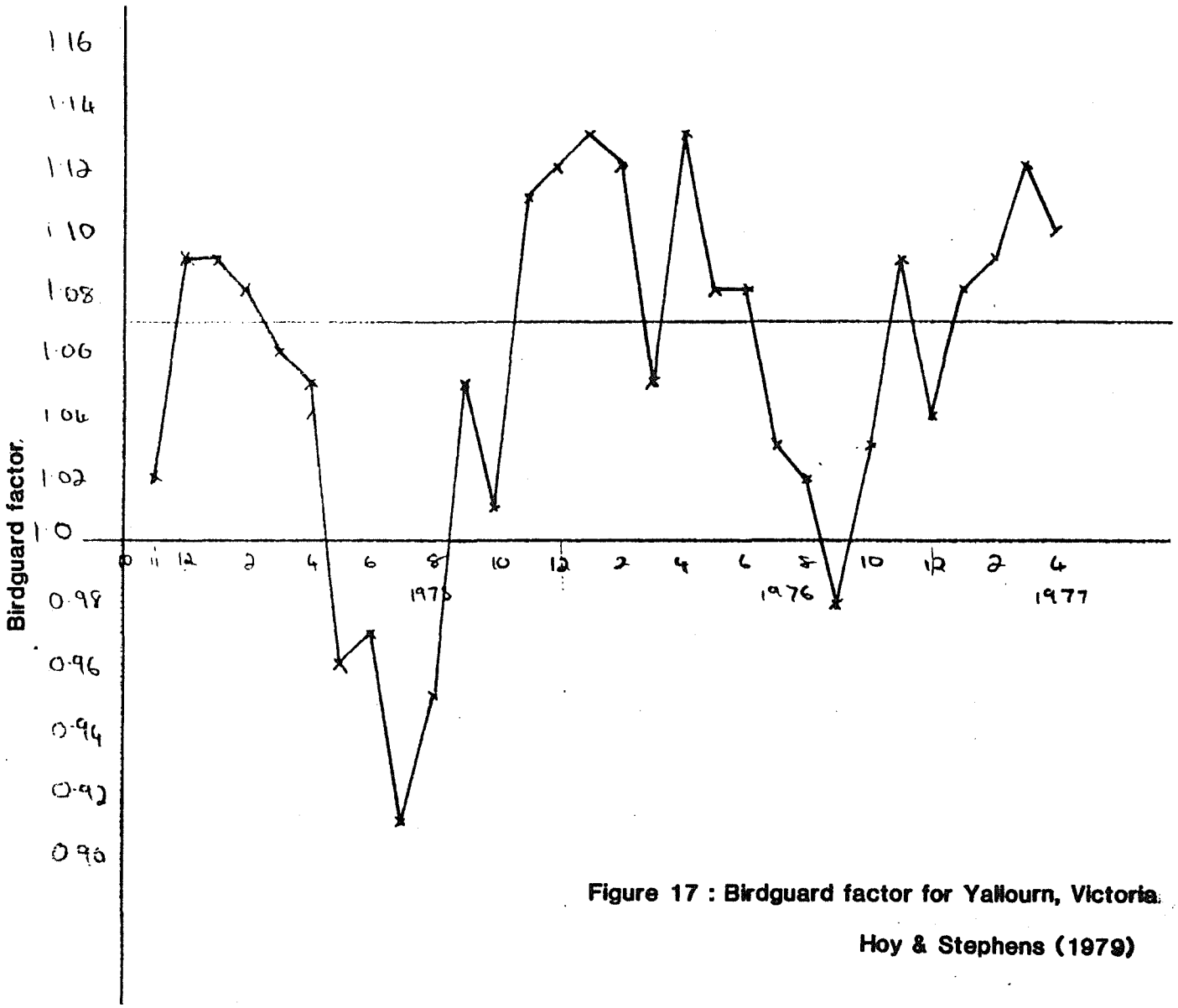

Figure 17 : Birdguard factor for Yallourn, Victoria.

Hoy & Stephens (1979)

The use of the +7% factor on anything less than yearly evaporation totals will introduce an uncertainty of the same magnitude into the "corrected" data.

It would seem more preferrable in the future to use uncorrected pan data and to develop a new standard based on the evaporation pans with birdguards.

The argument exists that all past work has been done on corrected pans and that new pan-lake relationships would be required, however these new relationships could easily be developed from existing relationships and data.

The corrected or uncorrected pan values are not significantly different when considered in terms of catchment or lake water balances, but when considered on the short term, as in the work here, the differences become very significant and need to be allowed for.

In view of the extent that pan evaporation data is used in short term water balance models, it seems that not enough is known of the pan itself and what evaporation it is actually modelling.

In addition to the effects of the lip and birdguard on the pan, are the effects of the pan material and the water in the pan.

As the pan is above ground, the sides will intercept incoming radiation and will heat up as a result. Heat will then be advected into the water in the pan, raising its temperature and enhancing evaporation.

The water temperature in the pan will also increase due to absorption of radiation penetrating the water surface.

The heating of the water due to this effect will remove available energy for evaporation and hence reduce the evaporation. However when the water begins to cool, energy will be released and this will be available for evaporation.

The combined heat storage and advection effects in the pan are represented here by the heat storage change, G, which is determined by the temperature change in the pan as discussed in section 2.2.6.

The effect of this is to reduce evaporation during the day and increase it at night. This effect is shown schematically in Figure 18. The delaying effect of heat storage is reflected in pan evapaoration data which tends to peak around 3pm. If there were no heat storage effects then pan evaporation would peak around noon.

In large water bodies the heat storage is much larger and temperature changes are expected to be lower, hence lake evaporation would be expected to peak before pan evaporation.

The inclusion of heat storage is only important however for modelling on intervals less than a day. For larger intervals the effects tend to balance out.

As discussed in section 2.2.5. The albedo of the water surface of the pan changes with sun altitude and causes a direct loss of short-wave radiation.

An additional loss of short-wave radiation, and hence available energy comes from the reflection of direct short-wave radiation off the bottom and sides of the pan.

A factor termed the "pan albedo" was applied to the pan to account for this reduction in available energy. The factor also includes allowance for absorption of short-wave radiation in the water in the pan, although this will be small. T.V.A. (1972).

Although the factor could vary through the day, it is assumed to be constant here. By fitting the Penman equation to the pan using this modification, a pan albedo of 0.1 was obtained. This indicates that approximately 10% of short-wave radiation penetrating the water surface is lost due to reflection out of the pan. This subsequently lowers the pan evaporation.

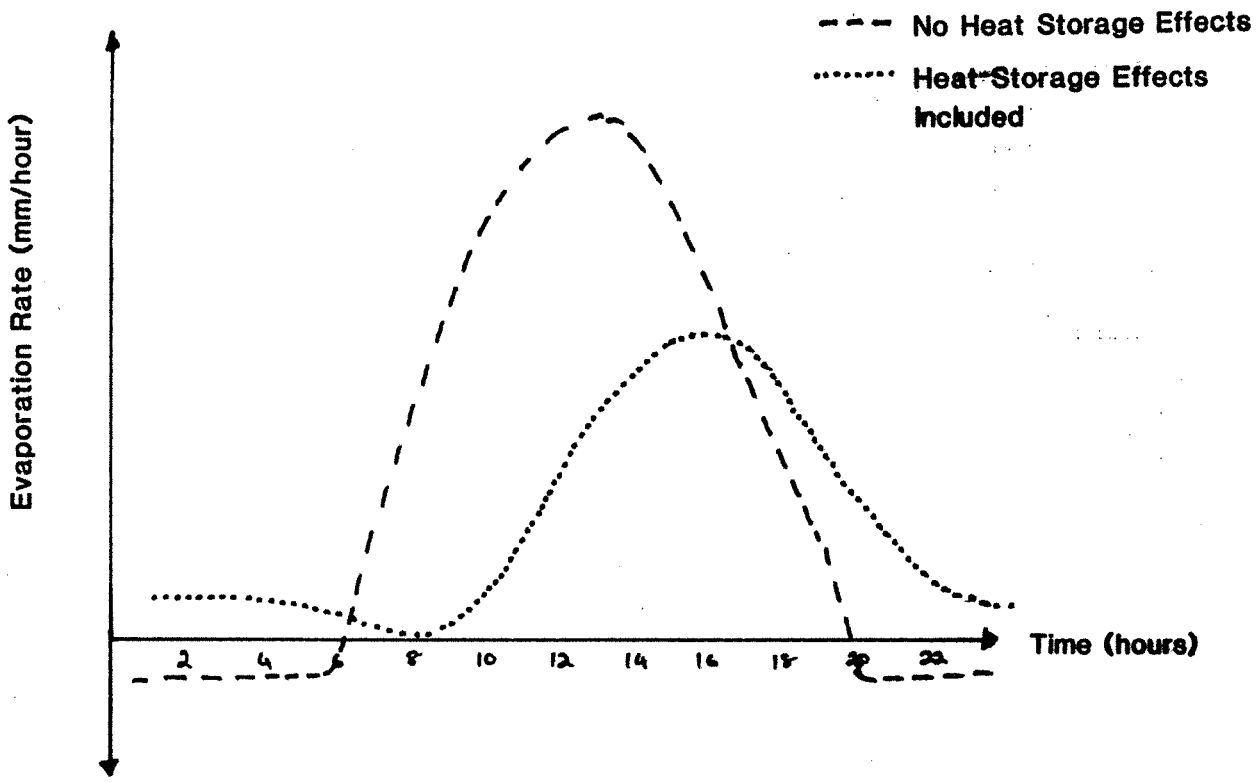

Figure 18 : Effect of Heat Storage on Pan Evaporation

It would then be expected that in black pans, where less radiation is reflected, the evaporation would be higher.

This was observed by Yu and Brutsaert (1967) where the evaporation from a white pan was 35-50% lower than the evaporation from a black pan.

Cunningham (1974) also observed lower evaporation from a white pan as compared to a grey pan, although in this case only a 5% difference was found.

No other reference to such effects has been observed.

4.4 Modelling Results

By including the pan albedo, heat storage and variable water surface albedo effects in the Penman equation, the short and long term behaviour of a Class A evaporation pan was simulated.

Only the July 1982 and December 1982 data sets were used and hence the values of pan albedo and roughness length found, could be biased towards these data sets.

However these factors do not influence forest evaporation and hence this was not considered a problem.

The main reason for applying the Penman equation to the pan was to determine the best way to estimate the net radiation from the measured short-wave radiation. This application was responsible for the development of the cloud factor approach.

By choosing a pan roughness length and pan albedo to best match the observed pan evaporations in the short and long term, the magnitude of the long-wave component of radiation was determined to fit the pan data.

Recognising that pan evaporation data is at best accurate to $\pm$0.2 mm, a trial and error fit to the data sets gave best results when a roughness length, z_o, of 1 mm and a pan albedo of 0.1 were used.

As the pan evaporation was least sensitive to roughness length, the value of 1 mm was chosen and the pan albedo then was estimated by subjectively minimising the observed deviations.

The result is that for December 1982 the "Penman Pan" over estimates the pan evaporation by 3% while during July 1982 it under estimates by 3%. These represent an over estimate of 0.18 mm/day in December and underestimate 0.03 mm/day in July, well within the errors generally accepted in evaporation estimates.

The fits to the data on a daily basis are shown in Figures 19 and 20. The data was not fitted for the first 6 days as no pan temperatures were available. The daily values and totals are given in Table 4.1.

Low overcast cloud conditions for water surface albedo were used in July, while low scattered conditions were used for December.

It is seen from this data that the Penman Pan estimates, although not exactly modelling the data, do produce the same patterns of evaporation. Only on days where extreme variations in the meteorological variables occur, do large variations in evaporation estimates occur.

The very large Penman Pan value for the 9th December is due to a high energy input from extensive low cloud cover and higher than average windspeeds. The high Penman Pan value on the 27th July is attributable to similar causes. Overall however the fit is quite good.

The further work that would be involved in getting a closer fit to the pan data is not justified, although it would be possible. The availability of true net radiation data and the better understanding of advective and heat storage effects in the pan should give a better fit.

The biggest limitation will be that for the short term modelling, the accuracy of the data becomes dominant and will limit the best fit possible.

In the analysis of the evaporation from the pan, the evaporation was divided into an energy component and an aerodynamic component.

The energy component is driven by the available energy, while the aerodynamic component is driven by the vapour pressure deficit and is restricted by the aerodynamic resistance.

Table 4.2 shows the proportions of evaporation from each source over the two modelled periods. Negative quantities indicate that condensation occured due to that particular mechanism operating. In most cases the net evaporation was positive and hence a loss occurred.

The low amounts of evaporation occuring in July made it difficult to model adequately. A particular problem was that the model was showing condensation in the pan (-ve evaporation) while the evaporation pan showed very low positive evaporation.

Much more confidence can be placed in modelling the higher evaporation rates of December.

Although the July data indicates that the evaporation comes approximately equally from both driving components, the December results probably reflect the true pan behaviour more accurately. It is seen that approximately 80% of pan evaporation is due to the available energy, with the remaining evaporation being driven by the vapour pressure deficit.

These figures are very dependent on the data set used and are subsequently expected to vary in different climatic regimes.

It is important to note that in pans the dominant mechanism seems to be the available energy, while for forests the aerodynamic component will be dominant. This indicates the unsuitability of using pan evaporation to model potential forest evaporation. Different mechanisms are dominant in each case.

As a final indication of the Penman Pan model's performance, Figure 21 shows the modelled and observed diurnal variation. The day chosen, was such that the daily totals were the same, and hence only differences in the diurnal variation are indicated.

The inaccuracy of the pan data is indicated by its large variations and the comparison in Figure 22 removes some of this by taking totals over 2 hours. All modelling was done at 15 minute intervals, and then summated over the longer periods.

The period of condensation indicated by the Penman Pan estimate seems to be due to a negative net available energy. This occurs because the water in the pan is taking up energy in heat storage at a greater rate than energy can be supplied by radiation.

This could indicate that the pan albedo factor is too high at this time or that advectional effects are causing this difference. The magnitudes involved are only small however and are not of great concern.

The most important observation with respect to the short-term data is that the same general diurnal pattern is being produced. This together with the same general pattern on a daily basis is very reassuring that the basic mechanisms involved in pan evaporation are being accounted for.

It is again noted that the modelling of the pan could be improved, but that it has not been done here as it is not considered justified.

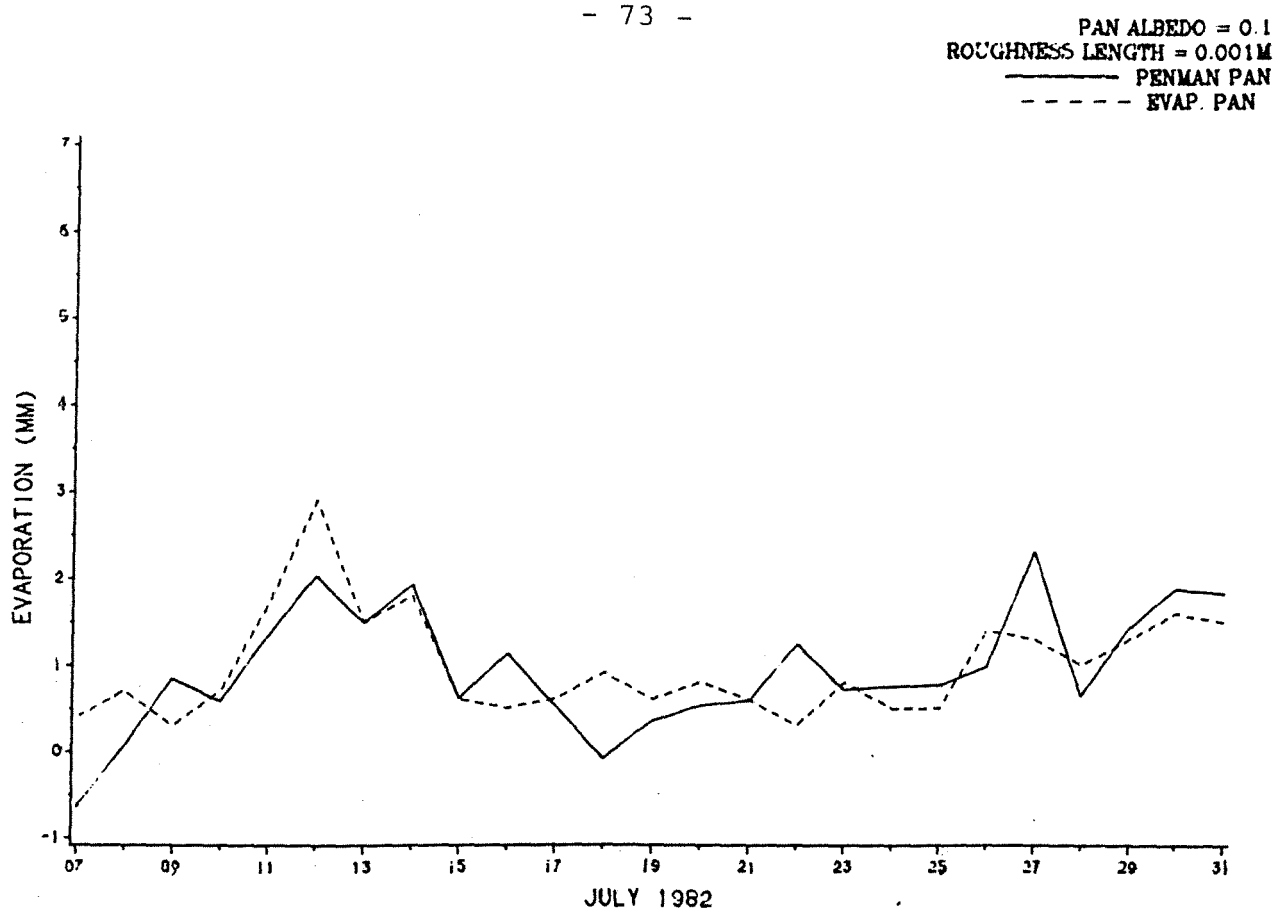

FIGURE 19 : JULY PAN SIMULATION

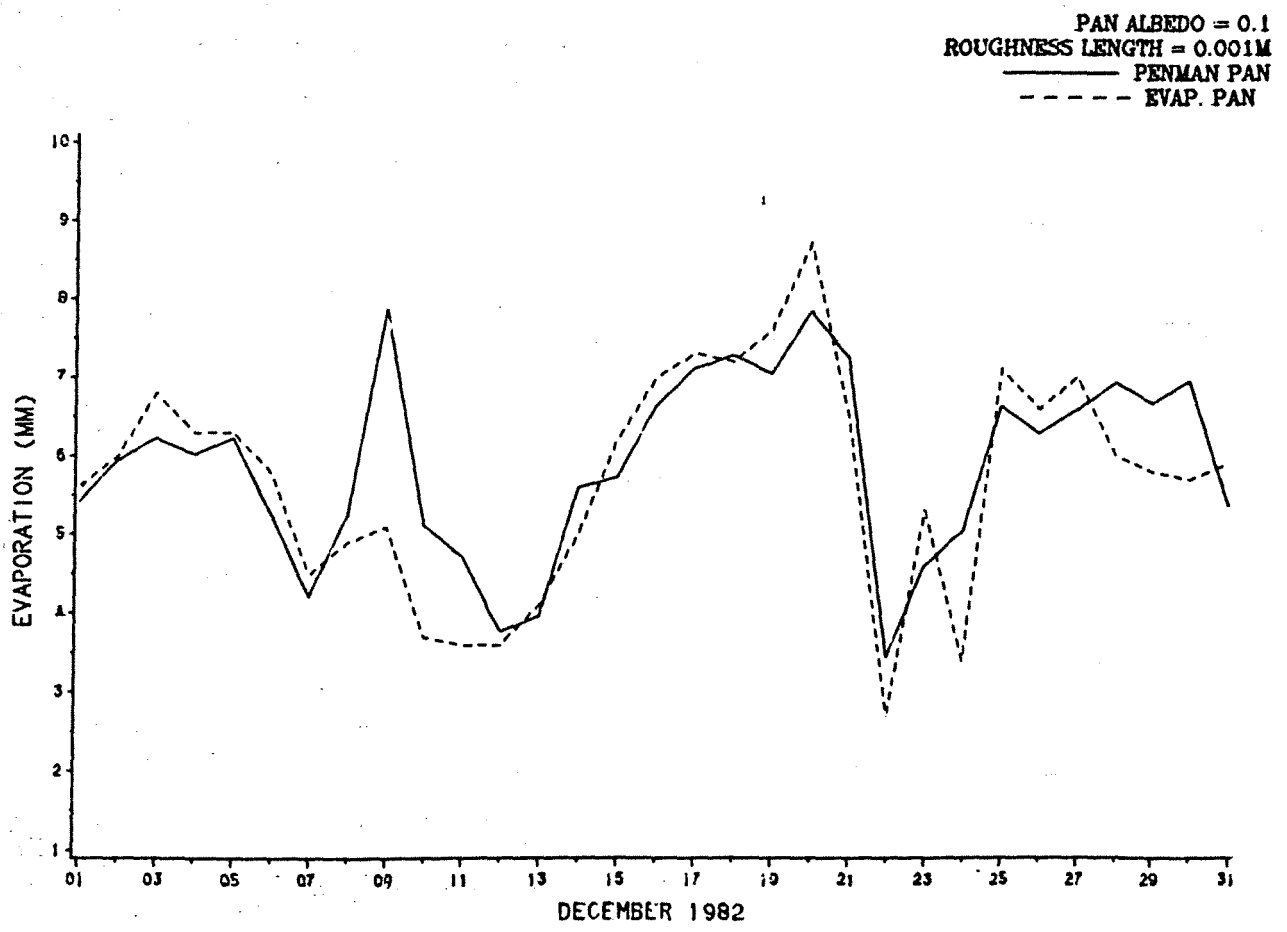

FIGURE 20 : DECEMBER PAN SIMULATION

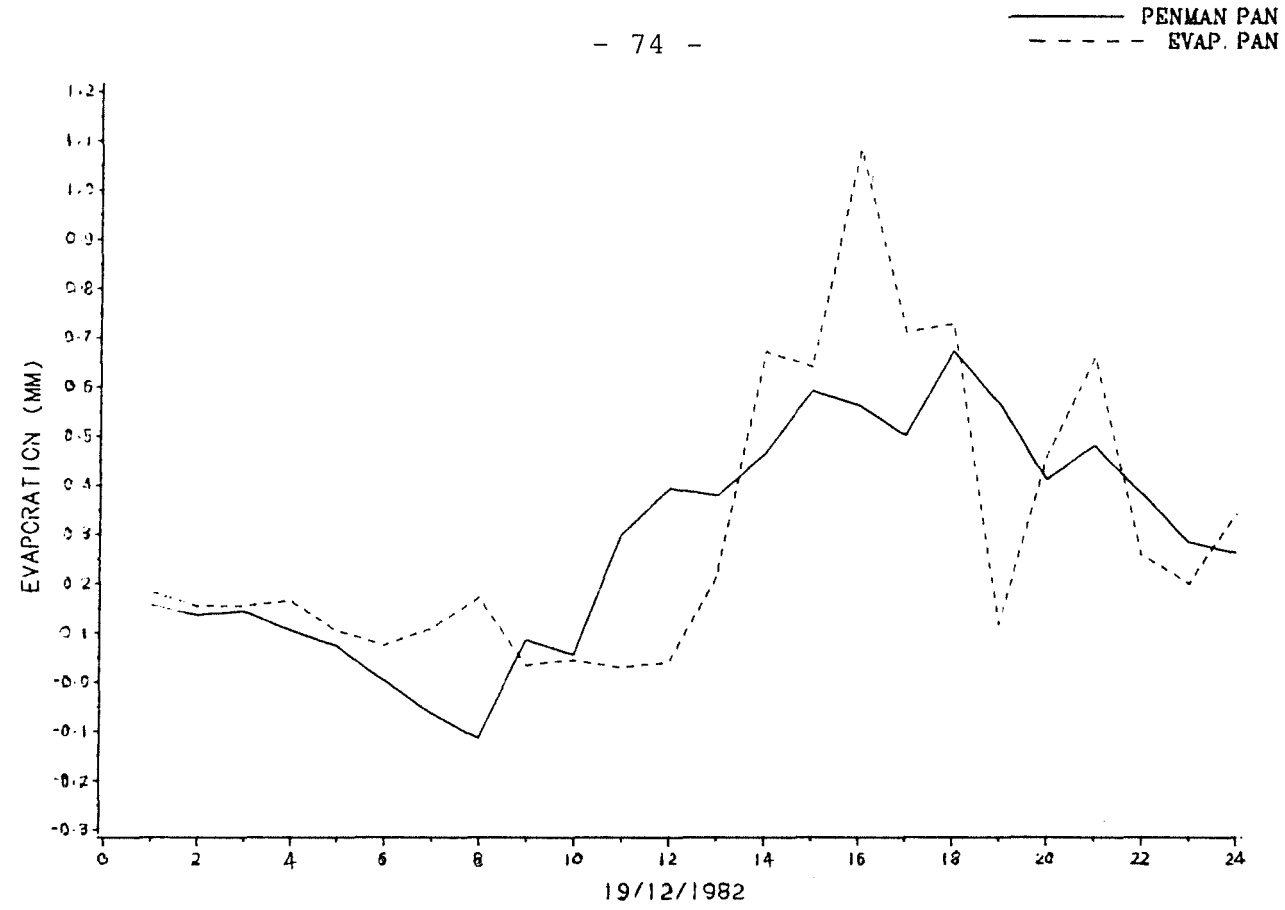

FIGURE 21 · HOURLY PAN EVAPORATIONS

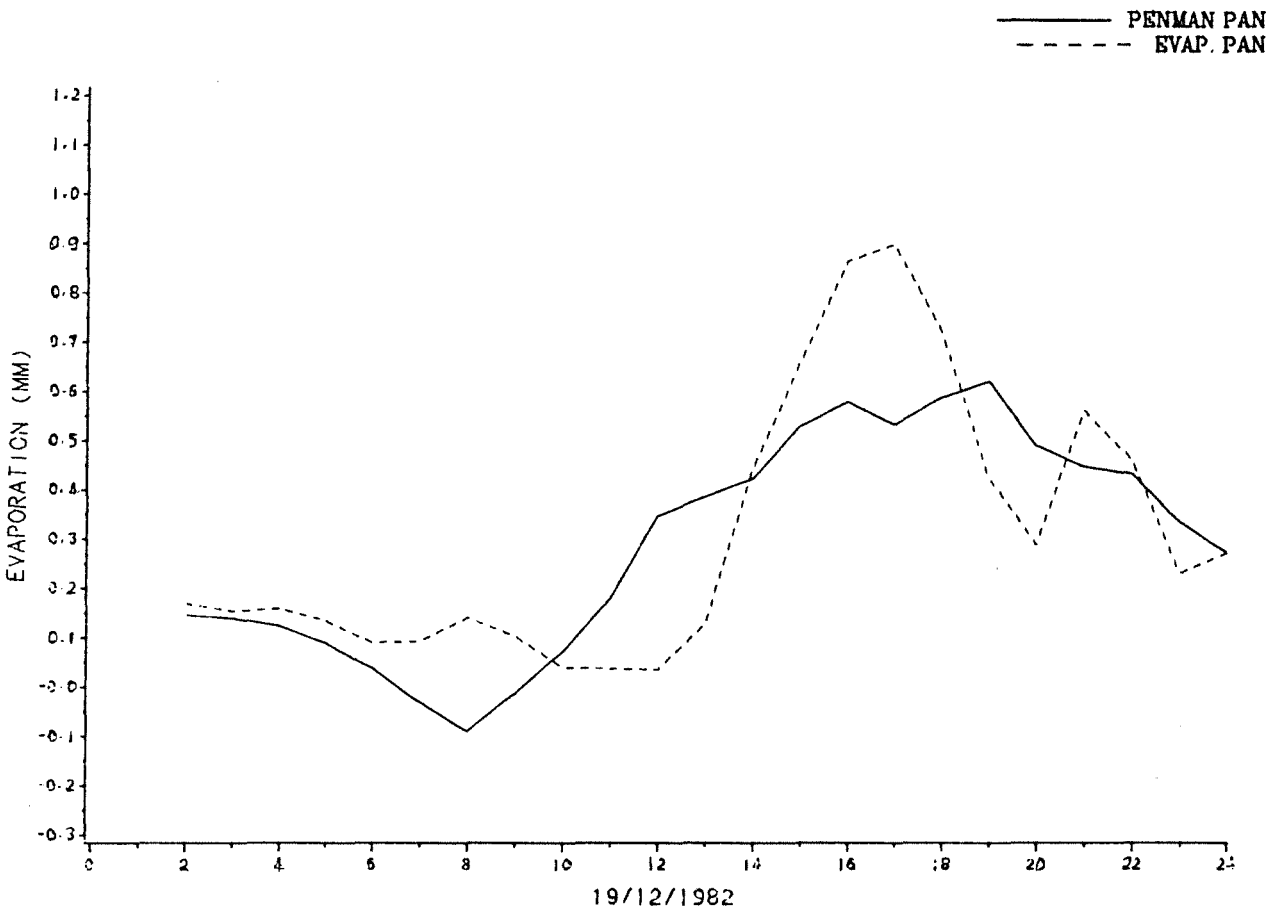

FIGURE 22 2 HOURLY PAN EVAPORATIONS

TABLE 4.1 Penman Pan model estimates

Day	July 1982 Pan (mm)	July 1982 Penman Pan (mm)	December 1982 Pan (mm)	December 1982 Penman Pan (mm)
1	-	-	5.6	5.40
2	-	-	6.0	5.94
3	-	-	6.8	6.22
4	-	-	6.3	6.02
5	-	-	6.3	6.22
6	-	-	5.8	5.26
7	0.4	-0.66	4.5	4.22
8	0.7	0.05	4.9	5.25
9	0.3	0.84	5.1	7.87
10	0.7	0.58	3.7	5.10
11	1.7	1.34	3.6	4.72
12	2.9	2.03	3.6	3.77
13	1.5	1.50	4.1	3.95
14	1.8	1.92	5.0	5.60
15	0.6	0.61	6.2	5.73
16	0.5	1.12	7.0	6.64
17	0.6	0.52	7.3	7.11
18	0.9	-0.09	7.2	7.27
19	0.6	0.34	7.6	7.04
20	0.8	0.52	8.7	7.83
21	0.6	0.58	6.5	7.25
22	0.3	1.23	2.7	3.44
23	0.8	0.72	5.3	4.60
24	0.5	0.75	3.4	5.04
25	0.5	0.76	4.1	6.62
26	1.4	0.97	6.6	6.28
27	1.3	2.31	7.0	6.58
28	1.0	0.65	6.0	6.92
29	1.3	1.44	5.8	6.67
30	1.6	1.88	5.7	6.94
31	1.5	1.83	5.9	5.37
Total	**24.8**	**23.7**	**177.3**	**182.9**

TABLE 4.2 Energy and Aerodynamic Components of Pan Evaporation based on Penman Pan Estimates

Day	July 1982		December 1982	
	Energy Component %	Aerodynamic Component %	Energy Component %	Aerodynamic Component %
1	-	-	85	15
2	-	-	87	13
3	-	-	86	14
4	-	-	84	16
5	-	-	85	15
6	-	-	88	12
7	116	-16	81	19
8	-276	376	87	13
9	97	3	77	23
10	92	8	79	21
11	77	23	81	19
12	54	46	81	19
13	88	12	75	25
14	78	22	83	17
15	99	1	81	19
16	91	9	85	15
17	86	14	79	21
18	241	-141	78	22
19	62	38	78	22
20	88	12	82	18
21	95	5	89	11
22	88	12	92	8
23	80	20	85	15
24	89	11	91	9
25	84	16	81	19
26	78	22	75	15
27	95	5	84	16
28	77	23	85	15
29	91	9	86	14
30	90	10	81	19
31	83	17	84	16
Total	78	22	83	17

4.5 Pan-Lake Comparison

It is interesting to compare here how well a pan can model lake evaporation.

Traditionally the approach for estimating lake evaporation has been to apply some factor to pan evaporation measurements.

Hoy and Stephens (1979) found that the mean annual lake to Class A pan coefficient for all Australian lakes was 0.78. This indicates that on an annual basis, lake evaporation is less than pan evaporation.

It was found however that the annual pan coefficient varied with climate, particularly relative humidity and rainfall, being greatest in the moist coastal areas and least in the arid interior. Monthly pan coefficients were found to vary significantly with lake depth and climate.

It is evident then that a direct correlation between pan and lake evaporation is not possible without considering some other factors.

From analysis of the Penman equation, it is seen for lake evaporation, that either there is less available energy for the lake, there is a higher vapour pressure deficit over the pan or the aerodynamic resistance of a lake is greater than for a pan.

Before investigating each of these possibilities, it is noted that there are significant heat storage differences between a pan and a lake.

Because of the small amount of water in an evaporation pan, its temperature and associated heat storage can change very rapidly. In comparison, a lake has a much greater heat storage capacity and hence its temperature does not change as much on a diurnal basis. As a result, pan evaporation is very dependent on present weather conditions, while lake evaporation can be strongly influenced by antecedent weather conditions, the influences of which will be carried over in the larger heat capacity of the lake.

These large differences in heat capacities of the pan and lake thus produce marked variations in daily pan coefficients in periods of changing weather. Kohler (1958).

As found from the application of the Penman Equation to the pan, a proportion (10%) of the short-wave radiation penetrating the water surface in the pan is lost by direct reflectance back out of the pan. If it is considered that heat storage effects will average out over a day, then it would imply that there is more available energy for lake evaporation than for pan evaporation. This would then give higher lake evaporation than for the pan.

This is not generally observed, so the effect of the additional available energy must be outweighed by some other factor to give a lower total evaporation.

It is reasonable to assume that there will be a lower vapour pressure deficit over a lake as compared to over a pan due to the larger source of moisture available. The effects of this type of difference have been included in pan conversion formulas such as that of Webb (1966) and take reasonable account of the differences due to such effects.

An additional effect that will reduce the lake evaporation in comparison to pan is that it will have a lower roughness length, z_o, and hence a higher aerodynamic resistance. The exact magnitude of these differences is unclear because of the wide variation in roughness values quoted for open water bodies.

Cunningham (1974) investigated and developed a pan to simulate evaporation from a shallow salt pond and found all these effects to be important. Only by developing a pan to minimise the differences in these effects was he able to get a reasonable estimate of salt pond evaporation on a daily basis.

The same case would apply to estimates of lake evaporation. If an evaporation pan is going to be used to estimate evaporation from a larger water body, then all measures should be taken to reduce or allow for these expected differences in some way. Only then will sensible short term (daily) correlations be obtained.

It is suggested that Class A pan evaporation data be used to model lake evaporation only on a yearly basis. Estimates on a monthly basis can also be made but with much less confidence. Reliable daily lake evaporation estimates can only be obtained by carefully located modified pans or tanks.

5. Application to forests

5.1 Climatic Data Transferral

In applying the Penman Monteith equation to a forest community it is desirable to use only climatic data which has been measured above the canopy.

Pearce et al (1980) investigated the effects of using climatic data measured over a grassland and applying it to a pine forest. It was found that the mean interception loss was overestimated by about 30% over a two year period.

The big problem with transferral of climatic data is that feedback mechanisms operate over plant communities and reduce the vapour pressure deficit and change the surface temperatures as evaporation occurs.

During rainfall, large amounts of water can be evaporated from forest canopies (in comparison to grass lands), and hence the air above a forest is cooled much more (than above a grassland), as energy is lost from the air to evaporate the water.

Thus the air temperatures and vapour pressure deficits are expected to be lower over forests than over grasslands.

Under wet canopy conditions, Pearce et al (1980) found that mean air temperature over the forest was $0.75^{o}C$ cooler than over a grass land and that the mean vapour pressure deficit over a forest was 0.4 mbar smaller. This subsequently affects the estimation of wet canopy evaporation from a forest.

McNaughton and Jarvis (1983) present a method based on planetary boundary layer theory for the transferral of climatic data from a grassland site to a forest. The method, as illustrated in Figure 23 starts with a set of meteorological measurements made over the grassland at some instrument height z_i. Two steps are then followed to predict the transpiration and evaporation from the forest.

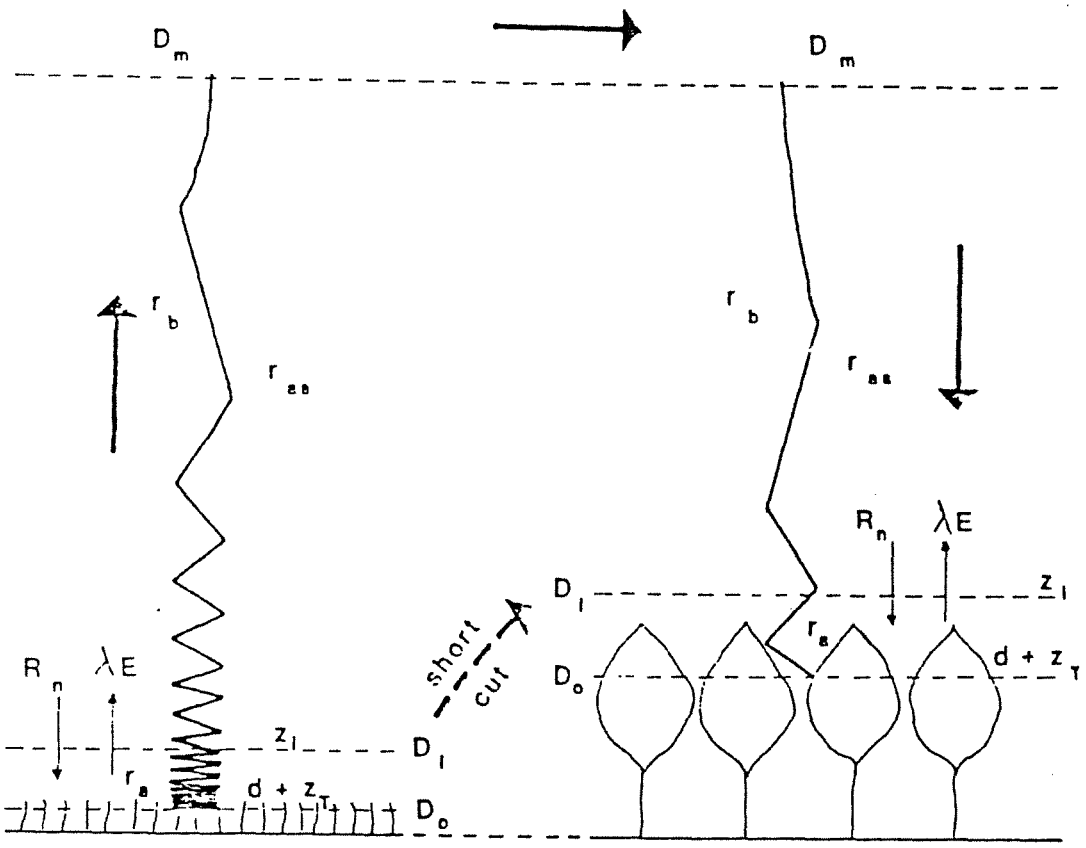

Figure 23 A diagram to show the proposed route (large arrows) to be followed in predicting forest transpiration and evaporation from meteorological data collected over grass. D_o, D_i and D_m are saturation deficits at the vegetation surface, at the instrument height (z_i) and at a reference level (100 m in unstable conditions), respectively. r_a is the resistance between the vegetation surface and z_i, r_b the resistance between z_i and the reference level and r_{as} the total resistance ($r_a + r_b$) between vegetation surface and reference level.

McNaughton & Jarvis (1983)

The first step is to move upwards above the instrument level and estimate the conditions at a suitable reference height sufficiently far above the grassland surface to be uninfluenced by it. The second step is then to move downwards to the forest canopy to get the conditions there.

This method involves considerable approximations regarding the planetary boundary layers at the sites and requires estimates of the aerodynamic resistance, r_b, above the instrument height and the advective exchange flux. This approach may be reasonable but requires a good understanding of planetary boundary theory for it to be applied with any confidence.

The approach that is generally used, and is used here is the "short cut" shown in Figure 23.

The data to be used here in application to a forest is obtained from Ernies Climat Station as discussed in chapter 3.

Ernies Climat Station is located in a small clearing in an extensively forested region, and as such would more closely represent the climatic conditions above a forest than would data from a grass land area.

Thus the differences observed by Pearce et al (1979) are expected to be greater than those that will occur between Ernies and the model site. The only means to confirm or dispute this would be to take above canopy measurements.

5.2 Forest Parameters

Based on an extensive search of the literature and on measurements conducted at the Arboretum Study site (Figure 2) as discussed in sections 2 and 3 and Appendix D,the following basic parameter set was used as representative of the reforestation sites under consideration:

Canopy height, $h = 7.2m$

Measurement height, $z = 1.2h = 8.64m$

Zero plane displacement, $d = 0.62h = 4.46m$

Roughness length, $z_o = 0.1h = 0.72m$

Albedo $r = 0.1$

Windspeed = 2 x Ernies Windspeed
Air Temperature = Ernies Air Temperature
Relative Humidity = Ernies Relative Humidity Direct and Diffuse
Shortwave radiation = Ernies Radiation

9am & 3pm Cloud Cover = Dwellingup recordings
and Type
Sunshine hours = Dwellingup recordings

This parameter set will be used as a reference set and should only be used until more information on each of the parameters becomes available.

The application of the results obtained here should recognise that they apply only for these conditions and that if they are to be used for other sites or tree types then large changes may be required.

5.3 Forest Evaporation

In application of the Penman equation or the Penman Monteith equation, it is important to understand what the results obtained actually represent.

The Penman equation applied to forest conditions strictly represents the potential evaporation of water from a surface where water is freely available, for example, a wet forest canopy.

If the use of the equation is to remain valid, then it should only be applied to climatic data recorded when the canopy was wet and evaporation was occuring. In this instance the feedback mechanisms are operating and the evaporation rate calculated is truly representative of that of intercepted water.

On the other hand, if the equation is applied to dry canopy climatic conditions, the evaporation rate does not strictly represent the rate that intercepted water would evaporate. This is because if rain was to occur, the air temperature and vapour pressure deficit would be actually lower and hence the actual evaporation rate would be lower. Hence, it is clearly incorrect to assume that the evaporative demand remains the same during wet and dry periods. Singh and Szeicz (1979) considered evaporation from a hardwood forest using the Penman Monteith equation. They found that evaporation rates based on dry canopy conditions need to be reduced by up to 50% to represent the equivalent evaporation rates that would occur under a wet canopy where the feedback mechanism alters the climatic variables.

Thus to estimate evaporation rates of intercepted rainfall, the Penman equation has been applied for both data sets for the forest, but only the "wet canopy" rates have been extracted. These are listed in Tables 5.1 and 5.2.

The results indicate that for July 1982 the mean wet canopy evaporation rate of intercepted rainfall was 0.12 mm/hr with a range from zero to 1.16 mm/hr. The zero wet canopy evaporation rates calculated during the given night hours are a result of the air temperature around the leaf cooling down to due point and hence no vapour gradient existing for evaporation. Under the December 1982 conditions the mean rate was 0.68 mm/hr and ranged from zero to 2.36 mm/hr. These are much lower than the wet canopy evaporation rates based on the full climatic data sets of July and December, 1982 (wet and dry canopy conditions), as given in Tables 5.3 and 5.4 and summarised in Table 5.5.

TABLE 5.1 July Wet Canopy Evaporations During Rainfall

Hourly Rainfall* (mm)	Wet Canopy Evaporation (mm/hr)	Vapour Pressure Deficit (mb)	Hour of Day
5.06	0.11	0.44	10
4.27	0.05	0.14	11
0.92	0.12	0.36	12
0.61	0.0	0.11	7
0.41	0.0	0.12	9
0.41	0.19	0.56	10
6.32	0.20	0.93	14
0.47	0.09	0.35	15
0.41	0.18	1.24	17
0.68	0.0	0.13	2
0.96	0.0	0.13	3
1.23	0.0	0.14	5
0.62	0.06	0.15	10
0.41	0.32	1.38	13
0.82	0.26	1.51	14
0.61	0.15	2.11	9
1.44	0.0	0.20	3
1.84	0.0	0.11	4
1.03	0.0	0.11	5
3.55	0.0	0.12	6
1.57	0.0	0.12	7
0.82	0.0	0.12	8
0.41	0.03	0.15	9
1.64	0.04	0.57	11
0.61	0.08	0.62	12
3.28	0.13	1.14	15
0.82	0.04	1.14	17
2.26	0.0	0.42	18
0.48	0.0	0.0	1
1.29	0.0	0.0	2
0.89	0.0	0.0	3
1.64	0.0	0.0	4
0.41	0.0	0.0	9
0.41	0.12	1.64	6
0.88	1.16	4.78	14
0.41	0.42	1.39	15
1.71	0.20	1.19	16
1.91	0.05	0.38	17
3.69	0.0	0.13	23
0.41	0.0	0.13	24
2.93	0.0	0.13	2
0.89	0.0	0.13	3
5.60	0.0	0.13	4
0.41	0.0	0.13	5
1.77	0.0	0.13	7
0.62	0.0	0.13	8
0.41	0.0	0.13	9
1.15	0.58	2.38	13

Hourly Rainfall* (mm)	Wet Canopy Evaporation (mm/hr)	Vapour Pressure Deficit (mb)	Hour of Day
0.41	0.14	1.37	14
1.23	0.0	0.10	24
3.15	0.0	0.12	1
1.36	0.0	0.12	2
0.48	0.0	0.11	5
0.55	0.0	0.12	6
0.41	0.0	0.13	7
0.41	0.37	1.13	11
0.41	0.0	0.14	20
0.41	0.0	0.14	21
0.41	0.0	0.14	1
0.41	0.07	1.02	18
0.75	0.03	0.35	20
0.82	0.05	0.42	23
0.67	0.04	0.27	24
0.97	0.03	0.16	1
0.61	0.14	0.62	2
2.37	0.18	0.77	3
2.34	0.07	0.36	4
0.41	0.03	0.34	5
0.41	0.08	0.47	6
0.56	0.93	4.29	13
0.98	0.92	4.23	15
0.45	0.86	4.45	16
Av. 1.28	0.12	0.68	

* only rainfall events greater than 0.3mm included

TABLE 5.2 December Wet Canopy Evaporations During Rainfall

Hourly Rainfall* (mm)	Wet Canopy Evaporation (mm/hr)	Vapour Pressure Deficit (mb)	Hour of Day
0.82	2.36	6.97	12
0.81	0.60	2.56	21
0.41	0.08	0.98	24
0.61	0.45	1.43	8
1.63	0.32	1.07	9
0.62	0.97	2.51	11
0.41	0.00	1.44	21
Av. 0.75	0.68	2.42	

* Only rainfall events greater than 0.3mm included

TABLE 5.3

July 1982 Wet Canopy Forest Evaporations

Day	Pan Evap (mm)	July 1982 Wet Canopy Forest evap (mm)	% Aerodynamic Component	Average Air Temp °C	Average Relative Humidity %	Average Windspeed m/s	Average Net Radiation w/m²	Average Vapour Pressure Deficit mb	Total Rainfall (mm)
1	0.3	5.32	78.2	3.46	89.0	0.74	28	1.3	0.41
2	0.7	7.10	80.6	1.37	82.3	0.72	38	2.0	0.21
3	0.1	8.96	91.4	5.96	83.4	2.07	37	1.7	10.66
4	1.5	6.59	77.5	4.39	83.1	0.79	68	2.2	0.0
5	0.1	3.68	86.1	7.84	94.3	1.50	18	0.8	8.81
6	0.6	4.25	70.7	4.00	89.0	0.42	25	1.7	0.0
7	0.3	5.14	78.1	7.58	89.4	0.65	41	1.7	0.0
8	0.6	8.77	83.3	9.92	87.5	0.94	48	2.2	0.0
9	0.1	2.19	42.7	11.06	95.1	0.44	51	0.8	5.33
10	0.4	2.65	64.4	9.12	93.9	0.75	44	0.8	0.20
11	0.5	13.30	86.7	11.70	79.5	2.07	76	3.5	0.21
12	1.3	35.90	96.7	15.01	49.8	2.97	49	8.9	0.00
13	0.5	8.31	83.8	12.90	72.8	0.85	56	4.5	0.82
14	1.1	17.50	89.7	9.24	70.2	1.14	48	5.4	0.0
15	0.1	0.86	39.6	6.93	95.9	0.39	23	0.5	19.88
16	0.1	5.24	73.9	4.36	91.2	0.86	58	1.0	4.72
17	0.3	4.03	67.1	5.94	92.1	0.62	52	1.1	0.20
18	0.4	6.23	76.5	6.06	87.4	0.81	61	1.8	0.0
19	0.2	6.17	79.8	10.31	88.3	1.60	52	1.5	9.64
20	0.4	3.85	61.6	9.29	92.6	0.61	60	1.1	14.35
21	0.2	2.24	50.1	7.81	95.6	0.43	50	0.6	1.84
22	0.2	7.29	77.0	8.50	89.2	1.06	58	1.5	4.92
23	0.4	7.14	76.5	8.98	89.5	0.92	66	1.7	0.82
24	0.1	4.35	70.3	10.43	94.9	1.35	52	0.8	3.70
25	0.1	5.77	79.9	12.60	92.7	1.54	47	1.2	3.50
26	0.4	8.92	8.2	13.17	87.6	1.83	29	2.2	1.90
27	0.5	5.63	73.0	8.22	90.5	1.72	64	1.2	9.60
28	0.6	7.76	71.1	4.77	85.3	0.60	98	2.1	0.20
29	0.9	7.11	69.8	8.92	83.3	0.51	71	2.9	0.0
30	1.1	9.28	73.4	6.44	82.4	0.58	87	3.3	0.0
31	1.2	14.4	82.6	6.92	878.2	0.82	87	4.4	0.0
TOTAL	15.3	235.88							101.92
AVERAGE		0.32mm/hr	74.8	8.16	86.3	1.04	53	2.1	

TABLE 5.4

December 1982 Wet Canopy Forest Evaporations

Day	December Pan Evap (mm)	Wet Canopy Forest evap (mm)	% Aerodynamic Component	Average Air Temp °C	Average Relative Humidity %	Average Windspeed m/s	Average Net Radiation w/m²	Average Vapour Pressure Deficit mb	Total Rainfall (mm)
1	3.4	36.4	81.0	18.21	54.9	1.70	256	12.9	0.0
2	3.6	35.5	79.7	18.53	59.6	1.69	265	11.8	0.0
3	4.4	39.5	82.6	21.40	60.8	2.40	253	12.8	0.0
4	3.9	41.9	83.8	21.76	62.6	2.67	249	12.3	0.0
5	4.0	40.5	83.2	19.48	64.2	2.12	242	11.0	0.0
6	4.3	29.5	77.7	18.80	61.7	1.61	250	10.1	0.0
7	3.0	35.0	85.4	21.35	58.8	2.21	185	14.3	0.0
8	2.0	30.2	80.8	23.91	58.3	1.33	207	15.6	0.0
9	3.2	71.3	92.6	22.48	61.4	6.01	207	11.2	1.02
10	2.4	45.1	89.6	17.87	77.9	4.82	193	5.1	1.63
11	1.7	38.4	88.5	13.89	76.9	3.78	189	4.2	3.88
12	2.5	31.8	84.7	13.73	71.2	2.82	189	6.3	0.41
13	2.6	42.3	87.6	16.85	71.9	2.99	201	7.1	0.0
14	3.0	40.4	85.8	18.06	70.9	2.99	223	7.3	0.61
15	3.1	46.8	83.5	18.23	64.0	2.07	263	12.1	0.0
16	3.7	44.0	84.1	21.02	62.8	2.57	254	11.9	0.0
17	4.3	60.9	88.5	20.58	56.3	3.53	257	13.2	0.0
18	3.5	65.9	88.5	22.90	59.4	3.95	273	14.9	0.0
19	4.5	64.1	88.4	27.98	53.1	3.20	253	23.6	0.0
20	4.7	60.8	86.4	27.55	58.8	2.56	266	20.1	0.0
21	4.2	36.5	80.8	22.9	71.2	2.59	257	10.4	0.0
22	1.7	12.7	75.1	19.43	78.6	1.37	127	5.4	0.0
23	2.8	31.9	80.1	21.09	68.2	1.70	218	10.8	0.0
24	1.8	21.9	77.1	20.18	74.3	1.46	195	7.5	0.0
25	4.4	54.2	85.8	21.86	60.0	2.25	258	15.3	0.0
26	4.1	42.2	83.8	22.15	61.2	2.13	240	13.2	0.0
27	4.6	47.0	82.8	24.00	56.1	2.00	272	18.4	0.0
28	3.6	45.1	87.5	19.88	66.6	3.15	212	9.9	0.0
29	3.3	43.4	81.4	16.30	60.8	1.84	305	11.6	0.0
30	3.5	56.8	86.9	16.49	68.4	3.35	283	8.4	0.20
31	3.9	38.1	83.8	18.12	63.1	1.87	227	10.1	0.21
TOTAL	105.9	1330.4	84.1	20.19	64.3	2.58	234	11.5	7.96
AVERAGE		1.79mm/hr							

TABLE 5.5

Summary of Wet Canopy Evaporation Rates

	July 1982	December 1982
Wet Canopy Evaporation based on full Climatic data set (mm/hr) 1.	0.32 (0-1.49)	1.79 (0-2.97)
Wet Canopy Evaporation based only on wet canopy climatic data (mm/hr) 2.	0.12 (0-1.16)	0.68 (0-2.36)

Values are means and ranges

1 Based on daily averages

2 Based on hour averages during periods of rainfall

Table 5·6 :

MEASUREMENTS OR ESTIMATES FROM A MODEL OF EVAPORATION RATES FROM SATURATED CANOPIES (E_1) OF TEMPERATE FORESTS*

Species	E_1 (mm hr^{-1})	Method[b]	Source
Coniferous forest			
Pinus sylvestris	0.17 (0.03–0.4)*	1	Stewart (1977)
	0.19 (0.05–0.55)	3	Gash (1979)
	0.33 (0.50–0.7)	3	Gash *et al.* (1980)
Pinus radiata	0.21 (0–0.5)*	2	Moore (1976b)
Picea sitchensis	0.19 (0.05–0.3)	1	James and Jarvis (1983)
	0.13 (0.05–0.25)	3	Gash *et al.* (1980)
	0.21 (0.1–0.45)	3	Gash *et al.* (1980)
Pseudotsuga menziesii	0.15 (0–0.4)	1	McNaughton and Black (1973)
Broad-leaved forest			
Fagus grandifolia –*Acer saccharum*	0.45 (0–0.9)*	4	Singh and Szeicz (1979)
Nothofagus	— (0.28–0.46)	3	Pearce and Rowe (1981)
–*Podocarpus*	0.37*+	3	Pearce *et al.* (1980b)

* The values are overall means or medians with ranges of means so that individual extreme values are excluded. Superscripts: *, indicates $E_1 > R_n$ at times; +, nights only.

[b] Methods: 1, direct measurement by the Bowen ratio method; 2, direct measurement by eddy correlation; 3, calculation from interception studies by the Gash (1979) model; 4, calculation from the Penman equation (6), using estimates of r_a from the neutral windspeed profile.

McNaughton & Jarvis (1983)

These rates compare well with those given in Table 5.6 during the July period but are higher during the December period. This is most likely due to the Mediterranean Climate at Ernies relative to the less extreme Temperature Climate for the values tabulated. Differences in the aerodynamics of the tree species could also account for the observed differences.

For both periods, the wet canopy potential evaporation rate is only 38% of that calculated using all climatic conditions, which mainly consisted of the stressed dry canopy condition. This is a greater reduction than that observed by Singh and Szeicz (1979) and indicates the importance of the feedback mechanism and its controlling effect on evaporation.

Figure 24 shows how during a period of low rainfall in December 1982, the vapour pressure deficit drops during the rainfall, and subsequently lowers the potential evaporation rate. The vapour pressure deficit during periods of no rain is much higher and would falsely give a high rate of evaporation if applied to intercepted water.

Also of importance as indicated in Figure 28 and tables 5.1 and 5.2, is the potential for night rainfall to produce much higher runoff than day rainfall because wet canopy evaporation is much lower at night time.

As indicated in Tables 5.3 and 5.4, the forest evaporation is largely dominated by the aerodynamic term of the Penman Equation which contains the vapour pressure deficit and the aerodynamic resistance. Pearce, et al. (1980) also found forest evaporation to be dominated by the aerodynamic component.

The other application of the Penman equation as used here is to determine the wet canopy evaporation rate and relate this to transpiration in a forest.

The Penman Monteith equation (82) effectively reduces the evaporation calculated by the Penman equation by an amount dependent on the surface or canopy resistance r_s, so that

$$\frac{Et}{Ec} = \frac{\Delta/\gamma + 1}{\Delta/\gamma + 1 + r_s/r_a} \qquad (84)$$

where Et = transpiration
Ec = potential (Penman) evaporation
r_s = surface resistance
r_a = aerodynamic resistance
= equation (38)

Thus in instances where the surface resistance is much greater than the aerodynamic resistance, the actual transpiration will be much less than the wet canopy evaporation that would be calculated for those climatological conditions.

Unlike the instance before, equation (84) can be applied in this manner over all the data set and is not restricted to wet canopy conditions.

The low amounts of water that will transpire are expected to have only a small effect on the climatic conditions, especially in the case here where only small groups of replantings are being considered.

Future work will investigate the behaviour of trees and their characteristic surface resistances, and the subsequent effect of this on forest transpiration.

Table 5.7 shows the magnitude of reduction that surface resistances can impose on wet canopy evaporations for estimating transpiration.

TABLE 5.7 Effect of surface resistance on transpiration rates

	r_s (s/m)			
	10^5	10^4	200	100
Et @ 20°C / Ec	2.2×10^{-4}	3.1×10^{-3}	0.13	0.23

* r_a = 10 s/m used

These results indicate that at a typical surface resistance of 100 s/m, the transpiration will only be of order 20% the wet canopy evaporation.

The major aim of the work here has been to estimate these wet canopy rates so that later when more is known about the surface resistance of the trees, the transpiration rates can be estimated. It is thus important to first understand the mechanisms involved in the wet canopy evaporation rates.

Figure 24 shows the diurnal variation of the wet canopy rates calculated from the full climatological data sets, while Figures 25 and 26 show the daily variations over the two months. As indicated before, the aerodynamic component is most dominant and represents 75% and 85% of the total evaporation in July and December respectively. The close harmony between the aerodynamic component and the vapour pressure deficit and windspeed is evident in Figures 25 and 26.

Based on mean monthly values, Table 5.8 shows that between July and December, the four-fold increase in average available energy produces a similar four-fold increase in the energy component of evaporation. The remainder of the increase in the evaporation is due to increasing windspeeds and vapour pressure deficit in December.

High windspeeds on the 9th December as shown in Figure 26 produce the large wet canopy evaporation rates estimated, again indicating the importance of the aerodynamic component.

Average air temp °C	23·9	22·5	17·9	13·9	13·7	16·05	18·06	18·33
Average windspeed m/s	1·33	6·01	4·82	3·78	2·02	2·99	2·99	2·07
Average relative humidity %	58·3	61·4	77·9	76·9	71·2	71·9	70·9	64·0

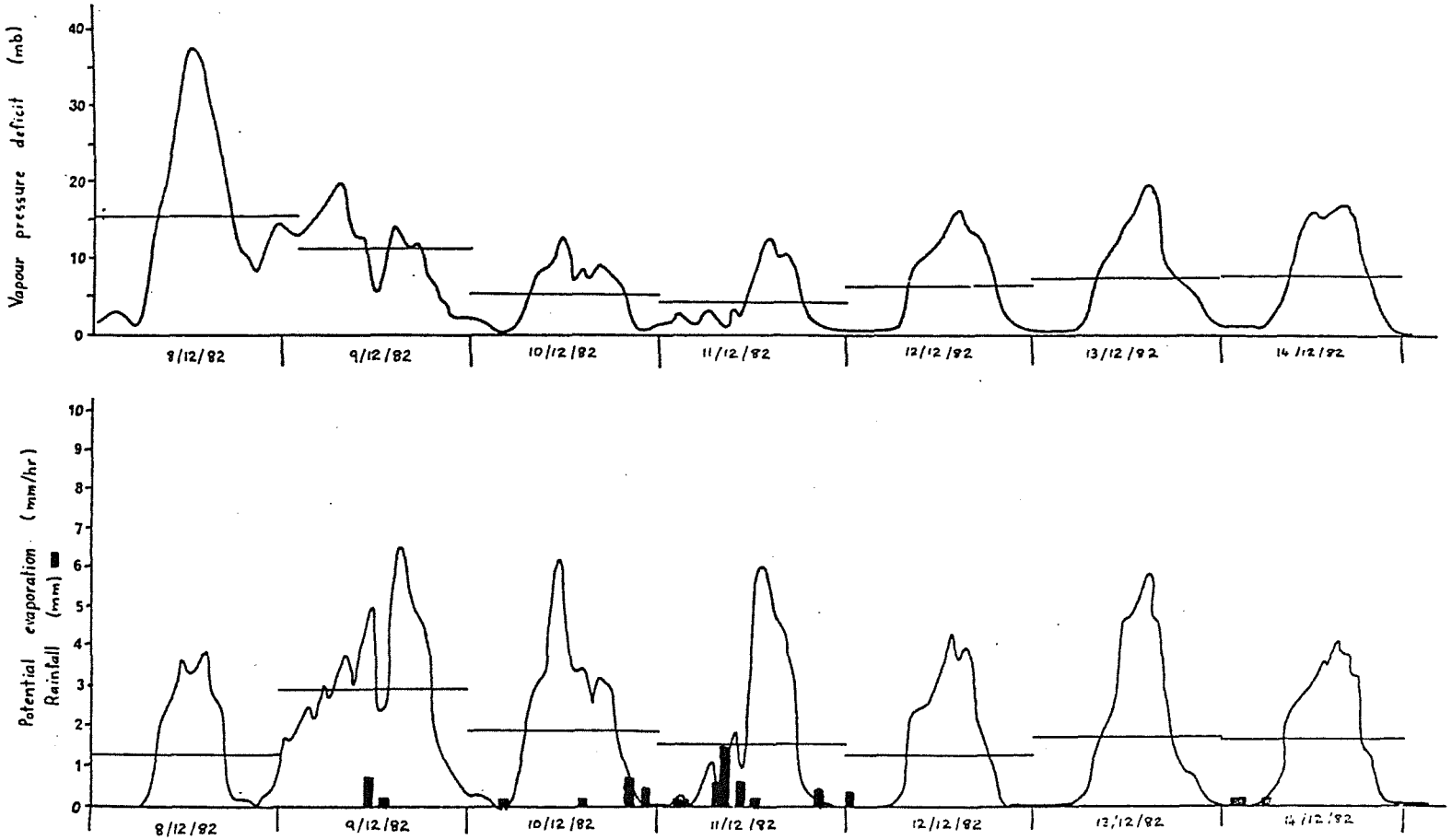

Figure 24 Diurnal effect of vapour pressure deficit on potential evaporation

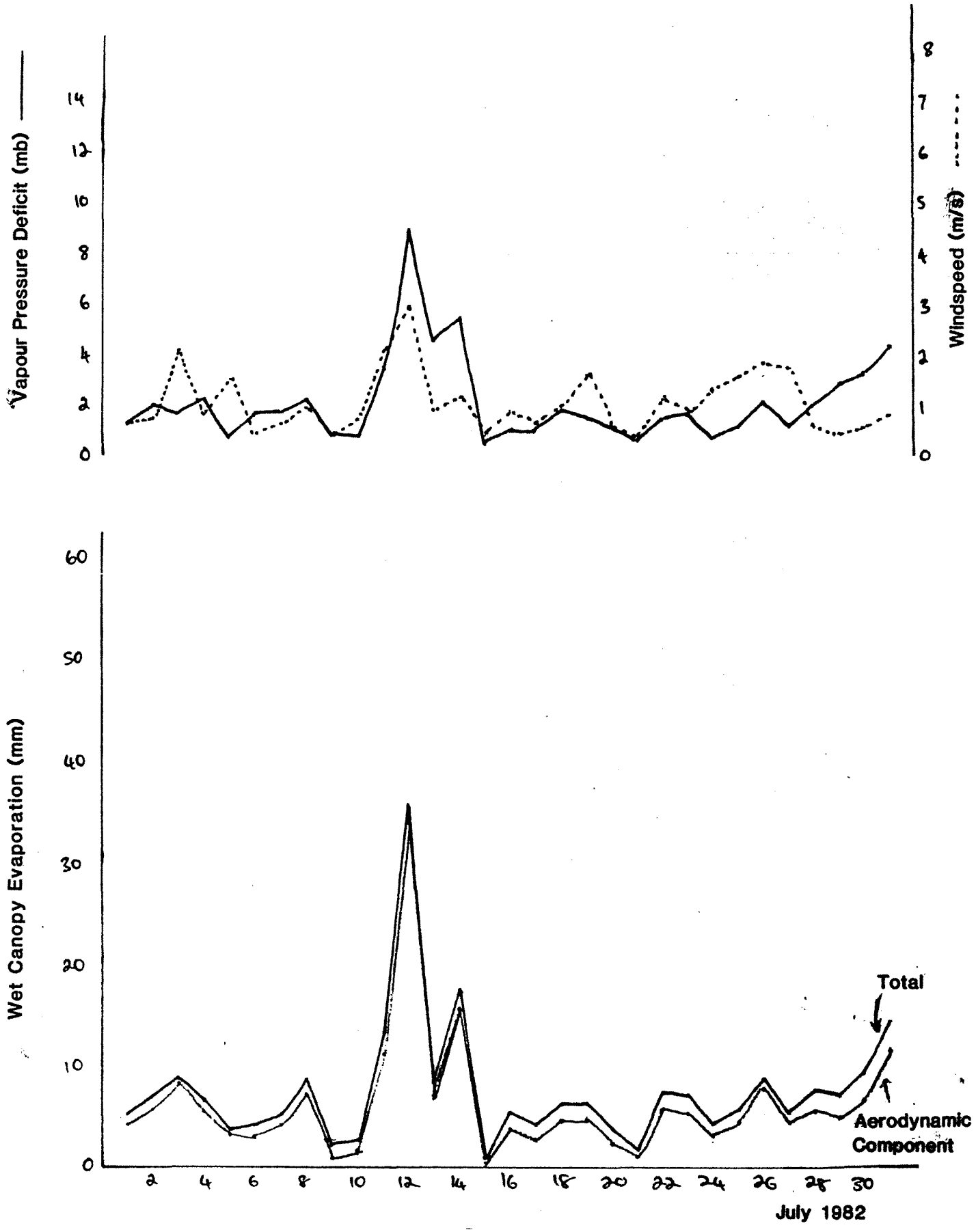

Figure 25 : July 1982 Daily values

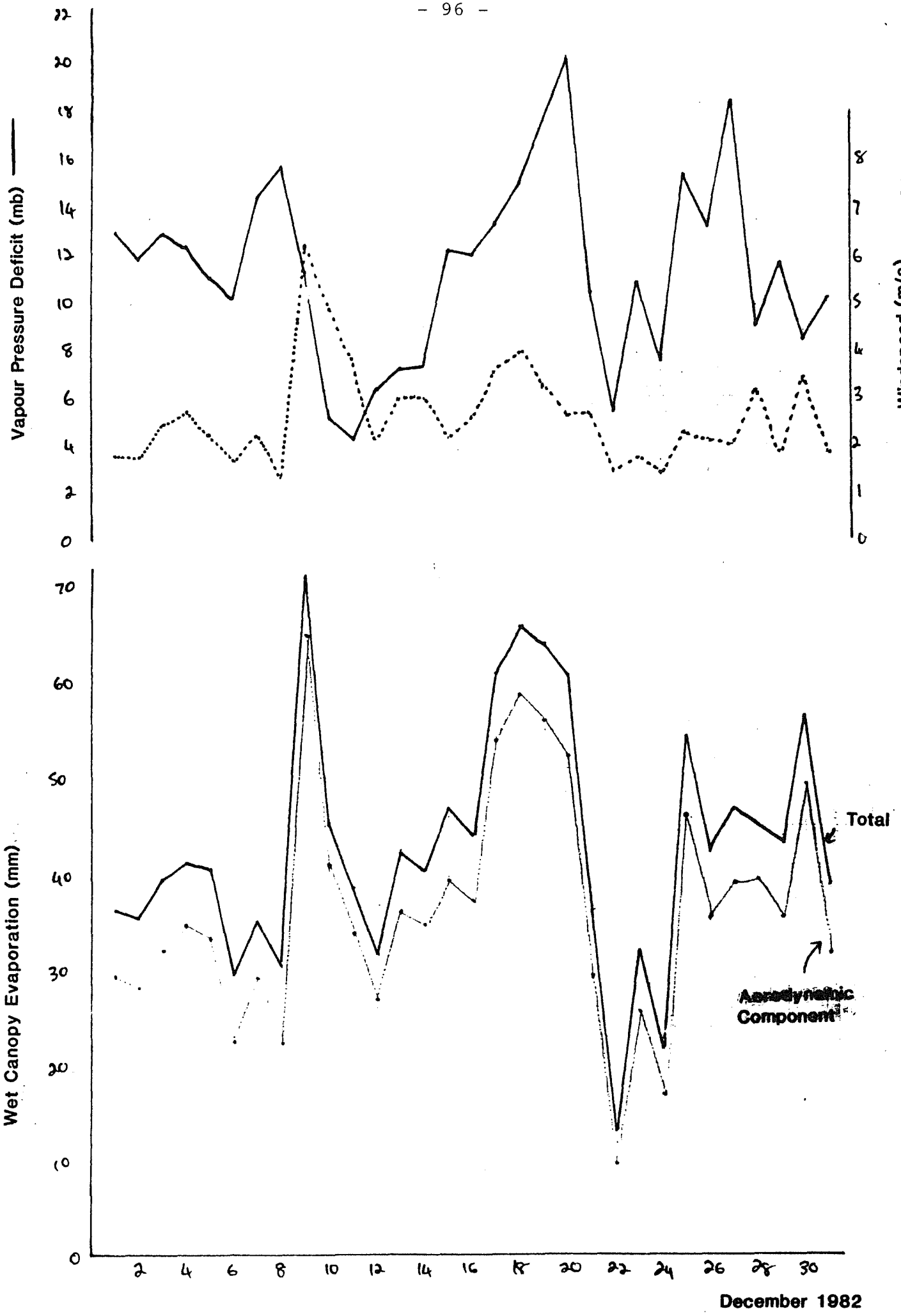

Figure 26 : December 1982 Daily values

TABLE 5.8 Monthly Components of Evaporation

	July 1982	December 1982	December / July
Vapour Pressure[1] Deficit (mb)	2.1	11.5	5.5
Windspeed (m/s)[1]	1.0	2.6	2.6
Available Energy[1] (w/m^2)	53	234	4.4
Aerodynamic[2] Component of Evap (mm)	176.43	1118.84	6.3
Energy Component[2] of Evap (mm)	59.45	211.53	3.6
Total Potential[2] Evaporation (mm)	235.88	1330.37	5.6

1. Values are means of daily values
2. Monthly totals

The dominance of the aerodynamic term stresses the importance of the correct determination of the vapour pressure deficit and the wind speed and profile.

5.4 Pan-Forest Comparison

To use the evaporations recorded from a Class A pan to represent forest evaporation on small time scales has been shown to be a very unsound approach. Even though the Penman equation has been applied to both pan and forest evaporation, important differences exist between the dominant mechanisms operating in each.

As discussed in section 4.3, the lip effect, heat storage and pan albedo all strongly influence pan evaporation, while for forests, the aerodynamic component tends to dominate. For example, in December approximately 85% of pan evaporation is due to the energy component (Table 4.2), while for forest wet canopy evaporation 85% is due to the aerodynamic component. Under wet canopy conditions in December the aerodynamic component still represents about 75% of the evaporation. Thus, the aerodynamic component drives the evaporation of intercepted water and hence would also drive transpiration in the forest canopy.

It must be advised that pan evaporation values should not be used in estimating wet canopy evaporation and hence forest transpiration because different mechanisms, as discussed above, dominate their behaviour.

6. Sensitivity Analysis

6.1 General

To aid in the application of the Penman equation to a forest stand, and to help in understanding the significance of the results obtained, a sensitivity analysis was carried out for each of the inputs required.

Two methods of sensitivity analysis may be used. One method is to obtain a solution from a set of variable values, then increase each variable value a small amount while holding all other values constant and note the change of the solution.

A second approach is to mathematically differentiate the equation or model under study to derive equations for the rate of change of the independent variable with respect to each dependent variable. This approach was used by Saxton (1975) who computed nondimensional sensitivity coefficients, Si, defined by

$$Si = \frac{dE}{dP_i} \frac{P_i}{E} \qquad (85)$$

where E = Penman equation

P_i = constant and time varying parameters.

The sensitivity coefficient is the fractional change in the output, E, divided by the fractional change in the input p.

Beven (1979) extended this approach to the Penman-Montieth equation and applied it to several sites in Britian.

Both Saxton and Beven found that the daily evaporation was most sensitive to net radiation, but Beven also found that for actual evaporation the resistance terms were important, increasingly so for taller vegetation.

Colleman and De Coursey (1976) extended this approach by also computing error variances by

$$\theta^2(E) = \sum_i \frac{(\partial E)^2}{(\partial P_i)} \theta^2(P_i)$$

where $\theta^2(E)$ is the expected variance in evaporation as a function of the analytical derivatives of the model E with respect to the input data P and the variances of these data $\theta^2(P_i)$.

Camillo et al. (1983) and Camillo and Gurney (1984) then eliminated the restrictions involved in these approaches by applying random errors to the input data and computing sensitivies from these. Biases were also added to the errors and the effects of these analysed with respect to the model of Camillo.

Because of the great amount of work that is required to apply this type of sensitivity analysis, the first approach will be used here. It is recognised that this simpler approach may not be the best one.

6.2 Base Data

The two data sets, July 1982 and December 1982 were used here and hence should give an indication of the effects of the climatic variations on the model sensitivity.

The sensitivity analysis here is also limited to unstressed wet forest canopy conditions although some discussion will be made of sensitivity under stressed conditions.

The sensitivies of each parameter will be considered in turn.

For application to a forest, the following parameters were used as reference values. Their development is discussed in chapters 2 and 5 and Appendix D.

canopy height, h = 7.2m
measurement height, z = 1.2h = 8.64m
zero plane displacement, d = 0.62h = 4.46m
roughness length, z_o = 0.1h = 0.72m
albedo, = 0.1
wind factor, WFAC = 2.0

6.3 Net Radiation

In the development of the algorithm for determining the net radiation, as discussed in section 2.2.5, great importance was placed on getting the best estimates of the diurnal variation of net radiation.

The determination of net radiation by factoring measured direct short-wave radiation was considered as a reasonable approach for a day and greater time periods, but it was not considered capable of giving good results for periods less than a day.

Figures 27 to 30 show the differences in net radiation for clear and cloudy days in July and in December by the factor approach as used by Schofield (1982, 1983) as compared to the cloud factor approach developed here.

The factor approach used by Schofield assumes the net radiation is 0.83 the measured direct and diffuse short wave radiation. For July 1982 it gave a monthly evaporation 2% higher than the cloud factor approach, and 0.4% lower in December 1982.

The differences for other factors are shown in Table 6.1

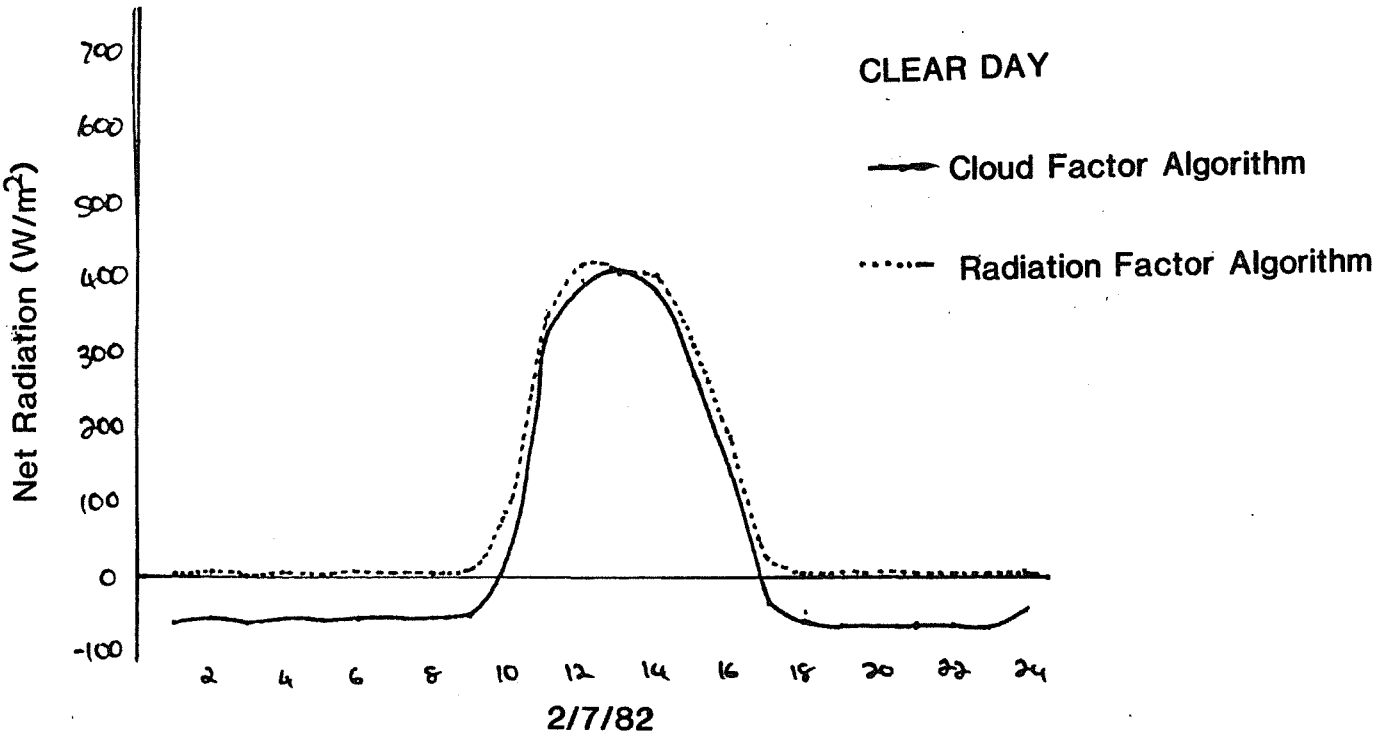

Figure 27 : July Clear Day Comparison

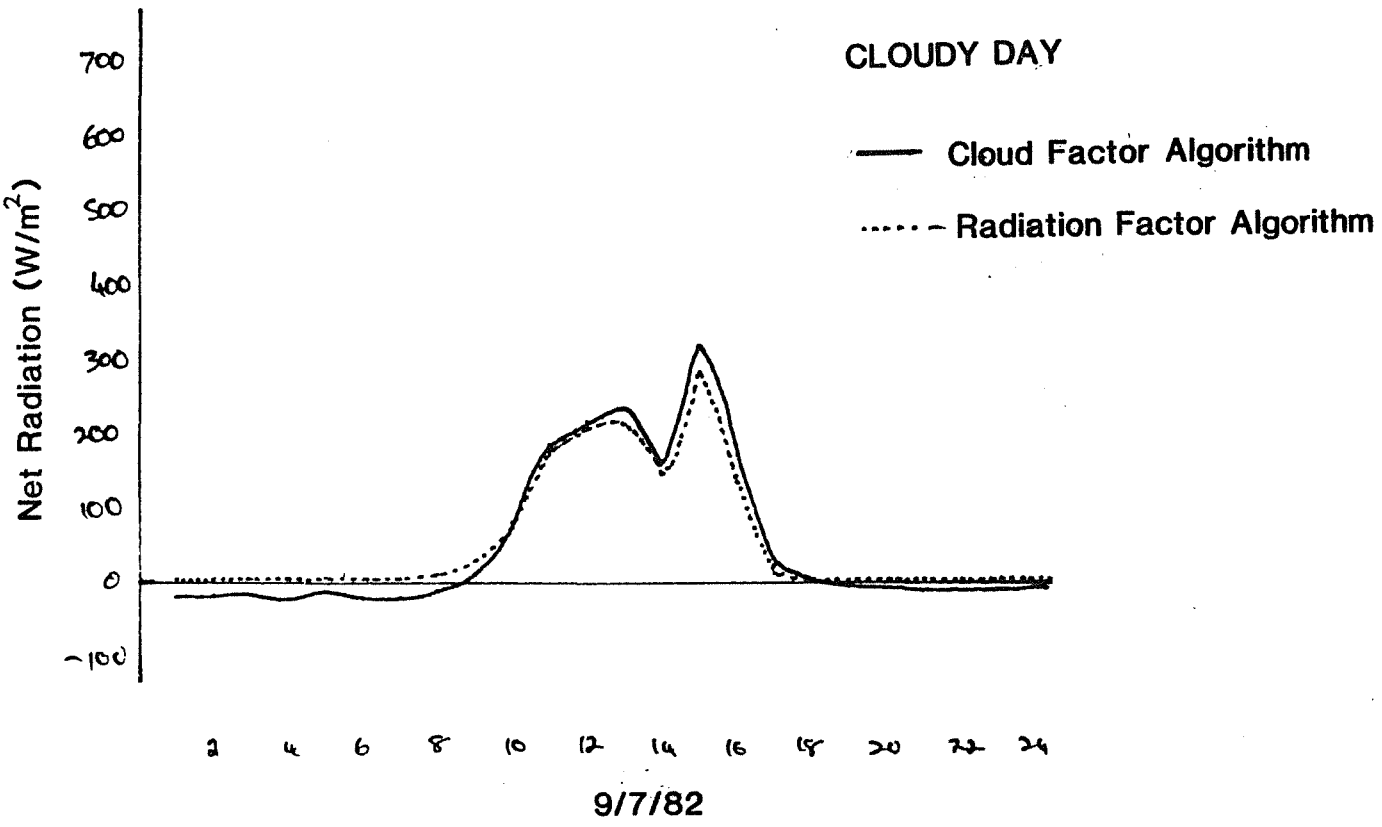

Figure 28 : July Cloudy Day Comparison

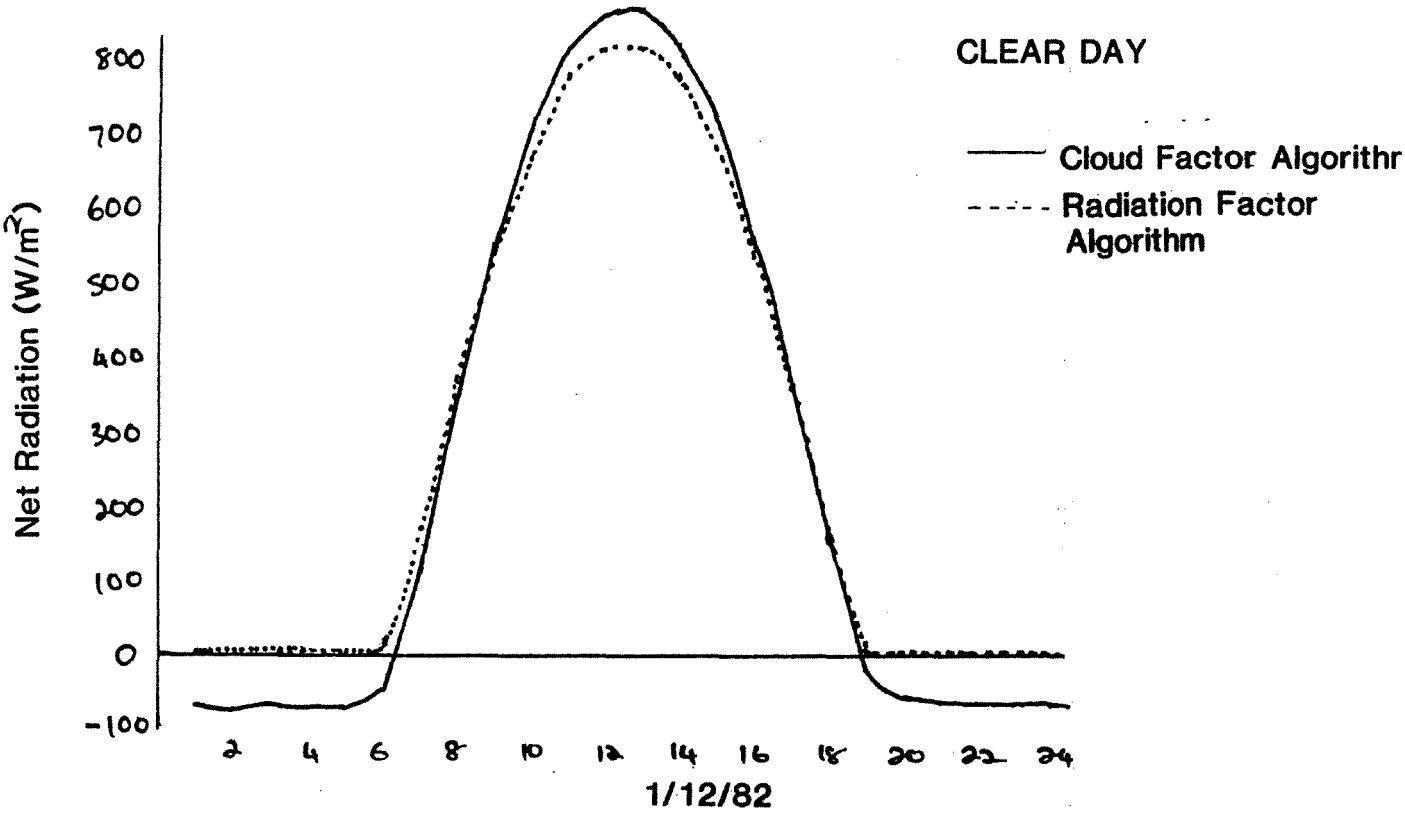

Figure 29 : December Clear Day Comparison

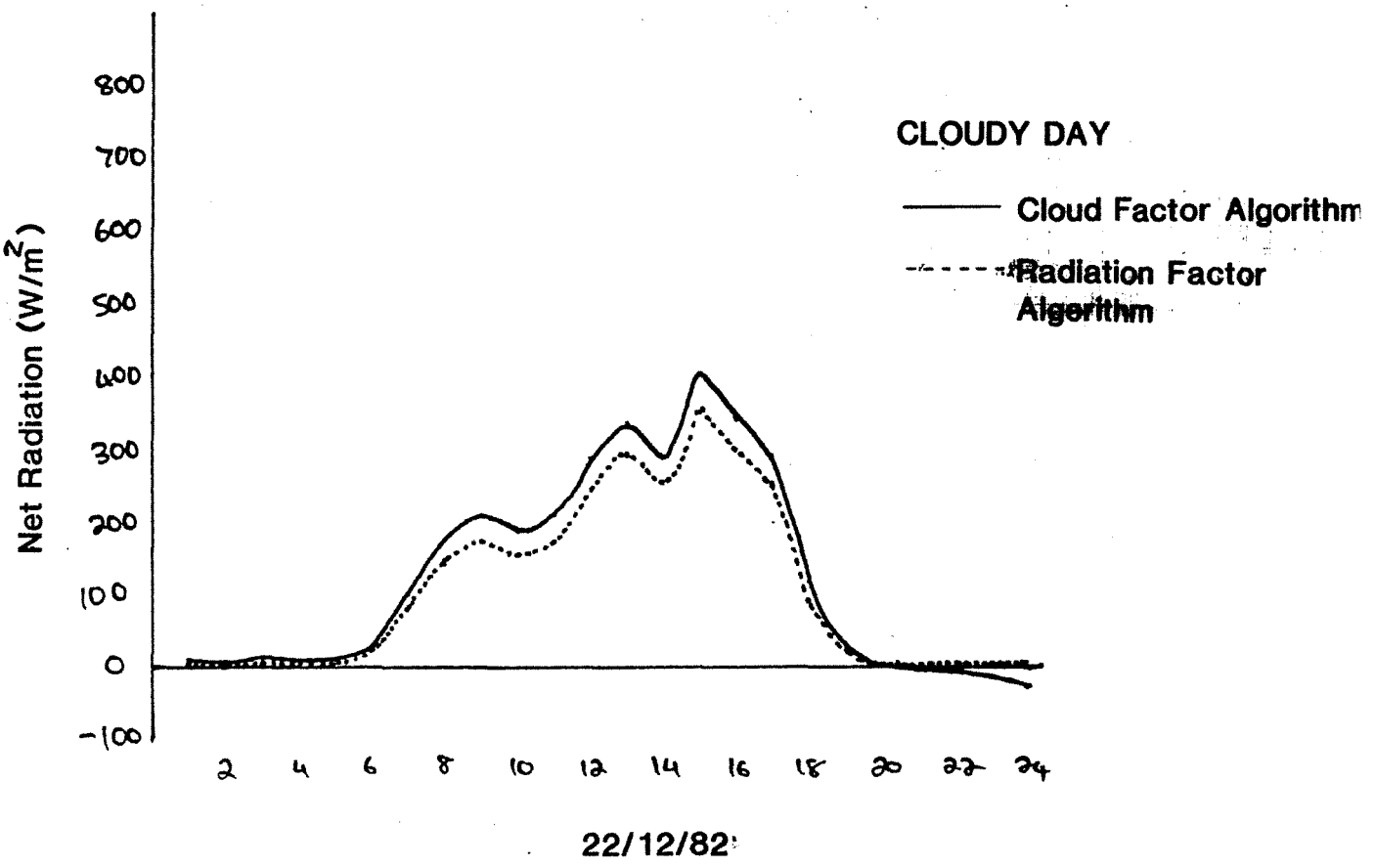

Figure 30 : December Cloudy Day Comparison

TABLE 6.1 Sensitivity of Radiation Algorithm

Radfac	July 82 evap (mm)	Δ%	Dec 82 evap (mm)	Δ%
Cloud factor Algorithm	235.88	0	1330.37	0
0.7	234.68	-0.5	1301.10	-2.2
0.8				
Schofield (1982, 1983)	240.75	+2.0	1325.31	-0.4
0.9	246.81	+4.6	1349.53	+1.4

R_N = Radfac x Rshortwave

The greatest difference between the two approaches occurs at night when there is no short-wave radiation.

The radiation factor approach gives zero net radiation at night while the other more complex approach accounts for the net long-wave radiation at night and the subsequent net energy loss.

This difference would have very little effect on transpiration estimates as most trees do not transpire at night, but it would affect evaporation estimates during this time.

For this reason, the algroithm which estimates long-wave radiation has been included, even though superficially it may seem unimportant.

Also in general, the simplified approach underestimates the net radiation by approximatey 10% at noon. This would thus cause a difference in both the transpiration and evaporation estimates during the day.

On a daily basis, the overestimate at night and underestimate during the day tends to balance out to give daily totals comparable with those found using the cloud factor approach.

To test the sensitivity of the model to variations in radiation, a scaling factor was applied to the total net radiation (short and long-wave) that was estimated. The results of these variations are shown in Table 6.2.

TABLE 6.2 Sensitivity of Radiation Estimate

Radiation Factor	July 82 Evap (mm)	Δ%	December 82 Evap (mm)	Δ%
0.8	227.01	-3.8	1290.36	-3.0
0.9	231.44	-1.9	1310.35	-1.5
1.0	235.88	0	1330.37	0
1.1	240.31	1.9	1350.39	1.5
1.2	244.75	3.8	1370.44	3.0

A 10% error in the radiation estimate only produces an approximately 2% error in the wet canopy evaporation estimate, hence indicating the low sensitivity to the radiation estimate.

On this basis, the only justification for including the estimates of long-wave radiation in the formulation is that the night time energy balance is more correctly defined. This could have a significant influence in a water balance model, where the negative radiation component would indicate condensation. Webb (1975).

If this model is also applied to smaller, thinner trees, say younger replantings, then the aerodynamics will be less important and the energy component will be more sensitive.

The sensitivity to variations in albedo are also not great as shown in Table 5.3. The estimates currently in use thus seem reasonable. Again for smaller trees the albedo will be more important.

TABLE 6.3 Sensitivity of Albedo

Albedo	July 82 Evap (mm)	Δ%	December 82 Evap (mm)	Δ%
0.0	241.80	+2.5	1354.51	+1.8
0.05	238.84	+1.2	1342.44	+0.9
0.10	235.88	0	1330.37	0
0.20	229.96	-2.5	1306.21	-1.8
0.30	224.06	-5.0	1282.07	-3.6

On the basis of this data, it then seems that the installation of a Net Radiometer although desirable, is not justifiable in terms of the sensitivities observed. Also, although better estimates of albedo are desirable they are not strictly necessary for the work here.

It is important however to maintain good quality measurements of direct and diffuse short-wave radiation, and 9am and 3pm cloud cover and type and sunshine duration at some location near the study site at the current accuracy.

It must be realised that these findings are with respect to forest evapotranspiration. Pan evaporation sensitivities should be considerably different to those observed above due to the energy component proportion of total evaporation being much larger than the aerodynamic component when simulating a pan.

6.4 Temperature and Humidity

As discussed in section 3.2.3, the accuracy of air temperature is thought to be only $\pm$ 2.0^{o}C.

If the temperature is considered to have a zero drift error given by TEMPFAC, then the sensitivities in Table 6.4 are obtained.

TABLE 6.4 Sensitivity of Temperature

TEMPFAC	July 82 Evap (mm)	Δ%	December 82 Evap (mm)	Δ%
+ 2.0	249.20	+5.6	1375.71	+3.6
0.0	235.88	0.0	1330.37	0.0
-2.0	222.62	-5.6	1282.45	-3.6

Similarly if a zero shift error, HFAC, is applied to the relative humidity readings the sensitivities in Table 6.5 are found.

A ±10% error in relative humidity is quite high and actual errors are more likely +5%. The sensitivities show that an error or ±2% is required to keep errors in wet canopy evaporation to the same levels as obtained by the other parameters. It is thus recommended that better humidity transducers be installed to record this information.

Previous high error data should not be discarded, but can still be used with caution, and with recognition of the error in evaporation estimates it may produce.

The errors in present measurements are indicated by recorded values of relative humidity greater than 100%.

TABLE 6.5 Sensitivity of Relative Humidity

HFAC %	July 82 Evap(mm)	Δ%	Dec 82 Evap (mm)	Δ%
+10	179.25	-24.0	1111.64	-16.4
+2	223.61	-5.2	1286.23	-3.3
0	235.88	0	1330.37	0
-2	248.89	+5.5	1374.55	+3.3
-10	302.52	+28.2	1551.58	+16.6

It is noted that the sensitivities to both temperature and humidity are greater in the winter period, and are both linear in their sensitivities.

6.5 Aerodynamic Components

The aerodynamic effects of the forest canopy are determined by the windspeed profile above the canopy and the associated roughness parameters. These are discussed in section 2.5 and in Appendix D.

The windspeed above the canopy is determined from that at Ernies and is related by a factor, WFAC. Based on the limited data available this factor, WFAC, is determined in Appendix D to be 2 and represents the windspeed at a height of 1.2 times the vegetation height.

This factor is very sensitive as shown in Table 6.6 and indicates the great need for above canopy measurements. Table 6.7 indicates the large sensitivity also to the selection of the reference level, z, assigned to this empirically related windspeed.

TABLE 6.6 Sensitivity of Wind Factor

WFAC	July 82 Evap (mm)	Δ%	Dec 82 Evap(mm)	Δ%
3.0	331.68	+40.6	1895.63	+42
2.1	245.46	+4.1	1386.88	+4.2
2.0	235.88	0	1330.37	0
1.9	226.30	-4.1	1273.86	-4.2
1.0	140.18	-40.6	765.66	-42

TABLE 6.7 Sensitivity of Reference Level

Reference Level z	July 82 Evap (mm)	Δ%	Dec 82 Evap (mm)	Δ%
1.1h = 7.92m	284.79	+20.7	1619.01	+21.7
1.2h = 8.64m	235.88	0	1330.37	0
1.3h = 9.36m	205.45	-12.9	1150.84	-13.5

h = vegetation height

Also of critical importance is the selection of the zero plane displacement, d, and roughness length, z_o.

Using values selected from Figure D2 in Appendix D, the very large differences in results that were obtained are shown in Table 6.8. The values selected for application to the forest in this study were

$$d = 0.62h = 4.46m$$

and $$z_o = 0.1h = 0.72m$$

In all except one instance, the present parameters used underestimate by up to 45% the wet canopy forest evaporation. Using a lower z_o will reduce the estimated evaporation, as will using a lower d.

It is important to note here how critical the roughness parameters are, and the need to evaluate them more accurately.

If values are simply chosen from the literature, say those quoted by Schofield (1982) in comparison to those given by Jarvis et al (1976) as given in Table 6.8, then the seemingly small difference in d of 7% will given evaporations up to 11% different and 30% different to the current values used.

It is recommended that above canopy profile measurements be taken to produce more reliable estimates of d and z_o and then continuous windrun measurements be taken above the canopy at the site in question. Considering how important and sensitive the aerodynamics of the forest are, this would be easily justified in future studies.

TABLE 6.8 Comparison of roughness parameters sensitivity

	$\frac{d}{h}$	$\frac{z_o}{h}$	r_a s/m	Δr_a%	July 82 evap (mm)	Δ%	Dec 82 evap (mm)	Δ%
(1)	0.62	0.1	4.8/u	0	235.88	0	1330.37	0
(2)	0.50	0.17	11.97/u	149	338.82	+43.6	1937.77	+45.7
(3)	0.75	0.05	8.8/u	83	167.10	+30.0	924.5	-30.5
(4)	0.75	0.1	13.4/u	179	306.27	+29.8	1745.71	+31.2
(5)	0.7	0.1	15.4/u	220	273.09	+15.8	1549.9	+16.5

d = zeroplane displacement (m)
z_o = roughness length (m)
h = vegetation height (m)
u = windspeed (m/s)
r_a = aerodynamic resistance (s/m)

(1) Values used in present modelling
(2) Upper point on observed relationship curve, Figure D2
(3) Lower point on observed relationship curve, Figure D2
(4) Point A, Figure D2. Schofield (1982) (leafy canopies)
(5) Point E, Figure D2. Jarvis et al (1976) (30m forests)

6.6 Surface Resistance

Although only wet canopy conditions are being assumed at this stage, future applications will include dry and partially wet canopy conditions.

This will then introduce a non-zero surface resistance term in the Penman Monteith equation. The aerodynamic resistance term is then retained in the denominator of equation (82). The high sensitivities to the aerodynamic related parameters will then be greatly reduced and their accurate determination will become far less important.

Future work on the transpiration losses of forests will look closer at the sensitivities in the Penman Monteith equation for stressed canopy conditions. Relative humidity and the associated vapour pressure deficit and the surface resistance term r_s, are expected to be the most sensitive terms under the stressed conditions.

7. Conclusions

This report has described the physical basis for the Penman-Monteith equation and has presented a detailed derivation of the equation data requirements for the short term application of the equation. Methods of estimating net long and short-wave radiation components without direct measurements are reviewed, and a means of estimating long-wave radiation is developed.

The Penman equation was used to model Class A pan evaporation and evaporation from a forest canopy typical of trees replanted as part of the reforestation project in the Wellington Catchment area.

The rates of evaporation of intercepted rainfall were also estimated to be of order 40% of the wet canopy evaporation rates calculated using dry canopy climatological data, indicating the significance of canopy feedback effects on reducing vapour pressure deficits above and within forest canopies.

An approach has been developed for estimating the long-wave radiation in the evaporation energy balance. The approach is suitable for short term (15 minute) modelling, but it is yet to be tested for longer term modelling. Cloud amount and type, and sunshine duration data at a nearby site is required.

Application of the Penman equation to the Class A evaporation pan indicated a pan roughness length of 1mm. It is also indicated that of order 10% of the short-wave radiation penetrating the water surface in the pan can be lost due to reflectance off the pan base and sides. Water heat storage effects were found to have a dominant effect on the diurnal distribution of pan evaporation.

In comparing pan and forest evaporation it was found that the lip effect, heat storage and pan albedo all strongly influence pan evaporation, while for forests, the aerodynamic component dominates. For example, about 80% of pan evaporation is due to available energy, while only about 20% of forest evaporation is due to available energy, the balance of the evaporation being due to the aerodynamic component.

An investigation into the use of birdguard factors on pans found them to vary considerably throughout the year, not remaining constant as is generally assumed.

A comparison of the dynamics of pan and lake evaporation identified the problems that can occur if pan evaporation is used as being truly representative of lake evaporation. It was found that modified pans can be used in some cases to give improved estimates of lake evaporation.

A sensitivity analysis on unstressed wet canopy forest evaporations demonstrated that the most sensitive terms in the Penman Monteith equation are relative humidity and the associated vapour pressure deficit, wind speed and the roughness parameters used to calculate the aerodynamic resistance.

Overall, this work provides the important basis for future evapotranspiration modelling. Only by a thorough understanding of evapotranspiration can the results of future modelling be utilised to the utmost.

8. References

Anderson, E.R. (1952). Energy Budget Studies in Water Loss Investigations. Vol 1 - Lake Hefner Studies Technical Report. U.S. Dept. Int. Geol. Surv. Circular 229.

Anderson, M., Loh, I., Stone, K. (1982). Groundwater Monitoring of Reforestation Strip Plantings Site. Bingham River Valley. PWD WRB Report 20.

Baumgartner, A. (1967). Energetic Bases for Differential Vapourization from Forest and Agricultural Lands in "International Symposium on Forest Hydrology". Ed. Sopper, W.E. and Lull, H.W.

Beven, K. (1979). A Sensitivity Analysis of the Penman-Monteith Actual Evapotranspiration Estimates. J. Hydrol., 44, 169-190.

Black, R.E. and Rosher, J.E. (1980). The Peel Inlet and Harvey Estuary System Hydrology and Meteorology. Dep. Cons. Env. Bull., 89.

Camillo, P.J. and Gurney, R.J. (1984). A Sensitivity Analysis of a Numerical Model for Estimating Evapotranspiration. W.R.R., 20, 105-112.

Camillo, P.J., Gurney, R.J. and Schmugge, T.G. (1983). A Soil and Atmospheric Boundary Layer Model for Evapotranspiration and Soil Moisture Studies, W.R.R., 19, 371-380.

Chapman, T.G. (1979). Hydrologic Process Modelling. Lecture notes, Dept. Civil Eng. U.N.S.W. (unpublished).

Coleman, G. and De Coursey, D.G. (1976). Sensitivity and Model Variance Analysis Applied to Some Evaporation and Evapotranspiration Models. W.R.R., 12, 873-879.

Cowan, I.C. (1968). Mass Heat and Momentum Exchange Between Stands of Plants and their Atmospheric Environment. O.J.R. Meteorol. Soc., 94, 523-541.

Cunningham, D.B. (1974). Evaporation Simulation between a Pan and a Solar Salt Pond. B.E. Honours Thesis U.W.A. Dept. Civ. Eng.

Edgeloe, R.W., Loh, 1.C. (1983). The Development of Humidity Record for Ernies Experimental Catchment. Collie Region, South Western Australia. PWD WRB Report 65, 1983.

Enz, J.W., Klink, J.C. and Baker, D.G. (1975). Solar Radiation Effects on Pyrgeometer Performance. J. Appl. Meteorol., 14, 1297-1302.

Fleming, P.M. (1971). The Calculation of Clear-Day Solar Radiation on any surface. Paper in AIRAH Federal Conference, May 1971.

Funk, J.P. (1958). Improved Polythene Shielded Net Radiometer. J. Sci. Instrum., 36, 267-270.

Gash, J.H.C. (1979). An Analytical Model of Rainfall Interception by Forests. Q.J.R. Meteorol. Soc., 105, 43-55.

Gash, J.H.C., Wright, I.R., and Lloyd, C.R. (1980). Comparative Estimates of Interception Loss from Three Coniferous Forests in Great Britain. J. Hyd., 48, 89-105.

Hawkins, B.J. (1981). J.C. Industires Evaporation Transducer. Operation and Maintenance P.W.D. W.R.B. Bulletin No. 12, Part B (iii).

Hawkins, B.J. (1982a). Rimco Digital Transducers (ii) Wind Run Standard Anemometer PWD WRB Bulletin No. 12, Part B.

Hawkins, B.J. (1982b). File Note, Water Resources Section, Stn No 509 249 History File.

Hawkins, B.J. (1983). Rimco Digital Transducers (iv) Global Radiation Integrating Pyranometer. P.W.D. W.R.B. Bulletin No. 12, Part B.

Hicks, B.B. (1973). Eddy Fluxes over a Vineyard. Agric. Meteor., 12, 203-215.

Hicks, B.B., Hyson, P. and Moore, C.J. (1975). A Study of Eddy Fluxes over a Forest. J. Appl. Met., 14, 58-66.

Holmes, J.W., Wronski, E.B. (1980). The Influence of Plant Communities Upon the Hydrology of Catchments. Land and Stream Salinity Seminar, Perth, Elselvier.

Hounam, C.E. (1964). An Advisory Note on the Australian Standard Evaporimeter and Expansion of the Network. Bureau of Meteorology Working Paper 64/1770 of August 1964.

Hoy, R.D. and Stephens, S.K. (1979). Field Study of Lake Evaporation - Analysis of Data from Phase 2. Storages and Summary of Phase 1 and Phase 2. AWRC Technical Paper No 41.

Idso, S.B. and Jackson, R.D. (1969). Thermal Radiation from the Atmosphere. J. Geophysical Research., Vol. 74, No. 23, Oct 20, 1969.

James, G.B. and Jarvis, P.G. (1983). Carbon Dioxide and Water Vapour Exchange by a Sitka Spruce Forest Canopy. 2: Evaporation and Surface Resistance. Plant Cell Environ. (in press).

Jarvis, P.B., James, G.B. and Landsberg, J.J. (1976). Coniferous Forests In "Vegetation and the Atmosphere" Vol. 2., (Ed. J.L. Monteith) (Academic Press : NY) 171-236.

Kohler, M.A. (1954). Lake and Pan Evaporation. Chapter in Water-Loss Investigation; Volume 1 - Lake Hefner Studies, Technical Report U.S. Geol. Surv. Prof., Paper 269, 127-146.

Leuning, R. and Attiwill, P.M. (1978). Mass, heat and momemtum exchange between a mature Ecualyptus forest and the Atmosphere. Agric. Meteorol., 19, 215-241.

Linacre, E. (1975). Aspects of Evaporation. Lecture Notes, 04320 Micrometeorology, Maquarie University.

McNaughton, K.G. and Black, T.A. (1973). A Study of Evapotranspiration from a Douglas Fir Forest using the Energy Balance Approach. W.R.R., 9, 1579-1890.

McNaughton, K.G. and Jarvis, P.G. (1983). Effects of Vegetation on Transpiration and Evaporation. Chapter in "Water Deficits and Plant Growth". ed. T.T. Kozlowski Vol VII Additional Woody Crop Plants. Academic Press, 2-47.

Mills, G.A. (1975). A Comparison of Some Formulae for the Calculation of Saturation Vapour Pressure over Water. Australian Bureau of Meteorology Meteorological Note 82.

Monteith, J.L. (1965). Evaporation and Environment. In : "The State and Movement of Water in Living Organisms". Sym. Soc. Exp. Biol., 19, 205-234.

Moore, C.J. (1976). Eddy Flux Measurement above a Pine Forest. Q.J.R. Meteorol., Soc. 102, 913-918.

Pearce, A.J., Gash, J.H.C. and Stewart, J.B. (1980). Rainfall Interception in a Forest Stand Estimated from Grassland Meteorological Data. J. Hyd., 46, 147-163.

Pearce, A.J. and Rowe, L.K. (1981). Rainfall Interception in a Multi-Storied Evergreen Mixed Forest, Estimates using Gash's Analytical Model, J. Hyd., 49, 341-353.

Penman, H.L. (1948). Natural Evaporation from Open Water, Bare Soil, and Grass. Proc. Roy. Soc. London, A193, 120-245.

Riou, Ch. (1984). Simplified Calculation of the Zero-plane Displacment from Wind Speed Profiles. J. Hyd., 69, 351-357.

Rouse, W.R. (1984). Microclimate at Arctic Tree Line. Radiation Balance of Tundra and Forest. W.R.R., Vol. 20, No. 1 57-66.

Rouse, W.R. and Wilson, R.G. (1972). A Test of the Potential Accuracy of the Water Budget Approach to Estimating Evapotranspiration. Agric Meteorol., 9:421-446.

Rutter, A.J., Kershaw, K.A., Robins, P.C. and Morton, A.J. (1971). A Predictive Model of Rainfall Interception in Forests. 1 : Derivation of the Model from Observations in a Plantation of Corsican Pine. Agric. Met., 9. 367-384.

Rutter, A.J., Morton, A.J. and Robins, P.C. (1975). A Predictive Model of Rainfall Interception in Forests : 11 Generalisation of the Model and Comparison with Observations in Some Coniferous and Hardwood stands. J. Appl. Ecol., 12, 367-380.

Sadler, B.S. and Williams, P.J. (1980). The Evolution of A Regional Approach to Salinity Management in Western Australia. Land and Stream Salinity Seminar, Perth, Elselvier.

Saxton, K.E. (1972). Watershed Evapotrasnpiration by the Comination Method. PhD Thesis. Iowa State Univ. Lib. Ames. Ia (Dissertatin Abst. Int. 33(4) : 1514b - 1515b. 1972).

Saxton, K.E. (1975). Sensitivity Analyses of the Combination Evapotranspiration equation. Agric. Meteorol., 343-353.

Sceicz, G. and Long, I.F. (1969). Surface Resistance of Crop Canopies. W.R.R., 5(3) : 622-633.

Schofield, N.J. (1982). A Hydrological Computer Model to Aid in the Design of Reforestation programmes for the Control of Stream Salinisation in Water Resource Catchments in the South-West Western Australia Part A : The Interception Model. W.A.1.T. School of Physics & Geosciences. Report No SPG 296/1982/AP36.

Schofield, N.J. (1983). InterI : A Numerical Model to predict annual interception losses for different reforestation species in south-west Western Australia, application to E. Globulus, E. Wandoo and E. Leucoxylon for two winter periods. Report No : SPG 329/1983/AP65.

Sellers, W.D. (1965). Physical Climatology (Univ. Chicago Press).

Shuttleworth, W.J. (1979). Evaporation. Institute of Hydrology Report No. 56.

Singh, B. and Szeicz, G. (1979). The Effect of Intercepted Rainfall on the Water Balance of a Hardwood Forest. W.R.R., Vol 15, No. 1, 131-138.

Stone, R.A. (1979). Climatological Stations, Purposes, Equipment and Operational Procedures. P.W.D. Water Resources Technical Report No 86.

Tajchman, S.J. (1971). Evapotranspiration and Energy Balances of Forest & Field. W.R.R., : 511-523.

T.V.A. (1972). Tennesee Valley Authority. Heat and Mass Transfer between a Water Surface and the Atmosphere. Lab Report No 0-6803.

Van Dijk, M.H. (1975). Evaluation of a Birdguard for Class A Evaporation Pans. Bureau of Meteorology, unpublished report.

Webb, E.K. (1966). A Pan-Lake Evaporation Relationship. J. Hydr. 4., 1-11.

Webb, E.K. (1975). Evaporation from catchments in "Prediction in Catchment Hydrology". ed T.G. Chapman & F.X. Dunin. 203-236.

Wiesner, C.J. (1970). Hydrometeorology. Chapman and Hall, London.

Yu, S.L. and Brutsaert, W., (1967). Evaporation from Very Shallow Pans. J. Appl. Meteorol., Vol. 6, No. 2, 265-271.

8250R
8252R

Appendix A

Simplified Derivation of Penman Monteith Equation

Appendix A

Simplified Derivation of Penman Monteith Equation.

Chapman (1979) gives a simple derivation of the Penman Monteith equation.

The basis of each equation is given in Chapter 2.

For any time period, an energy balance can be written as

$$R_n - G = H + \lambda E \qquad (A1)$$

where R_n = net radiation on the surface (w/m^2)
G = soil heat flux into ground (w/m^2)
H = sensible heat flux from surface to air (w/m^2)
E = evaporation from surface to air (kg/m^2s or mm)
λ = latent heat of vaporisation of water (J/kg)

The problem in equation (A1) is to determine H, as R_n and G can be measured or estimated.

The sensible heat flux H is related to the temperature gradient and wind profile by

$$H = \rho C_p f(u_z)(T_s - T_z) \qquad (A2)$$

where ρ = density of moist air (kg/m^3)
C_p = specific heat of moist air at constant pressure ($J/kg/^oC$)
z = 0 is a reference datum
s = denotes the evaporation surface
u_z = wind velocity at height z

$f(u_z)$ has units (m/s) and for a sufficiently large area can be given by the KEYPS profile.

$$f(u_z) = k^2 u_z \ (\phi + \ln ((z+d+Z_o)/Z_o))^{-2} \qquad (A3)$$

where k = Von Karmans constant (0.43)
ϕ = diabatic profile parameter
d = zero plane displacement (m)
z_o = roughness length (m)
z = reference datum

For irrigated crops ϕ = 0 and this is also generally applied to other surfaces also (Sellers (1965)).

In equation (A2), the measurement of the surface temperature T_s becomes the problem when dealing with vegetation. An alternative aerodynamic approach is the Dalton equation

$$E = \rho f(u_z)(q_s - q_z) \qquad (A4)$$

where q = specific humidity (m^3/kg)

The problem in equation (A4) is the measurement of q_s

The need to measure T_s and q_s can be removed by eliminating these terms from equations (A1), (A2) and (A3)

From equation (A4)

$$\begin{aligned} E &= \rho f(u_z)\ (q_s - q_z) \qquad (A5) \\ &= \rho f(u_z)\ (q_s - q_s^* + q_s^* - q_z^* + q_z^* - q_z) \end{aligned}$$

where * denotes the saturated value at the same temperature.

Now q_s^* will be approximately the specific humidity q_i in the sub-stomatal cavity so that the change in specific humidity between the inside and outside of the leaf is $q_s^* - q_s$, and in dimsionless form is $(q_s^* - q_s)$

Since the flow is E, a leaf surface resistance can be defined in analogy to Ohms law by;

$$r_s = \rho(q_s^* - q_s)/E \qquad (A6)$$

Similarly an aerodynamic resistance r_a can be defined for the change in specific humidity between the outside of the leaf and the general atmosphere, by

$$r_a = \rho(q_s - q_z)/E \qquad (A7)$$

which from equation (A4) is

$$r_a = 1/f(u_z) \qquad (A8)$$

The aerodynamic resistance r_a also has units (s/m).

The second pair of terms in equation (A5), the quantity $q_s^* - q_z^*$ is a function of temperature only, and can be written

$$q_s^* - q_z^* = \Delta(T_s - T_z) \qquad (A9)$$

where Δ = the slope of the saturation vapour pressure curve (q^* against T) at the midpoint between T_s and T_z.

Finally for the third pair of terms in equation (A5) we define the aerodynamic evaporation

$$Ea = \rho f(u_z)(q^*_z - q_z) \qquad (A10)$$

Substituting from equations (A6), (A9) and (A10) into (A5) gives

$$E = - \rho f(u_z) r_s E/\rho + \rho f(u_z) \Delta (T_s - T_z) + Ea$$

using equations (A8) and (A2) then gives

$$E = - E\, r_s/r_a + \Delta H/C_p + Ea \qquad (A11)$$

Defining the psychrometric constant

$$\gamma = Cp/\lambda \qquad (A12)$$

where γ has a value of about $4.2 \times 10^{-4}/^{o}C$ at $20^{o}C$

equations (A11) and (A12) combine to give

$$E = -\frac{r_s}{r_a} E + \frac{\Delta H}{\gamma\lambda} + Ea \qquad (A13)$$

Substituting from equation (A1) to eliminate H

$$E = \frac{-r_s}{r_a} E + \frac{\Delta}{\gamma}\left(\left(\frac{R_N - G}{\lambda}\right) - E\right) + Ea$$

rearranging gives

$$E = \frac{\Delta/\gamma\ (R_N - G) + \lambda\ Ea}{\lambda\ (1 + \Delta/\gamma + \frac{r_s}{r_a})} \qquad (A14)$$

the Penman Monteith Equation

When the vegetation is transpiring freely $r_s << r_a$ and the potential evaporation Ep is found by equating r_s to zero to give;

$$E = \frac{\Delta/\gamma\ (R_N - G) + \lambda\ Ea}{\lambda\ (1 + \Delta/\gamma)} \qquad (A15)$$

which is the same form as that obtained by Penman (1948).

In summary the Penman Monteith equation and units are given by equation (A14)

where E = evaporation (kg/m^2s or mm/s)
R_N = net radiation (W/m^2)
G = soil heat flux (W/m^2)
Ea = aerodynamic evaporation (mm/s)
Δ/γ = $\frac{\text{slope of the saturated vapour pressure curve}}{\text{psychrometric constant}}$
λ = latent heat of vaporisation of water (J/kg)
r_s = surface resistance (s/m)
r_a = aerodynamic resistance (s/m)

Appendix B

Calculation of Clear-Day Solar Radiation

Appendix B

Calculation of Clear-Day Solar Radiation

As there can be problems in the measurement of solar radiation, it is often desirable to check recorded values with estimates based on solar radiation through a model atmosphere.

Fleming (1971) presents a method for the calculation of clear-day solar radiation on any surface.

A model atmosphere approach to attenuate and partition clear-day solar radiation into direct and diffuse components is used.

The simple model consists of four processes:

(i) absorption by water vapour,
(ii) scattering by dust,
(iii) scattering by water vapour, and
(iv) scattering by a dry dust free atmosphere

It is assumed that absorption takes place first, followed by scattering and that scattering is half forward and half back scattering. The scattered radiation gives rise to the diffuse radiation component without further absorption. Absorption by ozone and carbon dioxide is assumed to have been allowed for in the dust free scattering.

Each component is given its own optical air mass which is a function of the geometric air mass, m, and the water vapour concentration relative to a standard concentration.

The standard concentration of water vapour is a precipitable water content of 1cm.

T.V.A. (1972) gives the geometric air mass corrected for local atmospheric pressure as

$$m = \frac{((288-0.0065.Z)/288)^{5.256}}{\sin\alpha + 0.15\ (\alpha + 3.885)^{-1.253}} \qquad (B1)$$

where α = solar altitude (degrees)
z = elevation of site above mean sea level (m)

The calculation of the solar altitude, is given in Appendix C. The optical path length water content u* is given by

$$u^* = u.m \qquad (B2)$$

where u = precipitable water content of a vertical sounding (cm)
m = geometric air mass

To determine precipitable water content accurately, soundings of pressure and humidity at intervals in a vertical column are required. In the absence of this data a linear relationship between surface vapour pressure and precipitable water content can be used

$$\text{ie} \quad u = \frac{pe}{10} \qquad (B3)$$

u = precipitable water content (cm)
e = surface vapour pressure (mb)
p = local constant = 1.5

The absorption by water vapour, a(u*), is then given by

$$a(u^*) = 0.077u^{*0.3} \qquad (B4)$$

the transmittance after scattering, t(u*), by

$$t(u^*) = 0.975u^* \qquad (B5)$$

the transmittance after scattering by dust, t(D), is given by

$$t(D) = 0.95^{mD} \qquad (B6)$$

where D = dust factor equal to 1 for average conditions and the transmittance after scattering by a clean dry atmosphere t(A) by

$$t(A) = 0.9m^* + 0.026\ (m^*-1) \qquad (B7)$$

where $m^* = P/Po$

P = average barometric pressure (mb)

Po = standard barometric pressure, 1013 (mb)

The average barometric pressure can be estimated by the elevation above sea level.

The direct beam intensity, I_{DN}, after passing through the model atmosphere is then given by

$$I_{DN} = I_o\ (1-a(u^*))\ t(u^*)\ t(D)\ t(A) \qquad (B8)$$

where I_o = direct beam intensity at the top of the atmosphere. I_o is a function of the sun-earth distance and the solar constant, I_c, related through the inverse square law.

$$I_o = I_c\ R_c^2/R_o^2 \qquad (B9)$$

where R_c = mean sun earth distance

R_o = actual sun earth distance

I_c = solar constant = 1395 (w/m^2)

The intensity of the beam which is incident to a horizontal surface at an angle equal to the solar altitude, α, is then given by

$$I_{DHOR} = I_{DN} \sin\alpha \qquad (BIO)$$

The diffuse component of radiation results from the scattered radiation attenuating the direct beam. The model assumes 50% is forward scattered in the direction of the beam and 50% is back scattered and so is lost.

The diffuse component intercepted by a plane normal to the direct beam I_{DIFFN} is given by

$$I_{DIFFN} = 0.5\ (I_o\ (1-a(u^*))-I_{DN}) \qquad (B11)$$

Thus the intensity on a horizontal surface, I_{DIFHOR}, is given by

$$I_{DIFHOR} = I_{DIFFN} \sin\alpha \qquad (B12)$$

The total direct and diffuse radiation component, I_{DD}, as measured by the P.W.D. pyranometers is given by

$$I_{DD} = I_{DHOR} + I_{DIFHOR} \qquad (B13)$$

This formulation was applied to a clear day in December 1982 at the Ernies Climat Station at noon to check the magnitude of direct and diffuse radiation being recorded.

For the 17th December 1982 the noon temperature was 26^{o}C and the humidity 41%. This gives a vapour pressure, e, by

$$e = e_{SAT} \times RH/100 \qquad (B14)$$

where e_{sat} = saturated vapour pressure at given temperature (mb)

RH = relative humidity (%)

ie e is approximately 18mb. Thus by equation (B3) the precipitable water content is 2.7cm, as compared to the standard of 1.0 cm.

Using as an approximation at noon, m=1 and $\alpha = 90^{o}$, by equation (B2) the optical path length water content, u*, equals 2.7cm.

Thus from equations (B4), (B5), (B6) and (B7),

$a(u^*) = 0.10$

$t(u^*) = 0.93$

$t(D) = 0.95$

$t(A) = 0.9$

Substituting into equations (B10), (B12) and (B13) gives

$$\text{direct beam intensity } I_{DHOR} = 0.7\ I_o$$
$$\text{diffuse beam intensity } I_{DIFHOR} = 0.1\ I_o$$
$$\text{total direct and diffuse } I_{DD} = 0.8\ I_o$$

where I_o is the direct beam intensity at the top of the atmosphere.

Thus at noon on this day, under the assumptions of the model, only 20% of the direct radiation incident at the top of the atmosphere would be lost on transit through the atmosphere.

On days with cloud cover, the loss of short-wave radiation would be greater and hence a lower recording would result. This would be partly compensated for by increase atmospheric long-wave radiation, but this is not recorded by the shortwave pyranometers.

The recorded direct and diffuse component on the 17th of December was 1033 w/m^2 which using a calculated I_o of 1417 w/m^2 represents a reduction of 27% as compared to 20% by the model.

The values of radiation being recorded are thus consistent with those expected and hence no gross errors are apparent. The differences can be attributed to different atmospheric conditions than those assumed. The precipitable water content is particularly doubtful.

Appendix C

Calculation of the albedo of a Water Surface

Appendix C

Calculation of the Albedo of a Water Surface.

Unlike other surfaces, the albedo of a water surface, R_t, can change dramatically with solar altitude, , and cloud cover.

T.V.A. (1972) gives

$$R_t = A \ \alpha^B \qquad (C1)$$

where α = solar altitide (degrees)
A,B are empirical constants
dependent on cloud covers

The coefficients A and B are given in Table C1 for different cloud covers and the resultant relationships based on equation (C1) are plotted in Figure C1.

It is observed that the value of albedo is most dependent on cloud cover for small solar altitudes.

For solar altitudes less than 3 degrees, Class A evaporation pans are shaded and recieve no direct short-wave radiation.

Low scattered cloud and clear sky conditions are typical for summer while overcast conditions are typical for winter. This indicates that for morning and afternoon when the solar altitude is low, more short-wave energy will be lost due to reflection from water surfaces in summer than in winter, with the effect being most critical near sunrise and sunset.

The solar altitude, α, required to calculate the albedo, R_t, is defined by T.V.A. (1972) as

$$\sin\alpha = \sin\Phi \sin\delta + \cos\Phi \cos\delta \cos h \qquad (C2)$$

where Φ = latitude (radians)

δ = declination of the sun (radians)

h = local hour angle (radians)

An approximate value of declination can be calculated from

$$\delta = 23.45\ (\Pi/180)\cos((2\Pi/365)(172-D)) \qquad (C3)$$

where D = number of the day

This calculation of declination assumes the observation is made at the centre of the earth, ie it gives the apparent declination. More accurate methods are available (TVA (1972)) but are not justified here.

The latitude, Φ, is given positive if in the northern hemisphere and negative if the in the southern hemisphere.

Figure C2 shows the definition of the local hour angle of the mean sun, LHA. It is the angle measured westward around the axis of the celestial sphere from the upper meridian of the observation point to the meridian of the mean sun.

When the sun is east of the local meridian the LHA is greater than 12 hours. When the sun is at the local meridian it is local noon and LHA = 0 (or 24 hours). In the afternoon when the sun is west of the local meridian, the LHA is less than 12 hours.

The angle measured westward around the axis of the celestial sphere from the lower meridian of the observation point to the meridian of the sun is the local true solar time, LTST.

Due to the irregular angular motion of the earth around the sun, an imaginary mean sun is used to get the LTST.

At solar noon, LHA = 0, thus when the sun is east of the local meridian.

$$LMST = LHA - 12 \text{ (hours)} \quad (C4)$$

and when the sun is west of the local meridian

$$LMST = LHA + 12 \text{ (hours)} \quad (C5)$$

where LMST = local mean solar time (hours)

To correct for the position of the true sun relative to the mean sun, the equation of time, ET, is used.

$$ET = -(0.123570 \sin d - 0.004289 \cos d + 0.153809 \sin 2d + 0.060783 \cos 2d) \quad (C6)$$

where $d = (2\Pi/365.242)(D-1)$ (radians)

D = day number

and then

$$LTST = LMST + ET \quad (C7)$$

The equation of time only varies the LTST by at most 15 minutes and can hence be neglected as a good approximation for models with time steps greater than an hour.

Standard time, ST, is determined from the lower celestial meridian of the time zone and is related to the LMST by

$$LMST = ST - DTSL \quad (C8)$$

where $DTSL = \xi/15\ (LSM-LLM)$ (C9)

DTSL = time difference between local and standard meridian (hours)

LSM = longitude of standard meridian (120^{o} for W.A.)

LLM = longitude of location (deg)

ξ = -1 for west longitude

= +1 for east longitude

Combining equations (C4) through to (C9), the local hour angle becomes:

for sun east of location

$$LHA = ST + 12 - DTSL + ET \qquad (C10)$$

for sun west of location

$$LHA = ST - 12 - DTSL + ET \qquad (C11)$$

and for input to equation (C2)

$$h \text{ (radians)} = \Pi/12 \text{ LHA (hours)} \qquad (C12)$$

These calculation are easily done on a computer and require as inputs

- longitude of location
  (116.17^{o} for Collie)
- longitude of standard meridian
  (120^{o} for Western Australia)
- latitude of location
  (-33.33^{o} for Collie)
- local time (clock time)
- coefficients A, B dependent on cloud cover (from Table C1)

TABLE C1

Coefficients A and B for estimating the total reflectivity of a water surface. T.V.A. (1972)

Cloud Cover	A	B
Clear	1.18	-0.77
Scattered	2.20	-0.97
Broken	0.95	-0.75
Overcast	0.33	-0.45
High Scattered	2.20	-0.98
Low Scattered	2.17	-0.96
High Broken	1.10	-0.80
Low Broken	0.78	-0.68
High Overcast	0.51	-0.58
Low Overcast	0.20	-0.30

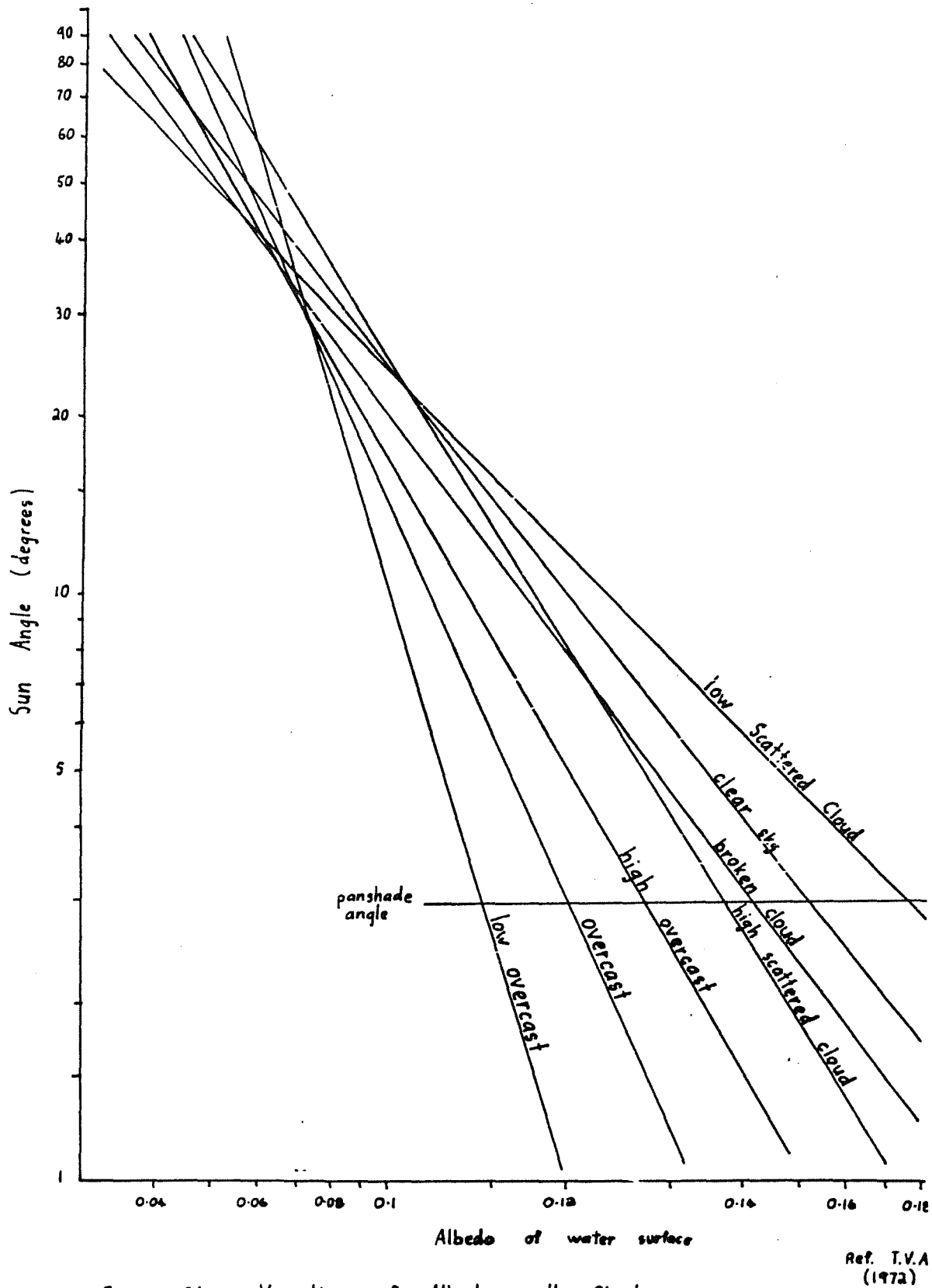

Figure C1 Variation of Albedo with Cloud cover

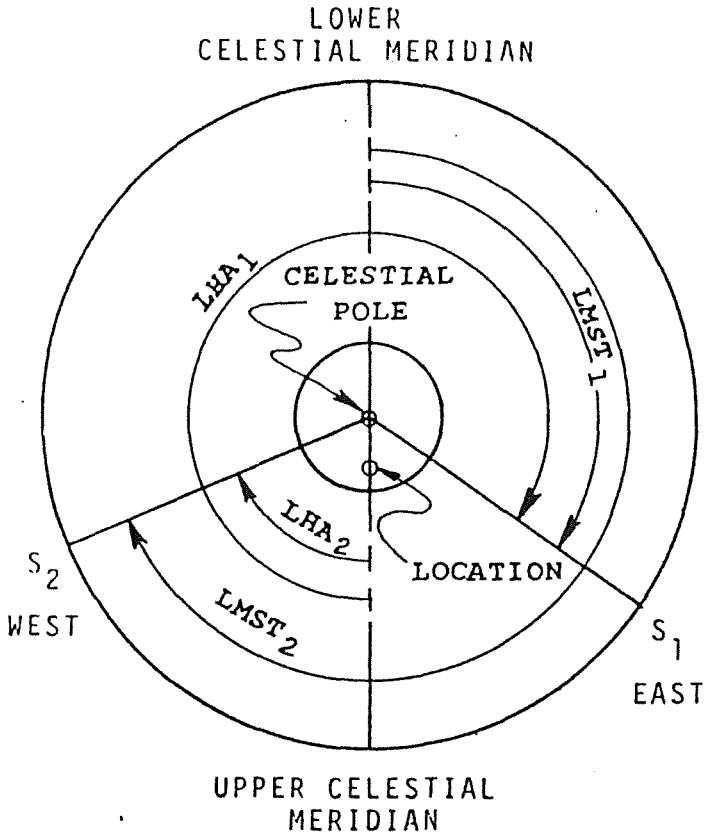

Time - hour angle relationship for mean sun*:

Sun east of the local meridian: S_1

$LMST_1 = LHA_1 - 12$ hours

Sun west of the local meridian: S_2

$LMST_2 = LHA_2 + 12$ hours

with: LMST local mean solar time

LHA local hour angle of mean sun in hours

*time is counted from the lower celestial meridian; the hour angle from the upper

Figure C2 : Time Diagram T.V.A. (1972)

Appendix D

Windspeed Profile above a Tree Canopy

Windspeed Profile above a Tree Canopy

In an effort to determine the nature of the windspeed profile above a forest canopy in a reforestation area, several measurements of windrun were taken at two elevations above the canopy of some replatings at the Arboretum Site (Figure DI), over a period of approximately one month.

Although it is desirable to take readings concurrently at 3 levels, only 2 anemometers were available and hence the data has its limitations.

The windrun measurements were taken in conjunction with measures of leaf conductance in the Arboretum replantings site. The anemometers were attached to the scaffolding used for this work and were located at fixed heights above the canopy at one location (Figure Dl).

The details of the anemometers are given in Table Dl and the recordings in Table D2.

TABLE Dl. Anemometer details

Anemometer Serial No.	Height Above Ground (m)	Vegetation ht (m)	Anemometer ht / Vegetation ht
27052	9.42	7.16	1.31
27073	8.60	7.35	1.17

As only values of windspeed at 2 levels can be obtained, no direct calculation of the zero plane displacement, d, or the roughness length, z_o, can be made. (Riou (1984))

However a relationship can be developed between d and z_o based on an assumed logarithmic profile in neutral conditions.

Under these conditions the windspeed profile can be given by:

$$u(z) = \frac{u^*}{k} \ln((z-d)/z_o) \qquad (D1)$$

where $u(z)$ = windspeed (m/s)

z = elevation (m)

d = zero plane displacement (m)

z_o = roughness length (m)

u_* = friction or eddy velocity (m/s)

k = Von Karman's constant = 0.41

The zero plane displacement is an indicator of the mean level at which momentum is absorbed by the plant community, while the roughness length indicates the bulk effectiveness as a momentum absorber.

If the ratio of the velocities at the two levels is taken then

$$\frac{u(z_2)}{u(z_1)} = \frac{\ln((z_2-d)/z_o)}{\ln((z_1-d)/z_o)} \qquad (D2)$$

should be a constant if d and z_o are strictly constants, and hence the windspeed profile maintains its logarithmic shape.

This ratio is plotted in Figure D2 for the data collected. The varying lengths of the segments indicate the periods over which the recordings were taken.

It is observed that there is a dominant mean value of 1.14 and that after 15th March the scatter is very small. Scatter prior to 15th March could have been due to non stable conditions. No temperature profile data is available to confirm this.

It will be assumed then that for the period represented by the data this ratio is representative of the profile above the canopy.

To determine a relationship between d and z_o, the generally accepted relationships

$$d = xh \qquad (D3)$$

$$z_o = yh \qquad (D4)$$

where x, y = constants

h = vegetation height

were used.

Substituting equations (D3) and (D4) into equation (D2) and using

$$\frac{u(z_2)}{u(z_1)} = 1.14, \text{ and}$$

rearranging gives

$$1.14\ln(z_1-xh_1) - \ln (z_2-xh_2) = 1.14 \ln (yh_1) - \ln yh_2)$$

and substituting $z_1 = 8.60m$

$z_2 = 9.42m$

$h_1 = 7.35m$

$h_2 = 7.16m$

and solving graphically for x and y gives the relationship plotted in Figure D3. This does not continue for values of $x < 0.3$ as this would give a roughness length greater than the zero plane displacement. The literature indicates the reverse is generally so.

To locate the actual x and y corresponding to the canopy and hence its d and z_o, another set of measurements at preferably a higher level is required. (Riou (1984))

The line plotted here only indicates the x-y combinations which would give the observed ratio in velocities.

Also plotted in Figure D3 are the values of x and y quoted in the literature.

They are

(a)	$d = 0.75\ h$ $z_o = 0.1\ h$	leafy canopies	Schofield (1982)
(b)	$d = 0.5\ h$ $z_o = 0.18\ h$	leafless canopies	Schofield (1982)
(c)	$d = 0.63\ h$ $z_o = 0.13\ h$	grass crop	Monteith (1973)
(d)	$d = 0.64\ h$ $z_o = 0.13\ h$	all surfaces	Cowan (1968)
(e)	$d = 0.7\ h$ $z_o = 0.1\ h$	30m forests	Jarvis et al (1976)

These all plot above the observed relationship and represent a considerable range.

The values most suited to our applications are those given by (a) and (e).

These variations in values will produce significant variations in the aerodynamic resistance and hence in the evaporation calculated from the Penman equation. (Refer section 5.5)

First consider y = 0.1 (ie $z_o = 0.1h$) as representative of the roughness length for the canopy. Then by the Schofield (1982) the zero plane displacements given by the relationship d = 0.75h while the observed data indicates d = 0.62h.

The aerodynamic resistance is given by:

$$r_a = \frac{(\ln ((z-d)/z_o))^2}{k^2\ u(z)} \qquad (D5)$$

where r_a = aerodynamic resistance (s/m)
k = Von Karmans constant = 0.41

Thus, if the upper level anemometer (27052) values are used,

$h = 7.16m$

$z = 9.42m$

then $z_o = 0.716m$

$d = 5.37m$ (Schofield (1982))

$d = 4.44m$ (observed data)

i.e. the observed data indicates a 17% lower zero plane displacement.

In equation D(5) the term $(\ln((z-d)/z_o))^2/k^2$

is a constant. The value calculated from the observed data is 25% higher than the Schofield (1982) relationship and hence at the same windspeed would indicate a 25% higher aerodynamic resistance.

Now the Penman combination equation is given by

$$\lambda E = \frac{\Delta/\gamma \; A + \frac{\rho Cp}{\gamma} \; \frac{(es(T) - e(T))}{r_a}}{(1 + \Delta/\gamma \; + r_s/r_a)} \qquad \text{(D6)}$$

where E = evaporation ($kgm^{-2}s^{-1}$, mms^{-1})

λ = latent heat of vaporisation (Jkg^{-1})

A = available energy (Wm^{-2})

D = slope of saturated vapour pressure curve vs. temp ($mb^{o}\ k^{-1}$)

γ = psychrometric constant ($mb^{o}\ k^{-1}$)

ρ = density of air ($kg\ m^{-3}$)

Cp = specific heat of air ($J\ kg^{-1}{}^{o}C$)

$e_s(T)$ = saturation vapour pressure (mb)

$e\ (T)$ = actual vapour pressure (mb)

r_a = aerodynamic resistance (sm^{-1})

r_s = surface resistance (sm^{-1})

The first term of this equation represents the energy component of evaporation, while the second term represents the aerodynamic component.

Under wet canopy conditions r_s = 0 and where the energy component of the evaporation is only small, a 25% increase in r_a could produce a 20% decrease in evaporation.

Thus at night when the energy component is relatively small, the determination of the roughness parameters is very critical.

Similarly if a zero plane displacement of d = 0.75h is taken as representative then the value calculated from the observed relationship of 0.36m and is half the value of 0.72m indicated by Schofield (1982). This subsequently gives a value of r_a 95% higher as compared to the Schofield (1982) estimate. Hence a possible 49% reduction in evaporation under wet canopy conditions as compared to that calculated using the values of Schofield (1982).

This is indeed very significant and will have a great effect on the evaporations estimated from a forest canopy.

It seems that the values from the literature are too often used with little thought towards the sensitivity of them when applied in the Penman forumla.

From the limited data used here, it appears that lower potential forest evaporations will result if the observed relationship is used in preference to the values quoted in the literature.

Although a relationship between x and y is found here that will fit the observed data, some choice must be made as to what values to use in the application of the Penman equation.

It has been decided here to be consistent with the literature and use z_o = 0.1h, but to then use the observed relationship and the resulting d = 0.62h.

This will be used throughout all future work unless further measurements or data come to hand.

One other problem in using windspeed profiles in the Penman equation is that unless measurements of windspeed are taken above the canopy under consideration, then values from other sites must be used and hence transposed in some fashion.

The only available windrun data near to the replantings sites is from Ernies Climat Station (509 249). (Figure 2)

Due to timing errors in the recording mechanism, only average values of windrun between visits was available for the period under consideration here.

The average windrun over the period as indicated by the primary recorder at Ernies was 62 km/day or 0.72 m/sec.

Corresponding windspeeds over the same period calculated from the two anemometers were 1.6 m/sec and 1.4 m/sec at the high and low levels respectively.

Although these are only averages over a period of approximately 1 month, they do show differences between the sites which must be accounted for.

For the purpose of the work here, and considering the accuracy of the results obtained and the assumptions made, it is assumed that for a summer period with light winds, the windspeed at elevation 1.2h is twice that measured at the climat station at Ernies.

This is reasonable provided it is used only in summer for above canopy conditions in the Arboretum reforestation area.

TABLE D2

Anemometer Results

h_1 = 7.35m h_2 = 7.16m

z_1 = 8.60m z_2 = 9.42m

Date	Time	t seconds	High m	Low m	u_2 u High m/sec	u_1 u Low m/sec	$\frac{u_2}{u_1}$
13/3/84	1130						
	1700	19800	3830	2270	1.93	1.15	1.68
14/3/84	0917	58620	4485	5099	0.76	0.87	0.87
	1315	14280	3442	3178	2.41	2.22	1.08
15/3/84	1222	76020	6935	7033	0.91	0.92	0.99
	1302	2400	891	809	3.71	3.37	1.10
21/3/84	1126	512880	79026	69250	1.53	1.34	1.14
	1225	3540	490	441	1.38	1.24	1.11
	1406	6060	1100	957	1.81	1.58	1.14
	1630	8640	1504	1333	1.74	1.54	1.13
22/3/84	1100	66600	5007	4159	0.75	0.62	1.21
	1207	4020	670	604	1.66	1.50	1.11
	1520	11580	2085	1835	1.80	1.58	1.14
	1640	4800	793	709	1.65	1.48	1.11
27/3/84	1205	415500	49121	42711	1.18	1.03	1.14
	1402	7020	1380	1248	1.96	1.77	1.11
3/4/84	1206	597840	73362	64541	1.23	1.08	1.14
	1214	480	106	85	2.21	1.77	1.25
	1401	6420	1445	1264	2.25	1.97	1.14
11/4/84	0926	674700	104716	91955	1.55	1.36	1.14
Average					1.65	1.45	1.14

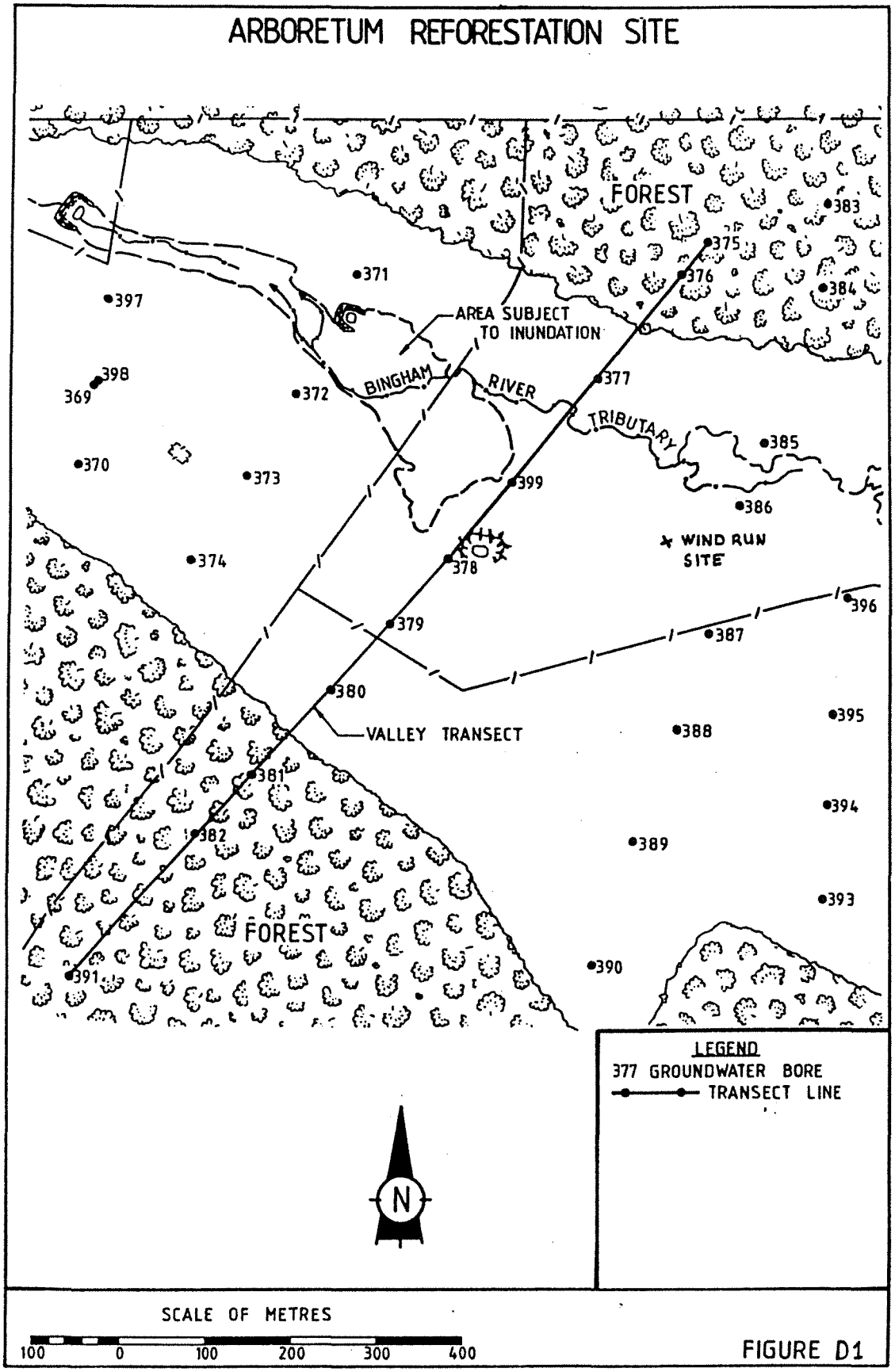
ARBORETUM REFORESTATION SITE
FOREST
383
375
371
376
384
397
AREA SUBJECT
TO INUNDATION
398
369
372
BINGHAM
RIVER
377
TRIBUTARY
385
370
373
399
386
WIND RUN
SITE
374
378
396
379
387
380
VALLEY TRANSECT
388
395
381
394
382
389
393
FOREST
390
391
LEGEND
377 GROUNDWATER BORE
TRANSECT LINE
N
SCALE OF METRES
100 0 100 200 300 400

FIGURE D1

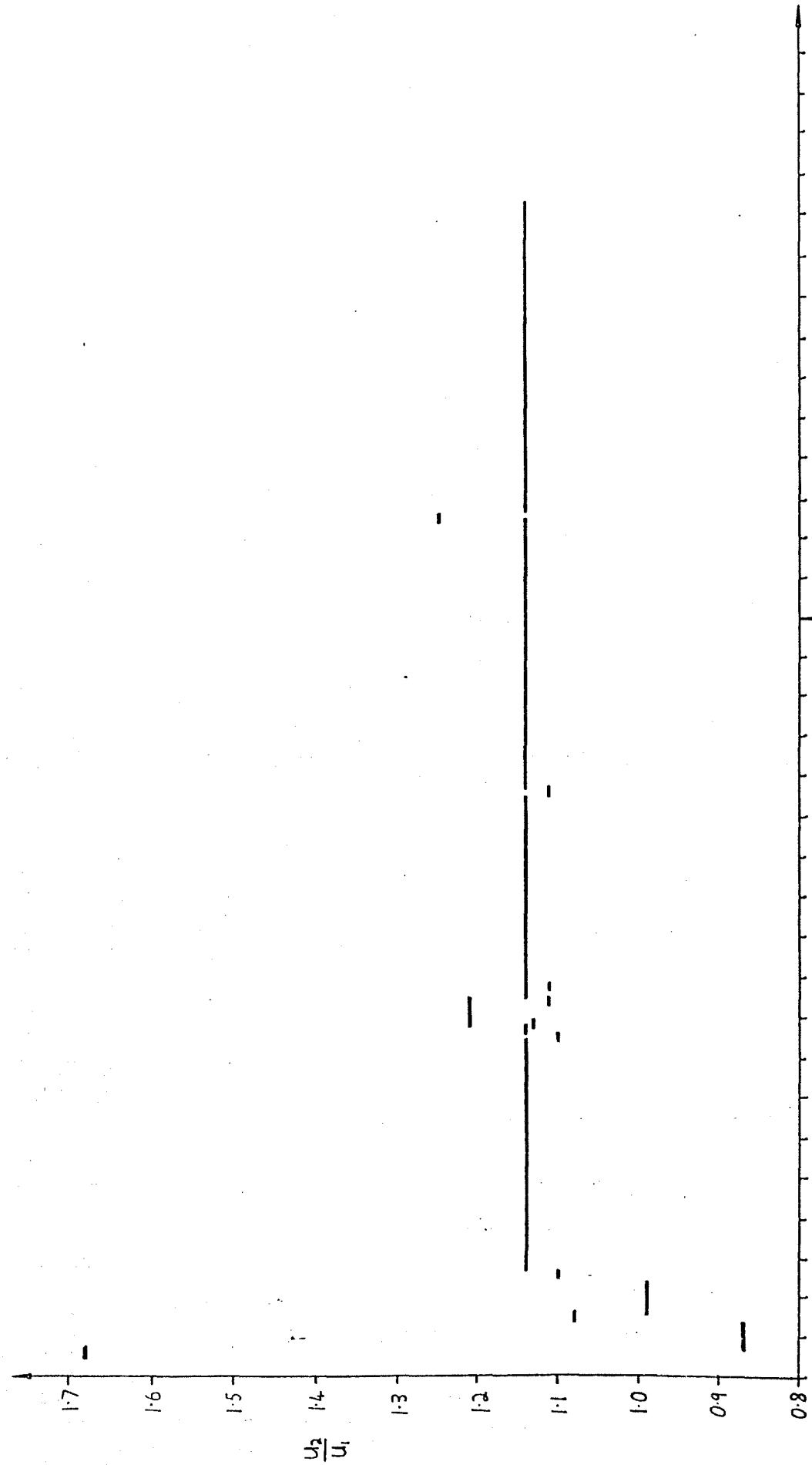

FIGURE D2 Ratio of wind velocities at two different levels above the vegetation

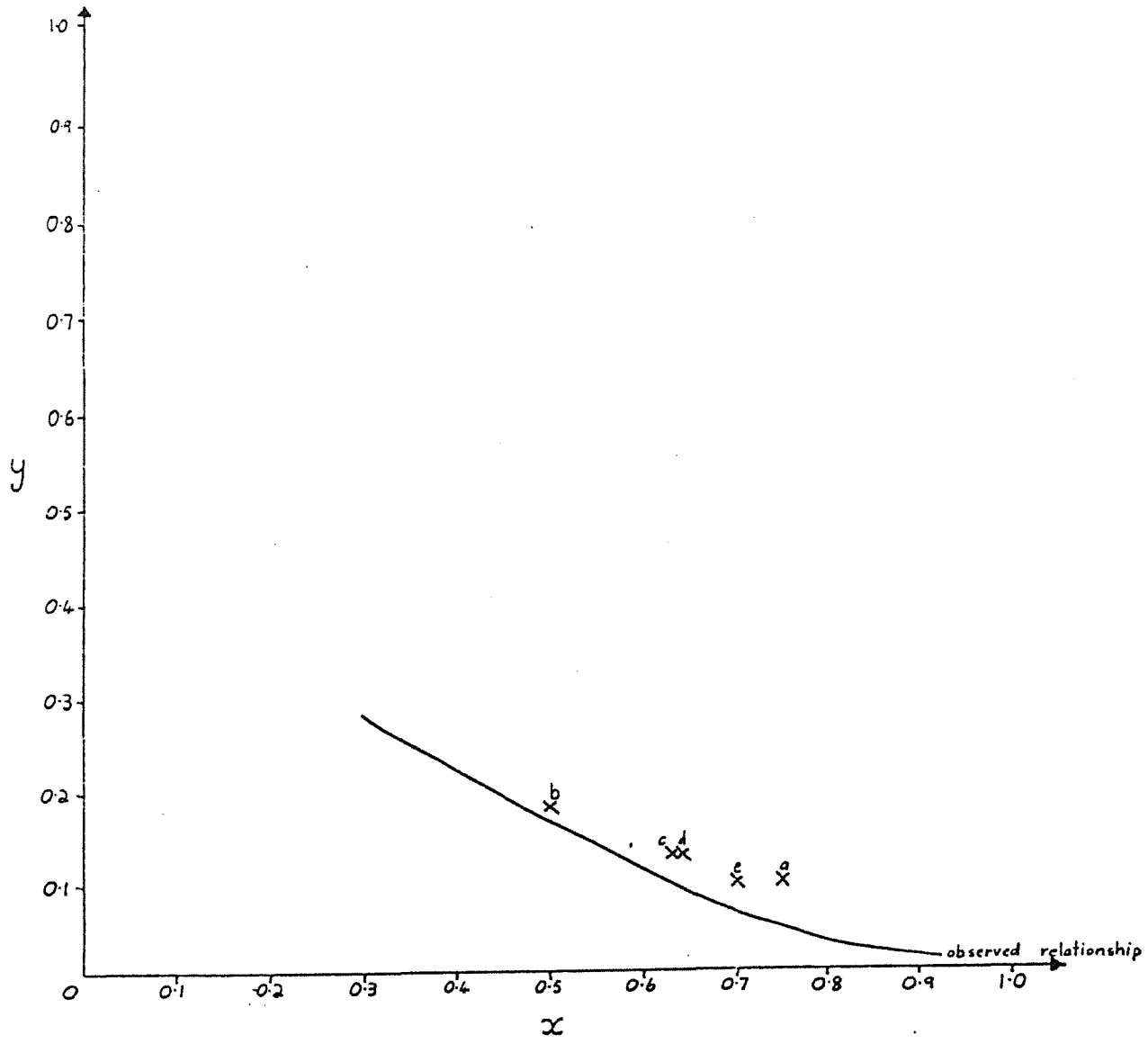

Figure D3 Zero plane displacement, Roughness Length relationships.

zero plane displacement $d = x\,h$

roughness length $z_o = y\,h$

h = vegetation height

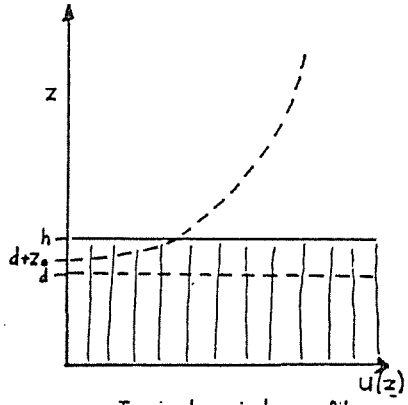

Typical wind profile over uniform level vegetation

Appendix E

Dwellingup Data Used

TABLE E1 Cloud Factors

Day	July 1982		December 1982	
	9am	3pm	9am	3pm
1	1.060	1.036	1.000	1.000
2	1.000	1.000	1.016	1.028
3	1.240	1.240	1.000	1.000
4	1.176	1.176	1.000	1.046
5	1.134	1.240	1.000	1.036
6	1.060	1.036	1.176	1.008
7	1.134	1.240	1.012	1.096
8	1.176	1.096	1.176	1.246
9	1.176	1.240	1.240	1.134
10	1.240	1.240	1.176	1.176
11	1.176	1.176	1.240	1.060
12	1.000	1.008	1.096	1.134
13	1.176	1.176	1.134	1.000
14	1.044	1.000	1.134	1.134
15	1.240	1.240	1.000	1.008
16	1.240	1.096	1.000	1.008
17	1.176	1.176	1.000	1.000
18	1.176	1.176	1.000	1.060
19	1.240	1.134	1.036	1.036
20	1.176	1.176	1.000	1.008
21	1.240	1.240	1.176	1.016
22	1.060	1.096	1.240	1.176
23	1.176	1.176	1.012	1.010
24	1.176	1.176	1.240	1.240
25	1.176	1.176	1.000	1.000
26	1.060	1.176	1.030	1.000
27	1.176	1.096	1.000	1.036
28	1.176	1.176	1.134	1.134
29	1.096	1.096	1.134	1.134
30	1.176	1.000	1.134	1.134
31	1.176	1.000	1.068	1.000

JULY 1982

SUNSHINE

Table E2 :

DATE	-6	6-7	7-8	8-9	9-10	10-11	11-12	12-1	1-2	2-3	3-4	4-5	5-6	6+	TOTAL
1-7-82				.5	1.0	1.0	1.0	.9	.8	1.0	1.0	.4	-	-	7.6
2-7-82				.6	1.0	1.0	1.0	1.0	1.0	1.0	1.0	.3	-	-	7.9
3-7-82				.6	-	-	-	-	-	.5	-	-	-	-	1.1
4-7-82				-	.1	.2	-	.1	.7	.1	-	-	-	-	1.2
5-7-82				-	.8	.7	.1	-	-	-	-	-	-	-	1.6
6-7-82				.4	1.0	.3	.1	.2	.8	.9	1.0	-	-	-	4.7
7-7-82				.8	.8	.8	.9	-	-	-	-	-	-	-	3.3
8-7-82			.1	.2	.6	.6	.8	1.0	.9	.8	.1	.1	-	-	5.2
9-7-82				.3	.3	.6	1.0	1.0	.4	-	.4	-	-	-	4.0
10-7-82				.1	-	-	.1	-	-	-	.1	.2	-	-	0.5
11-7-82				.2	1.0	1.0	1.0	1.0	1.0	1.0	1.0	.4	-	-	7.6
12-7-82			.4	1.0	1.0	1.0	1.0	1.0	1.0	.9	.1	.1	-	-	7.5
13-7-82				.9	1.0	.6	.3	.2	-	.2	.1	.1	-	-	3.4
14-7-82			.5	.4	.8	.5	1.0	1.0	1.0	1.0	1.0	.4	-	-	7.6
15-7-82				.3	-	-	-	-	-	-	-	-	-	-	0.3
16-7-82				.0	.4	.7	1.0	1.0	.9	.8	1.0	.2	-	-	6.0
17-7-82				.3	1.0	1.0	.6	.5	.6	.4	.4	-	-	-	4.8
18-7-82				.3	1.0	1.0	1.0	.8	.7	.3	.7	.7	-	-	6.5
19-7-82				.6	.6	.8	.5	.7	.4	.2	-	-	-	-	3.8
20-7-82				.1	.9	.5	1.0	1.0	.5	.1	.7	.4	-	-	5.2
21-7-82				.3	-	-	-	-	.3	-	-	-	-	-	0.6
22-7-82				.3	1.0	1.0	.8	.7	.9	.8	.7	.2	-	-	6.4
23-7-82				.7	.4	.6	.2	.8	.8	.5	.5	.2	-	-	4.7
24-7-82				.5	.8	1.0	.9	.6	.5	.8	.9	.2	-	-	6.2
25-7-82				.3	1.0	.9	1.0	.5	.4	.7	-	-	-	-	4.8
26-7-82				.6	.6	1.0	1.0	.5	.4	.4	.2	.1	-	-	4.8
27-7-82			.1	.4	.8	.6	1.0	1.0	1.0	.6	1.0	.5	-	-	7.0
28-7-82			.1	.3	1.0	1.0	1.0	1.0	.8	.4	1.0	.6	-	-	7.2
29-7-82			.2	.7	1.0	1.0	.8	.4	1.0	.5	.6	.6	-	-	6.8
30-7-82			.6	.6	1.0	1.0	1.0	1.0	1.0	1.0	1.0	.7			8.9

SUNSHINE **DECEMBER 1982**

Table E3 :

Date	-6	6-7	7-8	8-9	9-10	10-11	11-12	12-1	1-2	2-3	3-4	4-5	5-6	6+	Total
1-12-82		.7	1.0	1.0	1.0	1.0	1.0	1.0	1.0	1.0	1.0	1.0	.8	.1	11.6
2-12-82		.8	1.0	1.0	1.0	1.0	1.0	1.0	1.0	1.0	1.0	1.0	.9	-	11.7
3-12-82		.8	1.0	1.0	1.0	1.0	1.0	1.0	1.0	1.0	1.0	1.0	.8	.1	11.7
4-12-82		.8	1.0	1.0	1.0	1.0	1.0	1.0	1.0	1.0	.9	.7	-	-	10.4
5-12-82		.8	1.0	1.0	1.0	1.0	1.0	1.0	1.0	1.0	1.0	1.0	.7	-	11.5
6-12-82		.1	-	.5	1.0	1.0	1.0	1.0	1.0	1.0	1.0	1.0	.8	-	9.4
7-12-82		.2	1.0	.8	1.0	1.0	.8	.8	.9	.8	.6	.8	.1	-	8.5
8-12-82		-	-	1.0	.3	.7	-	-	-	-	-	-	-	-	2.0
9-12-82		.2	-	.3	.1	.1	.6	1.0	1.0	1.0	.5	.7	.5	-	6.0
10-12-82		.8	-	.1	-	.6	.1	.7	.9	.7	.8	.7	.8	-	5.7
11-12-82		.3	.1	-	.1	-	-	-	.3	1.0	.9	.9	.6	-	4.0
12-12-82		.8	.8	.5	-	.1	.2	.4	.1	.8	.7	1.0	1.0	.3	6.0
13-12-82		.2	.2	.5	.8	.7	1.0	1.0	1.0	1.0	1.0	1.0	.4	-	8.8
14-12-82		.2	.9	.7	1.0	1.0	1.0	1.0	1.0	1.0	.9	.7	.4	-	9.8
15-12-82		.8	1.0	1.0	1.0	1.0	1.0	1.0	1.0	1.0	1.0	1.0	1.0	.5	12.3
16-12-82		.8	1.0	1.0	1.0	1.0	1.0	1.0	1.0	1.0	1.0	1.0	1.0	-	11.8
17-12-82		.8	1.0	1.0	1.0	1.0	1.0	1.0	1.0	1.0	1.0	1.0	.9		11.7
18-12-82		.8	1.0	1.0	1.0	1.0	1.0	1.0	1.0	1.0	1.0	1.0	.8	.2	11.8
19-12-82		.8	1.0	1.0	1.0	1.0	1.0	1.0	1.0	1.0	1.0	1.0	1.0	.4	12.2
20-12-82		.8	1.0	1.0	1.0	1.0	1.0	1.0	1.0	1.0	1.0	1.0	.2	-	11.0
21-12-82		-	-	.5	.9	.8	.8	1.0	1.0	1.0	1.0	1.0	.7	-	8.7
22-12-82		-	-	-	-	-	.1	.3	.5	.2	-	.5	.3	.2	2.1
23-12-82		.7	1.0	.5	.8	1.0	1.0	1.0	1.0	1.0	1.0	1.0	1.0	.4	11.4
24-12-82		-	-	.5	-	.1	.1	.1	.2	-	-	-	-	-	1.0
25-12-82		.6	1.0	.6	1.0	1.0	1.0	1.0	1.0	1.0	1.0	1.0	1.0	.4	11.6
26-12-82		.8	1.0	1.0	1.0	1.0	1.0	1.0	1.0	1.0	.5	1.0	1.0	.3	11.6
27-12-82		.1	.1	.7	1.0	1.0	1.0	1.0	1.0	1.0	1.0	1.0	1.0	.4	10.5
28-12-82		.8	1.0	1.0	.4	.8	.9	.8	1.0	1.0	1.0	1.0	.9	.2	10.8
29-12-82		.8	1.0	1.0	1.0	1.0	1.0	1.0	1.0	1.0	1.0	1.0	1.0	.4	12.2
30-12-82		.5	1.0	1.0	1.0	1.0	1.0	1.0	1.0	1.0	1.0	1.0	.7	.0	11.2

Table E4 :

. DWELLINGUP . . . . . during the Month of . . . . . JULY . . . . . 19.82 . . .

CLOUD 0900 Amount (Scale 0-8)	CLOUD 0900 Types	CLOUD 1500 Amount (Scale 0-8)	CLOUD 1500 Types	Visibility 0900 km/metre	Visibility 1500 km/metre	Rain 24 hrs to 0900 (millimetres to nearest 0.2)	Evaporation 24 hrs to 0900 (millimetres to nearest 0.2)	River Height at 0900 (metres to second dec. place)	Daily Remarks on Weather (With notes of Phenomena such as Thunder*, Lightning*, Hail, Frost Fog*, Snow, Wind-storms*, Heavy Rain-storms*, Floods, Dust-storms, Coloured Rain, Funnel Clouds & Tornadoes* etc.) * Include Time of Occurrence or Duration	RH 0900	RH 1500	RH MAX	SUN HRS	AM WIND DIR	WIND RUN	EMC	ROS	FDI
								FROSTS									
4	Fs	3	Cu	50	50	13·1	01·5	·		90	60		7·5	20	115		
CLEAR		CLEAR		50	50	·0	02·2	YES		95	52		7·9	32	043		
8	Sc			50		2·2	04·0	YES		92			1·1	10	147		
7	Sc			50		17·9	03·5	·		100		63	1·2	0	096		
6	Fs	8	Fs	50	50	5·0	03·8	·		88	100	55	1·6	0	109		
4	Fc	3	Cu	50	50	15·4	00·0	·		97	62	60	4·7	0	109		
6	Sc	7	Fs	50	50	·5	02·3	·		82	73	59	3·3	13	013		
7	Fs	5	Cu	50	50	·8	01·4	·		78	65	7	5·2	24	069		
7	Fs	8	Fs	50	50	·8	04·2	·		100	96		4·0	35	088		
8	Sc			50		4·8	00·0	·		100			0·5	14	054		
3	Sc			50		·0	02·8	·		92			7·6	29	022		
1	Ci	2	Ci	50	50	·0T	04·8	·		52	38		7·5	52	134		
4	Fs	7	Fs	50	50	6·1	00·9	·		95	70		3·4	36	119		
4	Ac	1	Ci	50	50	·4	05·6	·		45	32		7·6	55	073		
8	Fs	4/2	Fs/Ac	50	50	39·0	03·4	·		100	87		0·3	0	131		
8	Fs	5	Cu.	50	50	36·0	08·0	·		95	75		6·0	0	058		
2	Ac			50		3·4	00·2	·		71			4·8	0	051		
CLEAR				50		·2	04·6	·		100			6·5	10	028		
5	Fs	6	Fc	50	50	11·2	04·6	·		96	89		3·8	0	065		
6	Fs	7	Fs	50	50	13·6	02·3	·		96	94		5·2	0	100		
6	Sc	8	Fs	50	50	5·0	00·3	·		99	94		0·6	0	042		
4	Sc	5	Fc	50	50	16·6	00·6	·		86	69		6·4	0	034		
6	Fs	6	Fc	50	50	6·8	00·4	·		100	71		4·7	0	086		
6	Sc			50		3·6	00·5	·		98			6·2	0	180		
6	Sc			50		3·4	00·6	·		97			4·8	0	182		
4	Fs	7	Sc	50	50	3·0	05·0	·		82	74	60	4·8	0	144		
7	Sc	5	Cu	50	50	21·6	01·4	·		92	65	56	7·0	0	269		
CLEAR		4	Cu	50	50	01·6	03·0	YES		100	60	47	7·2	0	047		
5	Cu	5	Cu	50	50	00·0T	03·0	·		73	60	54	6·8	12	071		
2	Sc	CLEAR		50	50	00·1D	03·1	Yes		98	42	36	8·9	29	019		
Clear				50		·0	00·6	Yes		91		33	9·2	52	023		
						·	·	·									

Table E5 :

. . . . . during the Month of . . . . DECEMBER . . . . 19.82 . . .

CLOUD 0900 Amount (Scale 0-8)	CLOUD 0900 Types	CLOUD 1500 Amount (Scale 0-8)	CLOUD 1500 Types	Visibility 0900 km/metre	Visibility 1500 km/metre	Rain 24 hrs to 0900 (millimetres to nearest 0.2)	Evap-oration	River Height at 0900 (metres to second dec.place)	Daily Remarks on Weather (With notes of Phenomena such as Thunder*, Lightning*, Hail, Frost, Fog*, Snow, Wind-storms*, Heavy Rain-storms*, Floods, Dust-storms, Coloured Rain, Funnel Clouds & Tornadoes* etc.) RH* Include Time of Occurrence or Duration 0900	1500	Min	Sun/hrs	9am MSDT	Max Rain	SMC	RDS	FDI
								FRCSTS										
Clear		Clear		50+	50+	.0	4.0	.	51	28	28	11.6	1240	0073	6	58	High
4	Ci	3	As	50+	50+	.0	5.6	.	75	19	19	11.7	1249	0089	9	34	Mod
Clear		1	Cu	50	50	.0	5.9	.	63	50	40	11.7	1258	0077	7	60	High
Clear		6	3 Cu 3 Ci	50	50	.0	8.0	.	59	31	31	10.4	1269	0115	7	51	High
Clear		3	Cu	50	50	.0	7.0	.	65	54	43	11.5	1280	0065	7	51	High
7	Cu	3	1 Cu 2 Ci	50	50	.0	7.2	.	69	32	32	9.4	1289	0097	8	42	High
3	2 Ac 1 Ci	5	Cu	50	50	.0	6.3	.	53	22	22	8.8	1298	0069	7	51	High
	Sc	8	Sc	50	50	.0	7.0	.	48	51	33	2.0	1310	0059	9	37	High
8	Sc	6	Sc	50	50	.1	5.3	.	77	50	50	6.0	1320	0048	8	58	High
7	Sc	7	Cb	50	50	2.6	6.0	.	75	66	58	5.7	1309	0279	24	17	Low
8	Cb	4	Cu	50+	50+	11.6	4.8	.	98	65	58	4.2	1210	0332	51	5	Low
6	5 Cu 1 Ci	6	Cu	50+	50+	09.0	5.8	.	61	53	43	6.7	1134	0111	95	3m	Low
6	Cb	1	Cu	50+	50	.1	4.1	.	71	45	36	8.8	1149	0075	50	4	Low
6	Sc	6	Sc	50	50	.6	3.0	.	71	53	44	9.8	1168	0125	18	24	Mod
1	Ci	2	Cs	50	50	T .0	8.4	.	62	43	35	12.3	1191	0109	12	23	Mod
2	1 Ns 1 Ci	2	Ci	50	50	T .0	5.6	.	63	54	36	11.8	1221	0166	14	19	Mod
Clear		Clear		50	50	.0	5.8	.	62	31	28	11.7	1230	0031	7	57	High
Clear		4	Sc	50	50	.0	8.6	.	62	31	30	11.8	1241	0120	7	57	High
4	3 Sc 1 Ci	3	Cu	50	50	.0	9.2	.	52	21	21	12.2	1253	0103	7	51	High
1	As	3	1 Cb 2 Ci	50	50	.0	10.0	.	55	50	48	11.0	1246	0186	19	37	Mod
7	Sc	2	Cu	50	50	.0	8.2	.	80	46	40	8.7	1277	0111	11	24	Mod
8	Sc	7	Sc	50	50	.0	6.8	.	84	59	52	2.1	1288	0089	9	37	Mod
3	1 Cu 2 As	4	1 Cb 3 Cs	50	50	.0	4.0	.	66	45	43	11.4	1296	0049	11	24	Mod
7	1 Cu 2 As 4 Ci	8	Sc	50	50	.0	5.4	.	73	55	45	1.0	1305	0061	9	44	High
Clear		1	Ci	50	50	.0	3.4	.	70	44	28	11.6	1313	0015	12	26	Mod
6	Ci	2	1 Cu 1 Ci	50	50	.0	4.0	.	53	38	38	11.6	1324	0094	8	59	High
Clear		3	Cu	50	50	.0	10.6	.	55	27	26	10.3	1333	0097	8	42	High
6	St	6	Sc	50	50	.0	6.6	.	70	45	45	10.8	1345	0103	11	27	Mod
1	Cu	6	Cu	50	50	.0	7.0	.	45	31	22	12.2	1354	0126	9	29	Mod
6	Cu	6	Ci	50	50	.0	7.6	.	59	51	42	11.2	1363	0075	8	44	High
6	4 Ci 2 Ci	1	Ci	50	50	.6	5.0	.	63	35	32	8.6	1367	0116	11	27	Mod
						.	.	.										

Appendix F

Computer Program Locations

Two Fortran 4 programs have been written for the estimation of evaporation from climatological data. Both require as input, working files of 15 minute data in the format.

Col 1 = Total Rainfall (mm)
Col 2 = Average Air Temperature (^{o}C)
Col 3 = Average Relative Humidity (%)
Col 4 = Total Windrun (m)
Col 5 = Total Direct and Diffuse Short-wave Radiation (J/m^2)

This file is attached as TAPE 1 for both programs.

The first program estimates evaporation from a Class A pan and requires as an additional input

Col 6 = Average Pan Temperature (^{o}C)

The Source and Binary versions are PANCSOURCE and PANCBINARY.

The second program estimates wet canopy evaporation from any type of vegetation surface.

All inputs are interactive and are self explanatory. The detailed explanation of the various input requirements is given in the previous sections of this report.

An additional input to both programs is TAPE 3, which is the file containing cloud factors.

TAPE2 is output and contains hourly potential evaporation totals.

Two sets of files have been produced for running the programs, one for July 1982 and the other for December 1982.

These files are summarised in Table F1

Table F1 Program Input Requirements

	July 1982	December 1982
TAPE1	JULY82PANEVAPDATA	DEC82PANEVAPDATA
TAPE3	JULY82CLOUD2	DEC82CLOUD2

All data and program files are located on P.W.D. Mag Tapes 4434, 4813, 4560 on the disc master file

POTENTIALEVAPMASTER

Note that the programs give hourly summaries printed out on a daily basis and at the end of the data file produce a total evaporation.

All working files must start at 24:00 hours and should cover calendar month periods.

A sample of the printout for 1 day is given in Figure F1.

Additional programs have also been written for estimation of forest transpiration using estimated vapour pressure deficit - leaf conductance relationships.

Modifications to programs to suit particular needs is relatively easy.

Figure F1 : A sample of the printout for 1 day

PENMAN EVAPORATION ESTIMATES FOR STN NO:509 249

RECORD DATE 3/12/82

HOUR	1 AVERAGE AIR TEMP (DEG C)	2 AVERAGE REL HUM (%)	3 TOTAL RAIN (MM)	4 AVERAGE WIND SPEED (M/S)	5 AVERAGE RADIATION (W/M2)	6 ENERGY COM EVAP (MM)	7 AERO COMP EVAP (MM)	8 TOTAL EVAP (MM)	9 AVERAGE RA (S/M)	10 AVERAGE VPD (MB)	11 6/8	12 7/8
1	13.942	88.299	0.0000	.717	-71.0058	0.	.804E-01	.229E-01	27.3	1.87	0.	3.51
2	13.640	88.680	0.0000	.836	-68.8050	0.	.903E-01	.371E-01	27.8	1.77	0.	2.43
3	13.853	85.832	0.0000	.556	-71.1065	0.	.723E-01	.156E-01	37.1	2.24	0.	4.64
4	14.041	84.575	0.0000	.505	-67.1606	0.	.728E-01	.208E-01	41.7	2.47	0.	3.51
5	14.213	83.369	0.0000	.884	-69.4894	0.	.137	.781E-01	26.9	2.69	0.	1.75
6	14.343	82.038	0.0000	1.228	-47.8773	0.	.207	.164	16.0	2.93	0.	1.26
7	14.885	79.919	0.0000	1.502	78.6502	.717E-01	.295	.367	14.4	3.40	.195	.805
8	17.736	70.692	0.0000	3.566	351.6138	.338	1.09	1.43	5.36	5.97	.236	.764
9	20.306	61.844	0.0000	3.556	545.5019	.549	1.46	2.01	5.42	9.08	.273	.727
10	22.565	55.217	0.0000	3.111	709.0301	.741	1.57	2.31	6.04	12.2	.321	.679
11	24.676	49.216	0.0000	3.434	798.1322	.861	2.06	2.92	5.51	15.7	.295	.705
12	26.234	44.122	0.0000	3.000	843.9324	.931	2.03	2.96	6.16	18.9	.314	.686
13	27.939	39.035	0.0000	3.343	856.9986	.966	2.53	3.50	5.53	22.7	.276	.724
14	29.431	35.909	0.0000	3.889	807.7778	.928	3.17	4.10	5.08	26.0	.226	.774
15	30.433	33.328	0.0000	3.767	715.1112	.831	3.24	4.07	4.94	28.6	.204	.796
16	31.248	31.275	0.0000	3.111	576.7202	.676	2.79	3.47	6.20	30.8	.195	.805
17	31.598	30.035	0.0000	3.111	377.1144	.444	2.86	3.30	5.92	32.0	.135	.865
18	30.161	30.887	0.0000	2.898	149.1609	.173	2.58	2.75	6.56	29.2	.631E-01	.937
19	26.739	39.397	0.0000	2.431	-18.0963	.330E-02	1.83	1.81	8.74	21.1	.183E-02	1.01
20	24.018	45.569	0.0000	2.231	-51.6490	0.	1.38	1.32	10.8	16.2	0.	1.04
21	21.339	62.621	0.0000	4.227	-60.4148	0.	1.75	1.69	4.37	9.53	0.	1.04
22	18.561	72.798	0.0000	2.995	-64.2604	0.	.848	.785	6.49	5.82	0.	1.08
23	16.606	79.038	0.0000	1.489	-64.4678	0.	.310	.250	15.0	3.81	0.	1.24
24	15.097	85.195	0.0000	1.169	-69.9093	0.	.167	.103	17.6	2.54	0.	1.61
DAY	21.481	60.820	0.0000	2.398	253.5626	7.51	32.6	39.5	13.2	12.8	.190	.826